Contents

Preface

Karl Beucke
Rector of the Bauhaus-Universität Weimar

The planning and construction of buildings and infrastructure require a complex interaction between involved disciplines with partially diverging interests as well as the recognition of their impact on the natural environment. They impose demands on safety and reliability for a long time, which might be different to other engineering disciplines being more focussed on the daily life impact. Thus, the civil engineer has to take responsibility for the creation and maintenance of technical constructions which claim to be unique and can't be tested or better recalled. Together with the rapid development of computer technology many aspects of the civil engineering practise can be understood and discussed more in detail now. But, it also leads to increased demands on young practioners as well as young researchers.

Like some other academic institutions and departments, the Faculty of Civil Engineering of the Bauhaus-Universität Weimar makes its experience and expertise in teaching and research available under the organizational leadership of the Institute of Structural Engineering (IKI). The extraordinary format of the interdisciplinary Summer School provides the opportunity for foreign and local students to study advanced levels of recent developments of numerical methods and sophisticated modelling in different disciplines of civil engineering far beyond traditional graduate courses. In addition, results of ongoing research and projects at the partner Universities of the Bauhaus-Universität Weimar involved as well as topics from neighbouring disciplines affecting and describing the demands on civil engineer structures are presented by invited guest lectures.

In August 2014 about 50 Students and 10 guest lecturers from 20 countries have participated at the Technical Summer Course "Forecast Engineering: Global climate change and the challenge for the built environment" and contributed to the international atmosphere, to the scientific and the intercultural exchange of experience and ideas which were noticeably appreciated by the guests and organizers. This volume of the series of the Institute of Structural Engineering summarizes the results of the conducted project work and provides the abstracts of the contributions by the participants and impressions from the accompanying programme and organized cultural activities.

On behalf of the University I would like to thank everyone for his/her contribution to the scientific content, the social events, the organization and the realization of the Summer Course 2014. Particular thanks to all the lecturers spending a part of their annual leave to join us for the Bauhaus Summer School. The University and in particular the Faculty of Civil Engineering are grateful for the sponsorship from the German Academic Exchange Service (DAAD). The successful Summer Course 2014 and its Annual Report (Volume III) would not have been possible without this generous financial support.

Prof. Dr.-Ing. Karl Beucke

Photo: Barbara Proschak

Bauhaus Summer School – Forecast Engineering
Global Climate Change & Challenges for Built Environment

ABRAHAMCZYK Lars, SCHWARZ Jochen
Earthquake Damage Analysis Center, Bauhaus-Universität Weimar, Germany

Targets and objectives

The objectives of the summer course are to emphasize the demands and solution approaches on civil engineering structures due to the climate changes and their consequences. In collaboration with social and natural sciences the consequences and probable needs are discussed to develop and provide successful solutions. Different disciplines are brought together. The core area of the engineering sciences and techniques (here: civil and structural engineering) are completed by themes out of the research domains of natural hazards, geography, geology, geodesy, mathematics and natural sciences. E.g. from the field of the mathematics elements of statistics and stochastics as well as informatics and computer science will be trained and applied. The exchange of ideas between the partner institutions, especially in the field of the consequences due to climate changes, itself add value.
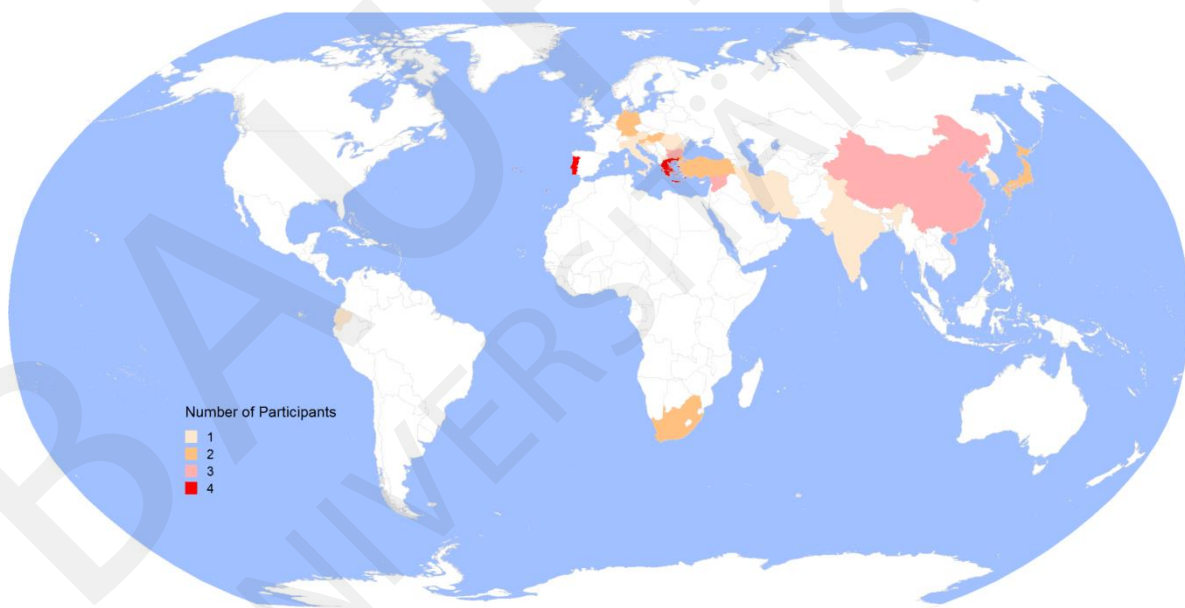
Participants

The course targets post-graduate students, i.e., second (M.Sc.) and third cycle (Ph.D.) from different institutions and countries to enable knowledge transfer between the participants. By providing students with advanced, scientifically-based interdisciplinary knowledge, skills and methods, they are trained to react to demanding engineering tasks in the areas of planning, construction and realization of structures under specific site, action and loading conditions.

In addition the soft skills of each participant (like team working and task sharing) will be trained in internationally composed project groups.

The Summer School has been supported by the EU Lifelong Learning Programme and "Strategic Partnerships and Thematic Networks". Students from our partner univeristies in China and Russia as well as from nearly all over the world attended the summer course, which leads to a very intercultural exchange of ideas, thinking and life styles (cf. Figure 1).

Its innovative character results from the ambitious engineering tasks and advanced modeling demands. Major course topics are derived from current research fields of the participating institutions at Bauhaus-Universität Weimar and involved European Project Partners. They are introduced by key lectures in civil engineering and condensed during the project related training of simulation and modeling techniques. The acquired knowledge is applied to scientific and practically relevant projects within a compact course. Such a "hands-on approach" is commonly not included in regular teaching programmes. Several targets harmonically overlap.

Figure 1. Home Countries of the Participants attending the Summer School "Forecast Engineering: Global Climate Change & Challenges for Built Environment" 2014.

Photo: Barbara Proschak

Course topics

The summer course is divided into two main parts: lectures and project work. This time sharing ensures theoretical and practical oriented work under holistic aspects and the use of modern analyses methods and tools for numerical simulation in structural and mechanical engineering. The young scientists get experience and modern scientific knowledge under realistic training settings.

The offered formats and forms of training can be summarized as follows:

- **Lectures:** The necessary theoretical basics, the current state of research (in project targeting fields) as well as special topics are presented by lecturers, leading scientists from the partner institution, and invited guest speakers (cf. Guest lecturers and invited speakers).

- **Project Work** (including presentation and submission of final results): This (for the participants mostly demanding) part of the course offers the possibility to work in interdisciplinary teams on different projects. The participants could choose between six offered projects dealing with advanced current engineering research topics:

  Project 1 | Implementation and Validation of Wireless Structural Health Monitoring Systems
  Project 2 | Image Analysis for Change Detection
  Project 3 | Evaluation of Existing Structures under Changed Extreme Impacts
  Project 4 | Special Aspects of Steel Structures
  Project 5 | Calibration of Engineering and Climate Models
 Project 6 | Wind-induced Vibrations of Long-span Bridges

The project work was conducted in small groups and intensively supervised. The outcome – presented by the herein compiled reports – reaches an impressive level of results and graphical elaboration (cf. Project Reports).

- **Presentation of the Participants** (workshop character): Participating students were requested to present their work in a special session and to defend their results in front of a broad scientific audience. Therefore each participant had to submit a short abstract together with his/her application. On the basis of these abstracts 15 titles were elected as presentation by the participants, which also shall honor the effort and work of the participant (cf. Papers Contributed by the Participants).

- **Excursion:** An excursion to just finalized construction sites emphasizes the practical relevance of the course topics and illustrates existing requests for real existing structures. Discussions with professionals provide the opportunity to link theoretical knowledge to practical experience.

So far and at the national level, no similar workshop to the International Summer School conducted by the Faculty of Civil Engineering at the Bauhaus-Universität Weimar is known. The relevance of the course topics is undisputable. Not at least the number of applicants indicates the existing demand for such an international and interdisciplinary oriented format of training and exchange between young scientists in structural and mechanical engineering.

Referring to recent European and International code developments, participants are invited to present national design practice and experience from applications, focussing on the efforts that contribute to new concepts, evaluation strategies and the quality assurance of structural models.

The Summer School combines theory and practice on the basis of advanced research and tool development. The modular structure of the programme allows the participants to address current and trendsetting problems and research topics.
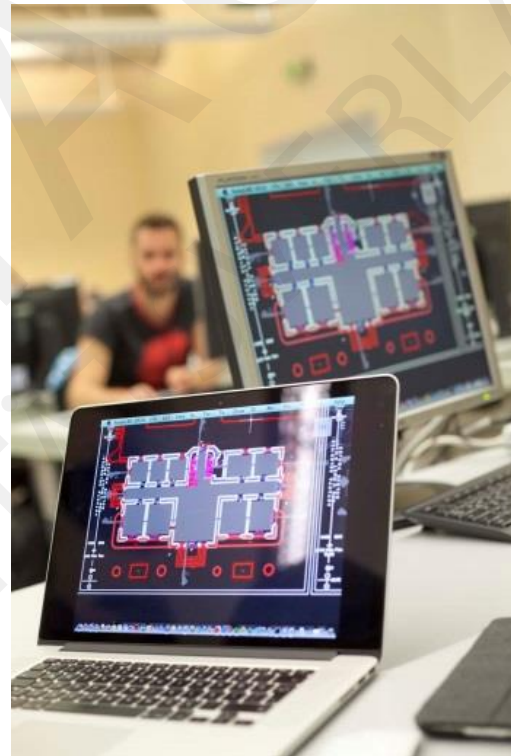
Photo: Barbara Proschak

Key aspects of the Summer School are linked to the Research Training Group 1462: Evaluation of Coupled Numerical and Experimental Partial Models in Structural Engineering – supported by the German Research Fondation DFG – which is involved within different projects.

7

Guest lecturers and invited speakers

In 2014 again internationally well-known and high-ranked scientist could be welcomed as guest speakers at the Engineering Summer Course at Bauhaus-Universität Weimar. The current state of research at the Project Partner's Universities as well as lecturers from other disciplines highlighted the future demands on Engineers to overcome future requirements on engineered structures.

- Buckling of steel plated structures | *Prof. Dr. L. Dunai (BME)*
- Improvements of the seismic response of existing structures using the high-performance plastics
  Prof. Dr. T. Isakovic (University of Ljubljana)
- Inelastic behavior of structures under earthquake loading: analysis, design and assessment
  Prof. Dr. A. Sextos (AUTH)
- Seismic collapse assessment | *Prof. Dr. Ch. Adam (University Innsbruck)*
- A Kalman filter based approach for the identification of structural systems
  Eleni Chatzi (ETH Zürich)
- Inelastic Seismic Analysis of Building Structures | *Dr. D. Dinev (UACEG)*
- Full-Scale Dynamic testing of a RC frame building by investigation the effect of brick-infilled frames | *Prof. M.C. Genes (Zirve University)*
- Bayesian Uncertainty Quantification and Propagation (UQ&P) in Structural Dynamics
  Prof. C. Papadimitriou (University of Thessaly)
- Topology optimization: basic concepts and robust design | *Dr. M. Schevenels (KU Leuven)*
- Fusing Big City Data with Civil Engineering Design Ideas
  Prof. T. Hartmann (University of Twente)
- Assessment of global change on hydrological systems - Methods and Applications
  Dr. M. Fink & Christian Fischer (Friedrich-Schiller-University Jena)
- Wind flow modelling and climate analyses | *Dr. M.P. Repetto (University of Genoa)*
- Damage Detection of Civil Engineering Structures by Analyzing the Changes of Dynamic and Static Characteristics | *Prof. S. Maas (Université du Luxembourg)*

Photo by:
Judith Rautenberg

Excursion

A special highlight of the Engineering Course at the Bauhaus Summer School is the annual excursion to current construction sites or already finished outstanding engineering projects in Thuringia. The participants became the once-only chance to visit modern bridge structures designed with different and sometimes unique super-structures not only from outside. The excursion was guided inside of the super-structures to highlight and impart knowledge about the special construction of engineering art in bridge design.

The excursion programm introduced bridges with:

Overall length:	280 to 845 m
Height over ground:	35 to 110 m

and including the highest arch bridge in Germany. All bridges are built as composite structures made of steel and concrete, whereas different techniques were applied (e.g. Pre-stressed concrete; external tendons steel).
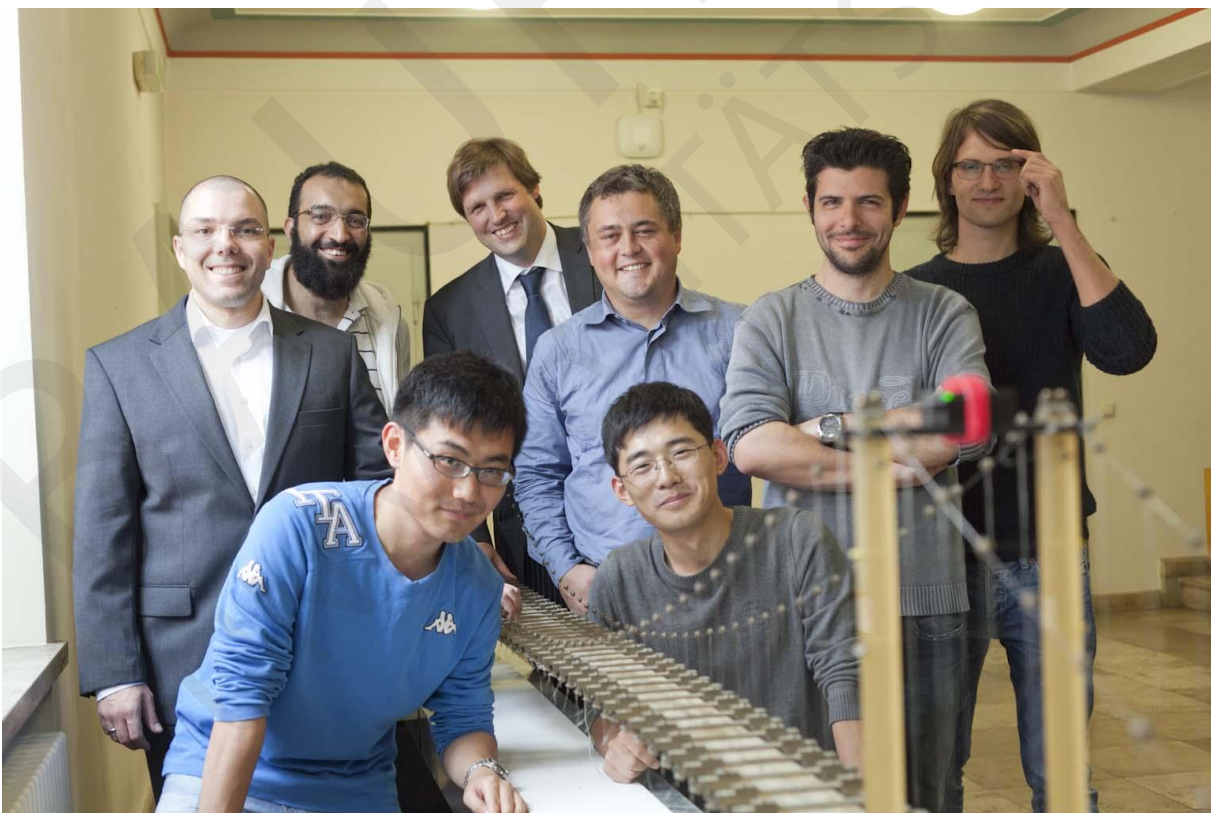

Photos by:
Judith Rautenberg

Federal Ministry of Education and Research

DAAD

Deutscher Akademischer Austausch Dienst German Academic Exchange Service

Lifelong Learning Programme

Project reports

Photos: Barbara Proschak

Implementation and validation of wireless structural health monitoring systems

DRAGOS Kosmas, THESSMANN Georg, FATHY Mohammad, WANG Shouqiang, LIANG Yufan

TAUSCHER Eike, SMARSLY Kay

Abstract. In recent years, the risks associated with structural deterioration of aging infrastructure have stimulated the development of structural health monitoring systems. While in conventional monitoring systems structures are instrumented using sensors connected to a central server through long coaxial cables, recent developments in the field of wireless technologies have led to the increasing adoption of wireless sensor networks for structural health monitoring. An important feature of wireless sensor networks is the combination of processing units and sensing modules within autonomous wireless sensor nodes. This paper summarises the results of a summer school project conducted at Bauhaus University Weimar, Germany, within the "Bauhaus Summer School 2014". In this project, an embedded computing approach for wireless structural health monitoring systems has been proposed. More specifically, an embedded computing algorithm has been implemented for transforming acceleration response data from the time domain into the frequency domain and for sending the transformed data to a central server. To validate the proposed approach, experimental tests have been performed on a laboratory model of an existing suspension bridge. In summary, the results of the experimental tests corroborate the applicability of the embedded computing approach for executing common monitoring tasks, such as system identification and condition assessment.

Introduction

Structural deterioration during the lifetime of structures might pose significant threats to public safety. In order to keep the safety levels of structures within acceptable limits, precise information on the condition of structures must be regularly obtained. To this end, the field of structural health monitoring (SHM) has been developed, facilitating condition assessment and damage detection on monitored structures. Conventional SHM systems employ wired sensors connected to a central server through long (and costly) coaxial cables. Owing to the significant merits of wireless sensor nodes in terms of cost and installation time, there has been a growing trend towards the use of wireless sensing technologies in SHM. Wireless sensor nodes are essentially integrated platforms able to autonomously execute several monitoring tasks. More specifically, both sensing modules and processing units are incorporated into wireless sensor nodes, while the use of radio transceivers for wireless communication eradicates the need for cabled connections. Furthermore, using embedded computing, the processing power present in wireless sensor node platforms can be exploited for data processing prior to wireless transmission. Drawbacks associated with the use of wireless sensor networks (WSNs) are the limited reliability of wireless communication and the power efficiency of the sensor nodes.

Several embedded computing approaches in wireless SHM systems have been proposed. Lynch et al. (2004) proposed embedded algorithms for damage detection based on autoregressive modelling with exogenous inputs (AR-ARX). Zimmerman et al. (2008) embedded system identification algorithms into wireless sensor nodes, while Cho et al. (2008) presented the wireless tension force estimation system for cable-stayed bridges. Lei et al. (2010) demonstrated the merits of incorporating data processing algorithms into the sensor nodes in terms of power reduction. Smarsly and Law (2014)

proposed a resource-efficient system using a migration-based approach, in which powerful software agents, automatically assembled in real time and migrating to the sensor nodes, analyse potential anomalies on demand.

In this paper, an embedded computing approach for wireless SHM systems is presented. First, a brief introduction to condition assessment techniques and SHM systems is given. Second, the theoretical background of the algorithms of the embedded computing approach is described. Finally, the implementation and experimental testing of the proposed approach is presented.

Condition assessment methods and systems

According to standard practice, there are three main categories of condition assessment techniques (Paik and Melchers, 2014):

- Visual inspection
- Non-destructive testing
- Destructive testing

Visual inspection is the most common technique for assessing the condition of structures. However, as can be seen in Figure 1, the equipment and specialised personnel required have rendered visual inspection particularly costly and labour intensive. Although reliable, visual inspection can only serve as an empirical condition assessment technique, but no prediction of actual structural performance can be made based on the outcome of this technique.

Destructive testing (DT) techniques, essentially, are associated with obtaining samples from structures. Depending on the type of the structure, the type of material and the objective of the test, the extracted sample can be of different size or shape, and it can be obtained from different parts of the structure. For instance, as shown in Figure 2, in concrete structures DT is usually performed by core sampling of cylindrical concrete specimens for estimating the material properties. However, in composite structures, such as masonry, larger specimens are needed since the structural performance depends on the arrangement of joints, the bonding stresses, and the material strength of individual components. While DT provides useful results about the actual properties of the extracted specimens, DT techniques are particularly expensive and labour intensive. Moreover, since DT affects the integrity of structures, the applicability of DT techniques is very limited, while the accuracy of the results is related to (and limited by) the number of specimens.

Figure 1. Visual inspection examples: Bridge, tower, wind turbine, pipeline, off-shore platform
Sources: Iowa State University, D&K Commincations, Inc., Technical Rigging Services NZ Ltd, Horizon Specialist Contracting Limited, Axiom NDT Ltd., Bachmann Entsorgungsfachbetrieb, geo OHG

Figure 2. Destructive testing (core sampling)
Source: http://www.testconsult.co.uk/itemdetail.aspx?id=43&dept=structural-investigation

Non-destructive testing (NDT) techniques encompass the estimation of structural properties by conducting tests directly on the structure. The performance of NDT is, by definition, not harmful to the integrity of the structure. Conventional non-destructive tests include Schmidt hammer testing, nail pull off testing, ultrasound testing, steel hardness testing, shaker testing (Figure 3), etc. The purpose of the tests is to estimate structural properties, such as the elastic moduli and strengths of materials, the size and positioning of reinforcement bars, etc. Furthermore, NDT can be used for damage detection by identifying cracks and voids.

Most of the tests described above provide useful information at a local level; however, to obtain adequate estimates regarding the global state of the structure, different strategies must be employed. Therefore, SHM techniques are applied based on the instrumentation of structures with sensors and the collection of response data. Common SHM techniques include, e.g. vibration-based system identification, operational modal analysis, auto-regressive models for damage detection. Depending on the type of instrumentation, SHM systems can be wired or wireless. In the following subsections, a brief description of wired and wireless SHM systems is given.

Figure 3. Shaker used for non-destructive testing
Source: http://www.measurement-testing.com/vibration-testing-2.html
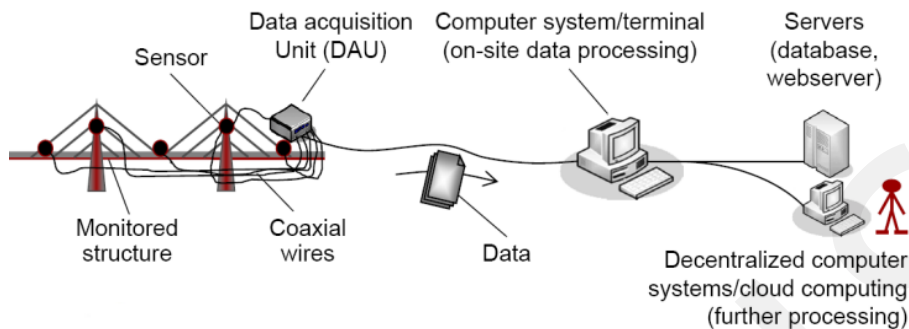
Figure 4. Schematic of a wired SHM system architecture

Wired structural health monitoring systems

Wired systems have been employed in early SHM approaches. In wired SHM systems the instrumentation is performed by means of wired sensors connected to a central server through long coaxial cables. The sensors are tasked to collect response data, which is transferred to the server for further processing. Data processing is performed either in real time or at specified intervals in order to assess the condition of the structure. From the architecture of wired SHM systems, shown in Figure 4, structural response data is collected by central data acquisition units for further processing; hence, condition assessment in wired systems is performed in a centralized manner.

Wired SHM systems have been applied in a broad field of SHM applications. Cable-based connections offer a reliable link between the sensors and the central server, effectively preventing data loss and synchronization errors. Wired systems have been proven efficient solutions for academic tests or small-scale field tests, as shown in Figure 5 (Dragos et al., 2014; Manolis et al., 2014). Furthermore, in full-scale field deployments, wired systems have been proven an attractive means facilitating a variety of engineering tasks, such as life-cycle management of structures (Smarsly et al., 2012). On the other hand, in full-scale SHM systems it has been reported that the cost of a wired system per sensing channel could reach the amount of $5,000 (Celebi, 2002). Thus, in an attempt to address the shortcomings of wired SHM systems in terms of efficiency, the research attention of the civil engineering community has been focused on alternatives, such as wireless sensor networks.


Figure 5. Wired data acquisition system applied on a small-scale academic instrumentation of a pedestrian bridge in Thessaloniki, Greece (Manolis et al., 2014)

Wireless structural health monitoring systems

Recent advances in wireless technologies have led to the introduction of wireless sensor networks to structural health monitoring. The use of wireless sensor nodes for SHM has been drawing increasing research interest, owing to the significant merits of wireless sensor nodes with respect to reduced cost and installation time. Typical wireless SHM architectures comprise wireless sensor nodes, installed on the monitored structure, communicating with each other and with a central server via wireless communication links (Figure 6). As mentioned earlier, wireless sensor nodes are basically integrated platforms combining processing units with sensing modules, facilitating the on-board processing of collected data prior to wireless transmission. However, there are some significant drawbacks associated with the use of wireless sensor nodes. The reliability of data transmission could be compromised due to wireless communication, while in long-term monitoring systems power efficiency is also a significant constraint.

In recent years, several approaches of wireless sensor networks have been proposed for SHM (Lynch and Loh, 2006). Most approaches focus on enhancing the ability of wireless sensor nodes, already at a "smart" level, to automatically execute various monitoring tasks on-board the sensor nodes. For that purpose, several embedded algorithms have been proposed covering a broad variety of SHM applications (Dragos and Smarsly, 2015). As discussed above, power efficiency is a substantial drawback in wireless sensor networks, and wireless communication has been proven one of the most power-consuming features of the sensor nodes. Consequently, most proposed embedded algorithms encompass data processing and data interrogation tasks in an attempt to reduce the size of the data to be wirelessly communicated. More sophisticated approaches are related to system identification, damage detection, fault detection, and structural control.

The hardware platform of a typical wireless sensor node consists of three basic components, the sensing/actuating module, the processing unit, and the communication unit, as shown in Figure 7. The sensing module, which might also include actuators, is responsible for collecting the data required to perform monitoring tasks. According to the type of monitoring task, the collected data could be accelerations, velocities, displacements, strains, temperatures, etc. The collected data is usually in the form of an analogue signal (typically voltage), which is digitised through an analogue-to-digital (ADC) converter. The processing unit, consisting of a microcontroller and memory modules, handles the storage and processing of collected data. The communication unit comprises the wireless transceiver.
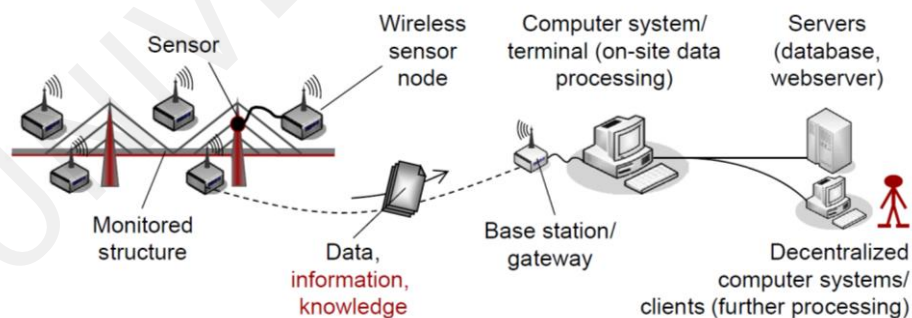
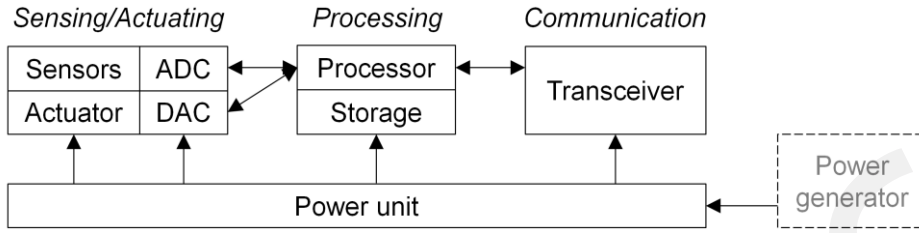**Figure 6.** Schematic of a wireless SHM system architecture

Figure 7. Schematic of the components of a typical wireless sensor node

An embedded computing approach for wireless SHM systems

As mentioned previously, embedded computing is an important aspect of wireless sensor networks. The embedment of powerful algorithms into wireless sensor nodes can reduce the size of the data to be wirelessly communicated leading to reduced power demands. In this section, an embedded computing approach for wireless SHM systems is presented. First, the mathematical background of the proposed approach is given. Second, the implementation of the approach in a wireless sensor network is described and, finally, the proposed approach is applied in laboratory experiments.

Mathematical background

The background of the embedded computing approach is related to structural dynamics and system identification through data processing. More specifically, the data, collected as time series, is processed on-board and information on the dynamic response of the structure is obtained. The aspects of structural dynamics and data processing are described in the following subsections.

Structural dynamics

The field of structural dynamics deals with the description of structural response under time-varying loading conditions. Contrary to static problems where structural response is estimated by only using elastic forces, in structural dynamics the effects of inertial forces and damping forces on structural response are non-negligible. Considering a structural system of mass M, damping C, and stiffness K, the equation of dynamic equilibrium is expressed as follows.

$$M \cdot \ddot{u}(t) + C \cdot \dot{u}(t) + K \cdot u(t) = F(t) \tag{1}$$

In Eq. 1, $\ddot{u}(t)$ is the acceleration of the system, $\dot{u}(t)$ is the velocity and $u(t)$ is the displacement, while $F(t)$ is the external force acting on the system. Due to the complexity of physical models, even of simple structures, it is impossible to formulate Eq. 1 in a straightforward way. Instead, it is useful to use discrete models, where mass, damping and stiffness are lumped into a finite number of points of the structural model ("finite element modelling"), termed "degrees of freedom" (DOFs) (Chopra, 2012). Hence, assuming a system of N DOFs, Eq. 1 is converted to:

$$\mathbf{M}_{N \times N} \cdot \{\ddot{u}_N\} + \mathbf{C}_{N \times N} \cdot \{\dot{u}_N\} + \mathbf{K}_{N \times N} \cdot \{u_N\} = \{f_N\} \tag{2}$$

where **M**, **C**, and **K** are the mass matrix, the damping matrix and the stiffness matrix, respectively, and $\{\ddot{u}_N\}$, $\{\dot{u}_N\}$, and $\{u_N\}$ are the acceleration vector, the velocity vector and the displacement vector, respectively, while $\{f_N\}$ is the force vector. It should be noted that Eq. 2 also describes a time-variant system; the variable of time has been suppressed for illustration purposes. A common tool used to analyse Eq. 2 is modal analysis, which provides information about the structural behaviour under vibration in terms of natural frequencies and mode shapes, according to the number of DOFs considered. Usual assumptions in modal analysis include considering "free vibration", i.e. no external force, and neglecting damping phenomena. Further, since the time variation is assumed to be equal for all DOFs, the displacement vector is analysed to a product of a time function $p(t)$ and a response vector $\{\phi\}$, as shown in Eq. 3.

$$\{u_N\} = \{\phi\} \cdot p(t) \Leftrightarrow \{\ddot{u}_N\} = \{\phi\} \cdot \ddot{p}(t) \tag{3}$$

Taking all the aforementioned assumptions into consideration and using Eq. 3, Eq. 2 is converted to:

$$\mathbf{M}_{N \times N} \cdot \{\phi_N\} \cdot \ddot{p}(t) + \mathbf{K}_{N \times N} \cdot \{\phi_N\} \cdot p(t) = 0 \tag{4}$$

Eq. 5 is obtained by rearranging the terms of Eq. 4.

$$\left[\mathbf{M}_{N \times N} \cdot \{\phi_N\} \right]^{-1} \cdot \mathbf{K}_{N \times N} \cdot \{\phi_N\} = -\frac{\ddot{p}(t)}{p(t)} = \lambda \tag{5}$$

where λ is a scalar that expresses the equivalency of the two fractions shown in Eq. 5, which can be re-written as:

$$\mathbf{M}_{N \times N}^{-1} \cdot \mathbf{K}_{N \times N} \cdot \{\phi_N\} = \lambda \cdot \{\phi_N\} \tag{6}$$

It is clear that Eq. 6 describes a quadratic eigenvalue problem. The scalar eigenvalues λ are the estimates of the squares of the natural frequencies ω of the structure. Moreover, the eigenvectors $\{\phi_N\}$, obtained by the solution of Eq. 6, are estimates of the mode shapes of the structure.

It is common in structural analysis to express the dynamic behaviour of structures in terms of natural frequencies and mode shapes. Consequently, experimental methods related to system identification focus on obtaining modal information by applying data processing techniques, such as the fast Fourier transform (FFT), to collected data.

The fast Fourier transform

The basic concept of Fourier analysis is to analyse any function of time into a sum of harmonic sinusoidal functions of different frequency ω and amplitude. Considering a continuous function of time $f(t)$, the Fourier transform is obtained from Eq. 7.

$$F(\omega) = \int_{-\infty}^{\infty} f(t)^{-2\pi i \omega t} dt \tag{7}$$

As explained earlier, in SHM systems, the sensing modules use ADC units to convert analogue signals to digital in a process termed "digitisation". Since converted signals are essentially discrete time series of length N, it is not possible to use the Fourier transform of Eq. 7. Instead, the discrete Fourier transform (DFT) is applied, calculating the amplitude F_k at each frequency expressed as k cycles per N data, as shown in Eq. 8.

$$F_k = \sum_{n=0}^{N-1} f_n \cdot e^{-2\pi i k \cdot \frac{n}{N}} \qquad k \in [0, N) \qquad N \in \mathbf{Z} \qquad \omega = k/N \tag{8}$$

From Eq. 8, it is evident that computing the DFT algorithm requires a total of $O(N^2)$ calculations, given that the equation produces N outputs of F_k and each output is obtained as a sum of N terms. In an attempt to reduce the computational cost of the DFT, several researchers proposed the use of "fast Fourier transform" (FFT) algorithms, where the number of calculations is reduced drastically to $O(N \cdot \log N)$. The most common FFT algorithm is the Cooley-Tukey algorithm, where the DFT algorithm of an arbitrary size is broken recursively into smaller DFT algorithms (Cooley and Tukey, 1965). The most common form of the Cooley-Tukey algorithm is the radix-2 decimation-in-time, where a DFT of size N is broken into two DFTs of size $N/2$ at each recursive stage. More specifically, using Eq. 8:

$$F_k = \sum_{n=0}^{N/2-1} f_n \cdot e^{-2\pi i k \cdot \frac{n}{N}} + \sum_{n=0}^{N/2-1} f_{n+1} \cdot e^{-2\pi i k \cdot \frac{n+1}{N}} = \sum_{n=0}^{N/2-1} f_n \cdot e^{-2\pi i k \cdot \frac{n}{N}} + e^{-\frac{2\pi i k}{N}} \cdot \sum_{n=0}^{N/2-1} f_{n+1} \cdot e^{-2\pi i k \cdot \frac{n}{N}} \tag{9}$$

Using the identity $e^{2\pi i n} = 1$ ($n \in \mathbf{Z}$), the symmetry property of the DFT is given in Eq. 10.

$$F_{N+k} = \sum_{n=0}^{N-1} f_n \cdot e^{-2\pi i (N+k) \cdot \frac{n}{N}} = \sum_{n=0}^{N-1} f_n \cdot e^{-2\pi i k \cdot \frac{n}{N}} \cdot e^{-2\pi i n} = \sum_{n=0}^{N-1} f_n \cdot e^{-2\pi i k \cdot \frac{n}{N}} \tag{10}$$

As a result from Eq. 9 and Eq. 10, the total number of calculations for the assumed division is $O(M^2)$, with $M = N/2$. Following the same concept, further recursive decimation is possible, eventually reducing the number of calculations to $O(N \cdot \log N)$.

Implementation

This section covers the implementation of the embedded computing approach, proposed in this study, in a wireless SHM system. Because the procedure presented in the previous section needs to be implemented into a wireless SHM system, embedded software enabling the sensor nodes to execute the calculations on-board needs to be written. In the following subsections, a description of the sensor node platform is given, and the embedded software designed is presented.

### *Wireless sensor node platform*

The wireless sensor nodes used in this study are the Oracle SunSPOTs (Small Programmable Object Technology) (Oracle Corp., 2007), shown in Figure 8. The hardware platform has been proven particularly reliable for rapid prototyping in a broad range of applications including structural health monitoring (Smarsly, 2014; Chowdhury et al., 2014). The sensor node platform features a powerful ARM 920T microcontroller with a 32-bit bus size running at 400 MHz. The flash memory used for storing application data is 4 MB, while the available volatile memory (RAM) is 512 kB. The operating system used is the Java Squawk Virtual Machine (Shaylor et al., 2003). As for the sensor board, an MMA7455L microelectromechanical system (MEMS) accelerometer is integrated into the sensor node platform, providing the user with three options with respect to the measurement range: ±2g, ±6g, or ±8g. According to the selected range, the resolution differs being 8-bit for ranges ±2g and ±6g, and 10-bit for ±8g. The maximum sampling rate of the accelerometer is 125 Hz. In addition, the sensor board of the node includes one light sensor and one temperature sensor.

Figure 8. The Oracle SunSPOT node

Embedded software

The design of the embedded software aims at executing the algorithms described previously on-board the wireless sensor nodes. To this end, two applications are developed; a "host application" that handles the tasks of the server and an "on-board application" that handles the tasks of each sensor node. An overview of the software design is shown in Figure 9.
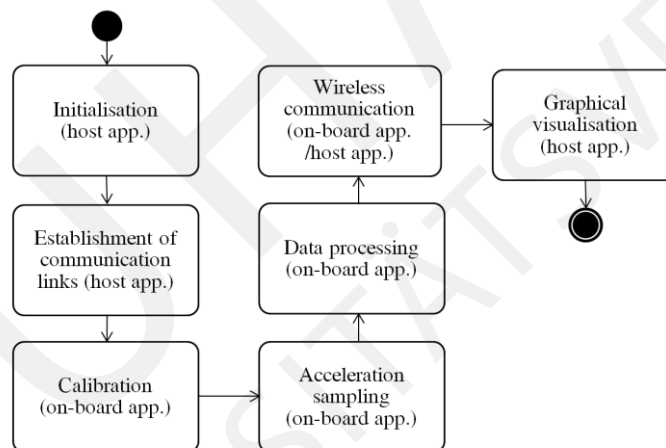
Figure 9. Overview of the designed software

The initialisation of the system is handled by the host application running on the server. The server is interfaced with the sensor nodes using another node designated as "base station". The base station is equipped with a radio transceiver, which is used by the host application to establish the communication links between the server and the sensor nodes. The next stage involves the calibration of the sensor nodes handled by the on-board application. More specifically, prior to excitation, the accelerometers are tasked to collect acceleration response data for a predefined time interval and to calculate the average acceleration value considered to represent the ambient noise, which is subtracted by the collected acceleration response data. The acceleration sampling stage starts once the acceleration exceeds a predefined threshold. If the acceleration drops under the predefined threshold, sampling stops and the collected acceleration response data is stored on-board the sensor nodes for further processing. Data processing involves transforming the collected acceleration response data into the frequency domain by applying the FFT algorithm. The processed data is then communicated via the wireless communication links to the base station and, subsequently, to the server. On the server,

the processed data received by the host application is plotted to obtain a graphical representation of the frequency spectrum of the structural response and to identify the peaks that correspond to the modes of vibration.

Experimental tests

The embedded computing approach proposed in this study is validated in experimental tests on a laboratory structure. The software described in the previous section is embedded into a wireless SHM system installed on a laboratory model of an existing suspension bridge. This section showcases the experimental tests of the proposed approach. First, a general description of the suspension bridge, modelled in the laboratory, is given. Second, the testing procedure is presented and, finally, the results of the tests are discussed.

The New Little Belt Bridge

The New Little Belt Bridge is a 1,700 m long suspension bridge located in Denmark between Jutland and Funen (Figure 10). The bridge was built in the 1970s in an attempt to relieve the congested Old Little Belt Bridge, which had been in service since 1935. The central and longest span of the bridge is 600 m long and is connected through two 240 m long side spans, one on each side, to the 31 m long concrete approach spans (COWI Group, 2015). The pylons have a height of 121 m and rest on piers shaped by caissons of 56×22 m dimensions. The deck girder has a depth of 3 m and a total width of 33 m. The vertical suspension cables are spaced at 12 m intervals, while the two 1,500 m long main suspension cables are made of 61 prefabricated strands. A detailed laboratory model, shown in Figure 11, has been built to represent the structural behaviour of the bridge to the best possible degree.

Figure 10. The New Little Belt Bridge in Denmark
Source: https://en.wikipedia.org/wiki/Little_Belt_Bridge_(1970)

**Figure 11.** Laboratory model of the New Little Belt Bridge
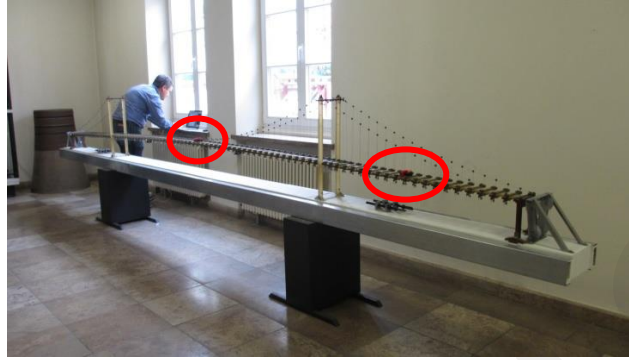
Figure 12. Experimental setup

Laboratory tests

The purpose of the laboratory tests is to collect acceleration response data of the structure, to perform automated on-board data processing and to communicate the processed data to the server. Given that the example presented in this study is a small-scale test of the proposed embedded computing approach, the use of two wireless sensor nodes for the instrumentation of the bridge model is considered adequate. By comparing the frequency spectra obtained by the two sensor nodes, an initial overview of the relation of spectral peaks to modes of vibration can be obtained.

The selection of the sensor node location follows the concept of modal analysis. One sensor node is placed at the middle of the central span (node 1), and the other sensor node is placed at the middle of one of the side spans (node 2), as shown in Figure 12. The basic idea of the experimental setup is to collect acceleration response data from the points with the highest amplitudes for the dominant modes of vibration. For the purposes of this study, one experimental setup is considered sufficient. Two tests are performed, test 1 exciting the structure in the vertical (z-axis) direction, and test 2 exciting the structure in the lateral/transversal (y-axis) direction with respect to the deck's longitudinal axis. The sampling rate for both tests is 25 Hz.

Acceleration response data from each excitation is collected and processed on-board the wireless sensor nodes, and the respective frequency spectrum data is wirelessly transmitted to the server for graphic visualisation. The frequency spectra of both tests are illustrated in Figure 13 and Figure 14.
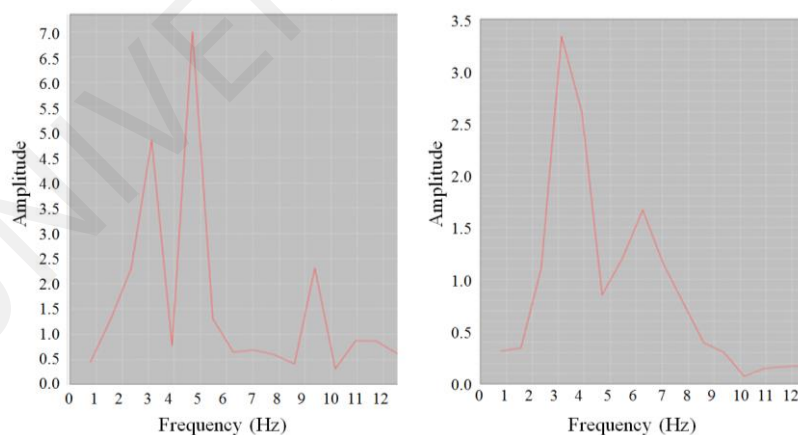
Figure 13. Frequency spectra of node 1 (left) and node 2 (right) from test 1
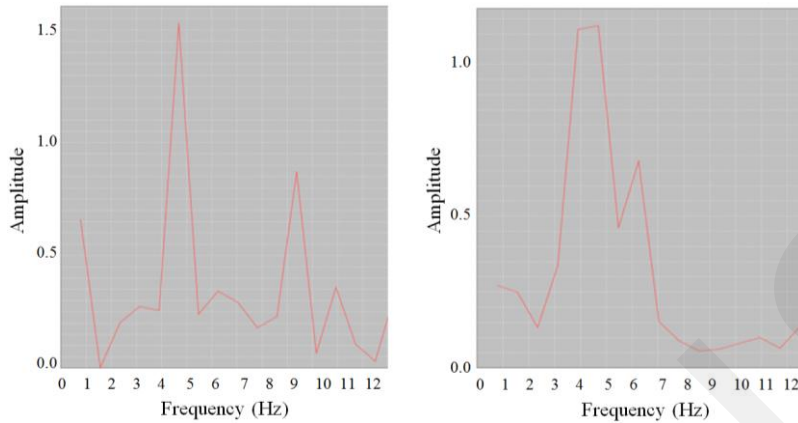
Figure 14. Frequency spectra of node 1 (left) and node 2 (right) from test 2

As can be seen from the results of test 1 (Figure 13), the first peak of the frequency spectra of both sensor nodes is identified at $f_{1,z} = 3.10$ Hz, which is concluded to be the fundamental Eigen frequency along z-axis. Although there is a second peak in both frequency spectra, it does not correspond to the same frequency and is therefore not considered the second modal peak. Considering that the second mode of vibration in multi-span beam structures usually has an antisymmetric half-sinusoidal shape with nodal (zero-amplitude) points at the middle of the spans, identification of the second modal peak is not likely with the current setup. Moreover, the highest detectable modal peak is restricted by the selection of the sampling rate; the highest frequency of the spectrum, also termed "Nyquist" frequency, is half of the sampling rate ($f_{max} = 12.5$ Hz). The results of test 2 (Figure 14) are quite similar to the results of test 1 with respect to peak detection. The first mode of vibration is identified at a frequency of $f_{1,y} = 4.80$ Hz, while no other modal peaks are identified. It is worth mentioning that there is an additional peak at the frequency spectrum of node 1 in test 1 at the same frequency as $f_{1,y}$. This result could be indicative of coupling between one lateral and one vertical component for this mode of vibration.

Summary and conclusions

System identification and condition assessment of structures is of utmost importance for maintaining the integrity of ageing infrastructure and for mitigating potential risks posed to public safety. To this end, structural health monitoring has been introduced aiming at successfully detecting adverse changes in the condition of structures that could indicate damage. In the field of structural health monitoring, wireless sensor networks have been drawing increasing research attention, as an alternative to conventional wired systems, which have been proven particularly costly and labour intensive. Wireless sensor nodes are autonomous platforms where sensing modules are collocated with processing units. The exploitation of the processing power of wireless sensor nodes has been demonstrated in various research efforts in the form of embedded algorithms used to execute monitoring tasks on-board the sensor nodes.

In this study, an embedded computing approach for wireless SHM systems has been presented. More specifically, an embedded algorithm has been proposed for transforming collected acceleration response data from the time domain into the frequency domain using the fast Fourier transform. The proposed approach has been implemented into a wireless SHM system, and embedded software has

been written using the Java programming language. The proposed approach has been validated in experimental tests on a laboratory model of an existing suspension bridge. Two tests have been conducted; in the first test, the bridge model has been excited in the vertical direction and in the second test, it has been excited in the lateral (transverse) direction. Collected acceleration response data has been transformed into the frequency domain using the fast Fourier transform, and the processed data has been sent to the server for graphic visualisation. The results have shown that the peaks of the calculated frequency spectra correspond to the dominant modes of vibration and can be used for system identification and condition assessment.

Further extension of the embedded computing approach will encompass the design of more sophisticated algorithms to enable the execution of system identification tasks of increasing complexity. More specifically, the embedment of algorithms that handle peak-picking on the extracted frequency spectra, frequency domain decomposition, or stochastic subspace identification could be investigated as an attempt to facilitate the decentralised system identification and condition assessment of monitored structures.

Acknowledgments

References

Celebi, M. (2002). Seismic instrumentation of buildings (with emphasis on federal buildings). *Technical report No. 0-7460-68170*. United States Geological Survey, Menlo Park, CA, USA.

Cho, S., Yun, C. B., Lynch, J. P., Zimmerman, A., Spencer Jr., B. and Nagayama, T. (2008). Smart wireless sensor technology for structural health monitoring. *Steel Structures* **8** (4): 267-275.

Chopra, A. K. (2012). *Dynamics of Structures: Theory and Applications to Earthquake Engineering*: *4th Edition*. Prentice Hall, Englewood Cliffs, NJ, USA, 2012.

Chowdhury, S., Olney, P., Deeb, M., Zabel, V. and Smarsly, K. (2014). Quality assessment of dynamic response measurements using wireless sensor networks. In: *Proc. of the 7th European Workshop on Structural Health Monitoring (EWSHM)*; Nantes, France, 08/07/2014.

Cooley, J. W. and Tukey, J. W. (1965). An algorithm for the machine calculation of complex Fourier series. *Mathematics of Computation* **19** (90):297-301.

COWI group A/S (2015). Operation and maintenance of the New Little Belt Bridge. *Technical Report No. 0233-1704-029e-00a*. Kongens, Lyngby, Denmark.

Dragos, K., Meixedo, A., Bonifácio, C., Sassani, A., Kamezi, A., Schommer, S., Makisha, N., Deeb, M. and Zabel, V. (2014). System identification model updating and simulation. In: Abrahamczyk, L., Schwarz, J. (eds), *Model Validation and Simulation-Vol. II*; Weimar, Germany, 04/08/2013. Paper No. 1, 23 pp. Bauhaus University Weimar, Faculty of Civil Engineering, Institute of Structural Engineering, 2014.

Dragos, K. and Smarsly, K. (2015). A comparative review of wireless sensor nodes for structural health monitoring. In: *Proc. of the 7th International Conference on Structural Health Monitoring of Intelligent Infrastructure*; Turin, Italy, 01/07/2015 (accepted).

Lei, Y., Shen, W. A., Song, Y. and Wang, Y. (2010). Intelligent wireless sensors with application to the identification of structural modal parameters and steel cable forces: from the lab to the field. *Advances in Civil Engineering* **2010:** 1-10.

Lynch, J. P. and Loh, K. (2006). A summary review of wireless sensors and sensor networks for structural health monitoring. *The Shock and Vibration Digest* **38** (2): 91-128.

Lynch, J. P., Sundararajan, A., Law, K. H., Sohn, H. and Farrar, C. R. (2004). Design of a wireless active sensing unit for structural health monitoring. In: *Proc. of SPIE's 11th Annual International Symposium on Smart Structures and Materials*; San Diego, CA, USA, 14/03/2004.

Manolis, G. D., Athanatopoulou, A., Dragos, K., Arabatzis, A., Lavdas, A. and Karakostas C. (2014). Identification of pedestrian bridge dynamic response through field measurements and numerical modelling: case studies. *BAS Journal of Theoretical and Applied Mechanics* **44** (2): 3-24.

Oracle Corporation (2007). *Sun Small Programmable Object Technology datasheet*. Redwood Shores, CA, USA, 2007.

Paik, J. K. and Melchers, R. E. (2014). *Condition assessment of aged structures*. Elsevier Publishing B. V., Amsterdam, Netherlands, 2014.

Shaylor, N., Simon, D. N. and Bush, W. R. (2003). A Java virtual machine architecture for very small devices. In: *Proc. of the 2003 Conference on Languages, Compilers, and Tools for Embedded Systems (LCTES 03)*; San Diego, CA, USA, 11/07/2003.

Smarsly, K. (2014). Fault diagnosis of wireless structural health monitoring systems based on online learning neural approximators. In: *Proc. of the International Scientific Conference of the Moscow State University of Civil Engineering (MGSU)*; Moscow, Russia, 12/11/2014.

Smarsly, K. and Law, K. H. (2013). A migration-based approach towards resource-efficient wireless structural health monitoring. *Advanced Engineering Informatics* **27** (4): 625-635.

Smarsly, K., Law, K. H. and Hartmann, D. (2012). Towards Life-Cycle Management of Wind Turbines based on Structural Health Monitoring. In: *Proc. of the First International Conference on Performance-Based Life-Cycle Structural Engineering*; Hong Kong, China, 12/05/2012.

Zimmerman, A., Shiraishi, M., Schwartz, A. and Lynch, J. P. (2008). Automated modal parameter estimation by parallel processing within wireless monitoring systems. *ASCE Journal of Infrastructure Systems* **14** (1): 102-113.

Evaluation of existing masonry structure under multiple extreme impacts

BOUGATSAS Konstantinos, COLAÇO Aires, FURTADO André, GARCIA Hernan, GIOTIS Georgios, MIKEC Janez, MUKHERJEE Avisek, PAP Zsuzsa, SANTOS Ricardo, TRILLER Petra, PSYRRAS Nikolaos, ZIAKAS Rafail, SHETTY Naveen

ABRAHAMCZYK Lars, SCHWARZ Jochen, GENES M. Cemal

Abstract. It is well known that masonry buildings are complex to study and analyze, especially when they are subjected to intensive loading. The current study attempts to determine the capacity of these types of buildings for the seismic action. This is achieved by the inspection of the response of a two – storey masonry building located at a high seismicity area under the impact of earthquake loading. Initially, the dynamic response of the building is determined through ambient vibration measurements. The building is modeled by using the equivalent frame method and its inelastic behaviour is taken into account in determining and assigning the different types of non-linear hinges to each element.

Introduction

The aim of this project is the performance evaluation of an existing unreinforced masonry building under multiple extreme earthquake impacts. Since there were no damaging accelerograms available for a full-scale non-linear time history analysis, it was decided that a standard pushover analysis to be performed both for the primary seismic event and the aftershock event.

The present work is divided into five main tasks that includes:
1. manipulation of obtained structural response data of the undamaged building in order to derive the first Eigen modes;
2. generation and calibration of a 3D analytical model of the building using the commercially available software SAP2000, according to the provided plans and vibration tests;
3. assessment of a set of available existing mathematical expressions for the definition of plastic hinges on the basis of experimental tests on masonry wall and the adoption of the most suitable one for the model;
4. damage prediction for consecutive seismic actions through the estimation of the capacity of the building;
5. conduction of a small scale testing.

The building selected for this study is located in an area of high seismic risk – Antakya, Turkey. It is a 2 – storey governmental building with a rectangular ground plan and regular openings (Figure 1). The principal dimensions of the building in plan are 26.3 m x 14.5 m and the total height of the building is 12 m; with a storey height of approximately 5 m [Abrahamczyk *et al.,* 2012].

As far as the material is concerned, the exterior walls are constructed with concrete masonry units; the interior walls are constructed with different types of masonry units: bricks, hollow – bricks, concrete blocks and stone masonry. The thickness of the interior walls varies from 10 cm to 60 cm, while the thickness of the exterior walls varies from 50 cm to 55 cm. Moreover, all the slabs are constructed with reinforced concrete and their thickness is 12 cm (Figure 2).
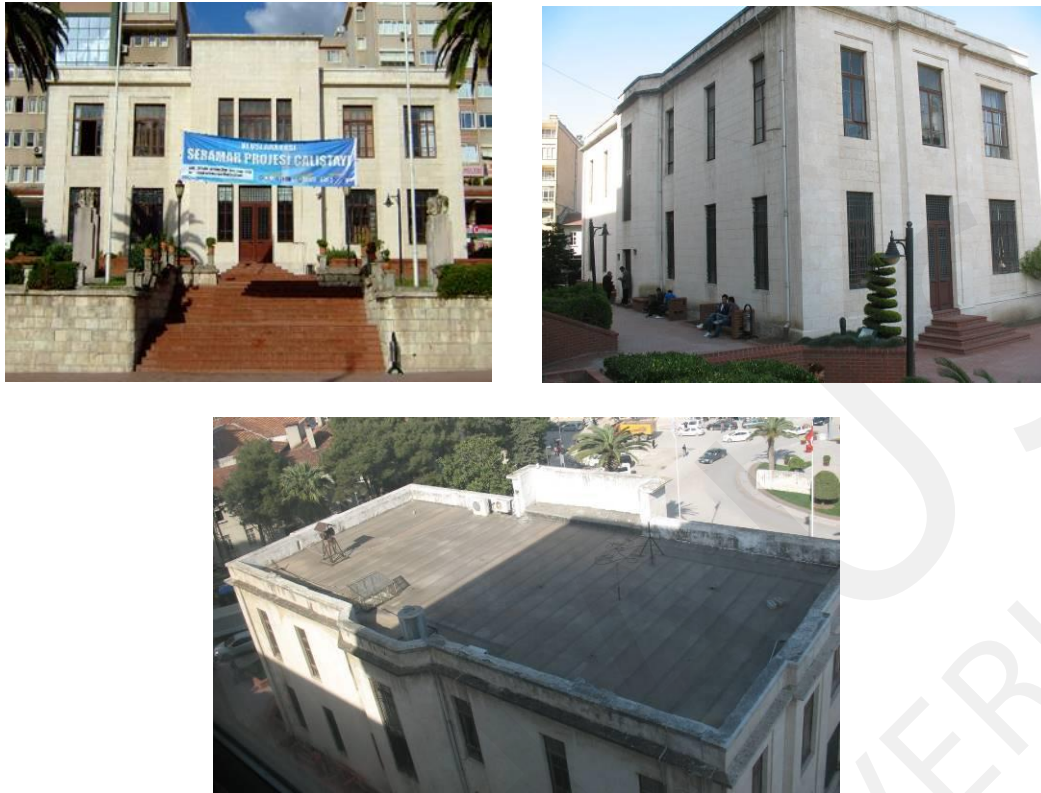
Figure 1. Different perspectives of the study building [Genes *et al.,* 2012].

In order to assess the seismic performance of masonry buildings, the geometry of the plan and elevation are also an important issue that has to be investigated [Erberik *et al.,* 2013]. The regularity and symmetry in plan and elevation with the placement of regular openings in this respective building (see Figure 1 & 2) indicate that it has good seismic resistance capacity and leads to the less damage mechanism.

However, in order to determine the dynamic behaviour, i.e. the fundamental frequencies and mode shapes of the building under an ambient excitation, it was instrumented by 4 tri – axial strong – motion recorders (Figure 3). The instrumentation scheme for this particular study building is followed by the scheme from the previous instrumentation of RC buildings in Antakya [Abrahamczyk *et al.,* 2008]. But there were some limitations regarding the space around the building, hence it was unsuccessful to install the free field station. Therefore, one sensor was installed on the second floor in a vertical line with the other sensors from the ground floor to the roof [Abrahamczyk *et al.,* 2012].
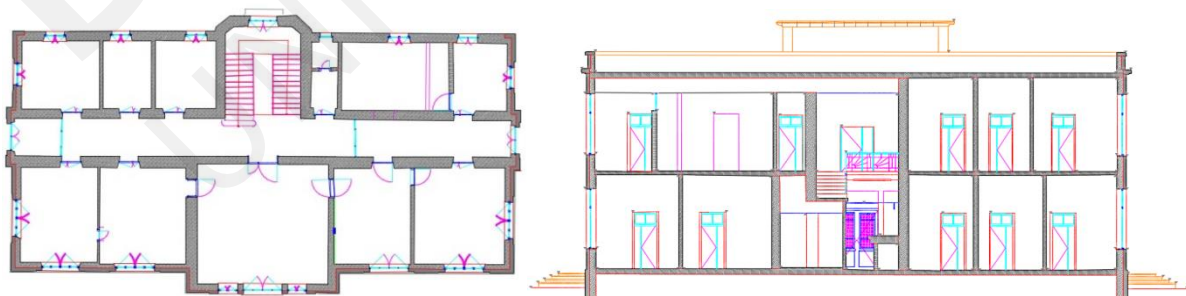
Figure 2. Principal dimensions (exterior and interior) of the study building [Genes *et al.,* 2012].

Figure 3. The 4 tri-axial strong-motion recorders used in the building [Genes *et al.,* 2012].

Modeling

For modeling this particular unreinforced masonry building, the equivalent frame method (EFM) has been used, because it has found to be an effective and reasonably accurate way for conducting non-linear analysis, which yields more realistic results [Belmouden *et al.,* 2009; Lagomarsino *et al.,* 2013]. The piers, spandrels and rigid zones are assigned in EFM according to the following rules:

- The piers and spandrels are represented by a frame element which are placed at the middle of each wall. These frame elements are subdivided into deformable elements and rigid offsets.
- For external piers, the rigid offsets are considered from the 30° inclination rule [Dolce, 1989].
- For internal piers, it is mainly dependent on the geometry of the openings. If the edge of the openings is at the same uniform level, then the length of the rigid offset is up to the uniform level. If the edge of the openings are at the different level, then it is the same procedure as external piers.
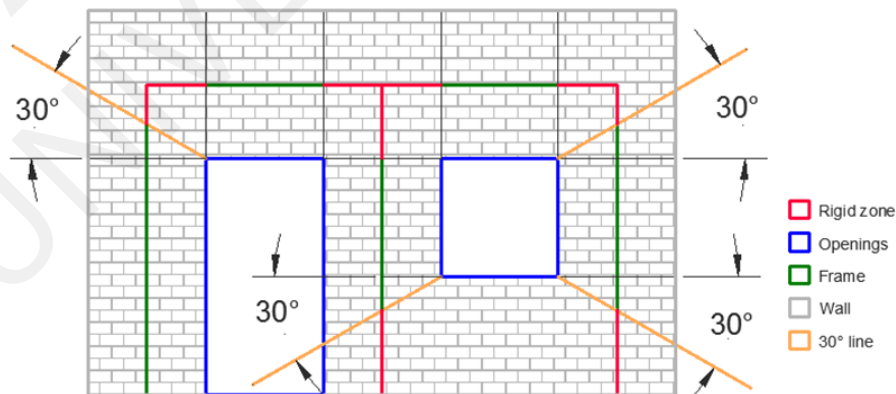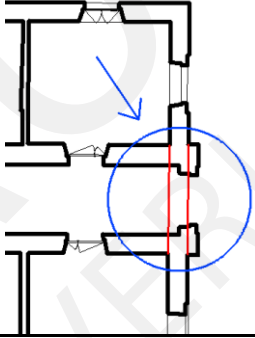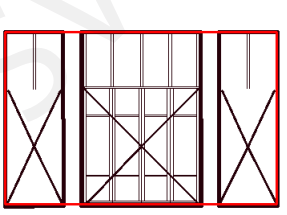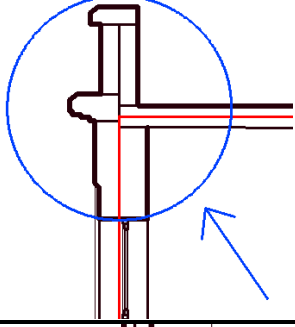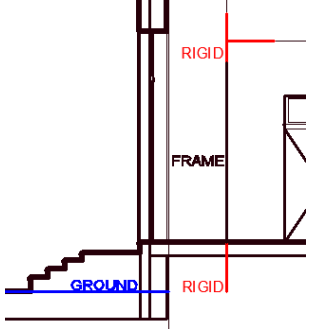

Figure 4. Equivalent frame model of the building according to [Dolce, 1989].

For the seismic analysis of masonry buildings, a user friendly commercial software SAP2000 v. 14 was used. All of the walls were modeled as an equivalent frame in SAP2000 (Figure 5), with the approximations and assumptions which are explained in Table 1.

Table 1. Assumptions for the model developed in SAP2000.

|				
Material	1	Reality	Stone, crushed stone, perforated brick, concrete masonry	
		Model	One material with combined characteristics	
Geometry	1	Reality	Parts of the outer side walls are out of the main plane.	
		Model	The side walls are considered as one plane.	
	2	Reality	There are separate windows on the middle of the front wall.	
		Model	Windows on the middle of the front wall are merged into one opening.	
	3	Reality	There is a parapet on the top of the building.	
		Model	In the modeling no parapet is considered.	
	4	Reality	The ground levels of the walls are different.	
		Model	Rigid parts are considered at the bottom of the columns to compensate the differences between the levels.	
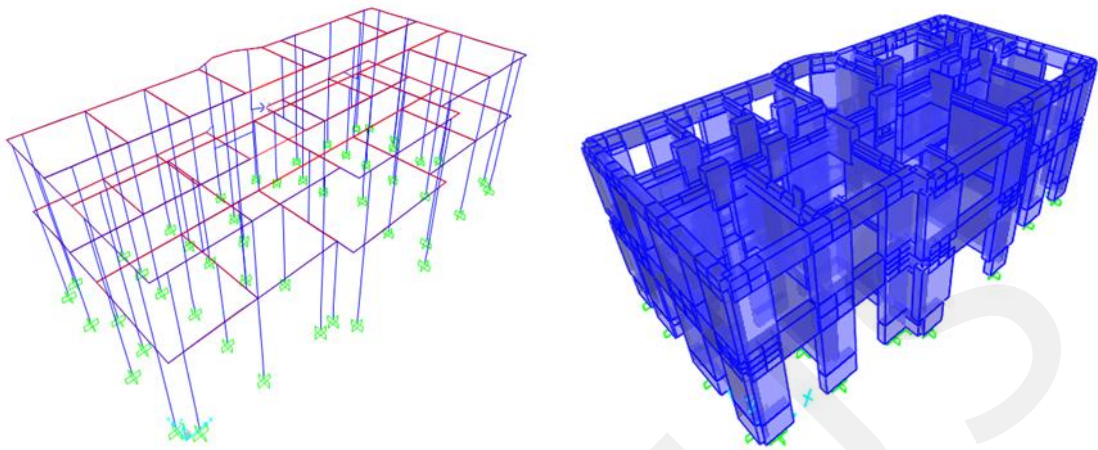
Figure 5. Three dimensional model in SAP2000.

Initially, in order to create a 3D model, the ground floor and first floor plans were imported from AutoCAD to SAP2000. In the next step, the equivalent frames were designed by taking into account the calculated dimensions of the rigid zones (Figure 6).

The masonry walls and the reinforced concrete slabs were modeled with two different materials. The software automatically calculates the mass of the building. The dead and live load on the slab is 0.7 KN/m^2 and 2 KN/m^2, respectively.

Approximately 70 different sections were used for the simulation of columns and beams. In case of columns, the width of the sections varying in the range of 125 to 650 cm and the height varies from 10 to 60 cm. Similarly, for the beams, the height of the sections varying in the range of 100 to 225 cm and the width varies from 10 to 55 cm. For the rigid zones of beams and columns, the same dimensions are used, only some of their properties (shear area in 2 direction and the moment of inertia about 3 axis) are modified.

For each wall there are some differences between the height of the levels, but as a simplification, the beams are designed to be at the same level in order to be able to define the slabs.
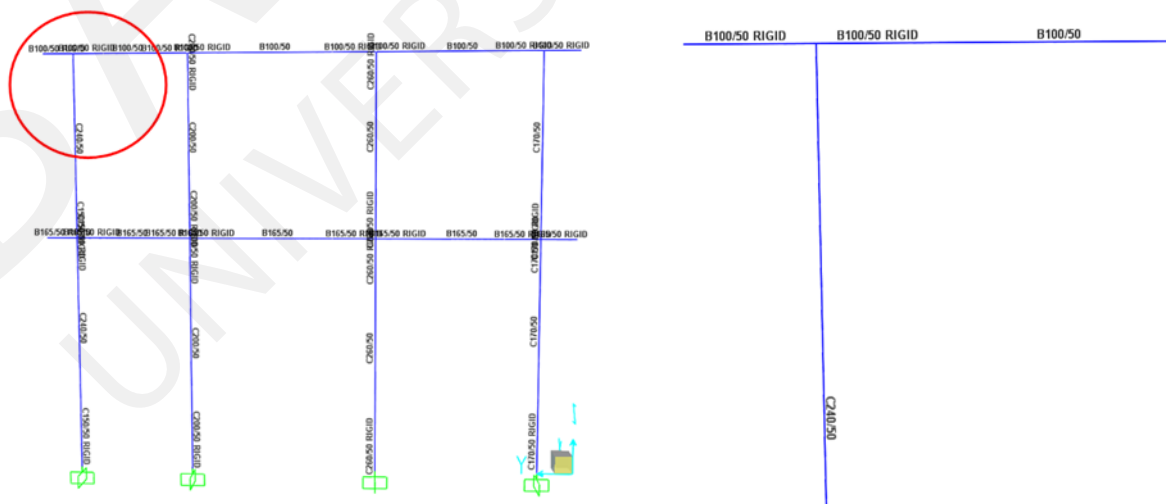
**Figure 6.** Side view of the frame with the sections.
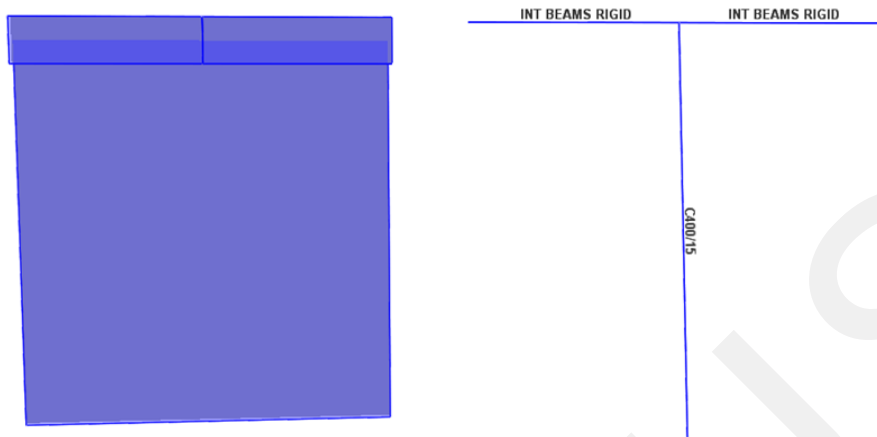
Figure 7. Simulation for the interior walls without openings.

In this building, there were some interior walls without openings. These walls were modeled with the same procedure as explained before, using an equivalent frame for the body of the wall and rigid beams to connect these walls with the other parts of the building, as illustrated in Figure 7. For these rigid beams, the same property modifiers have been used. The frames, which are positioned in different planes or direction has been connected with rigid beams.

In order to estimate the impact of the angle variation on the modal analysis results, different equivalent frame models were considered. Initially, the 30° rule [Dolce, 1989] and the other two additional ones have been implemented. The smaller and larger rigid zones were defined by changing the angle to 20° and then to 40°. In Table 2, the results of the modal analysis for each different method are displayed.

Table 2. Modal periods and frequencies for different angle values.

Angle [°]	Modal Periods [s]	Frequencies [Hz]
20	0.208	4.810
	0.184	5.448
30	0.213	4.691
	0.192	5.216
40	0.219	4.566
	0.202	4.951
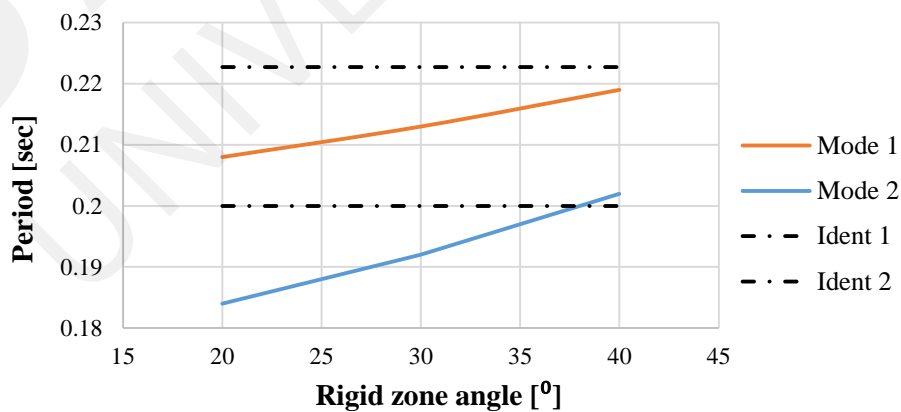
Figure 8. Relation between rigid zone angle and Eigen period.

Definition of non-linear hinge properties

In order to capture the behaviour of structures under seismic effects, the use of non-linear analysis is essential. For the current analysis, modeling is one of the important steps. The non-linear behaviour of the individual structural elements has to be considered in the model. The assignment of hinges to the model requires the definition of the non-linear properties for each structural element. These properties are quantified by strength and deformation capacities. The implementation of different criteria for the non-linear definitions results in different strength and deformation capacities. Several non-linear hinge definitions in terms of mathematical expressions have been proposed by various researchers based on the results of the past experiments [Pasticier *et al.,* 2008; Bal *et al.,* 2008, Diogo, 2009; Bucchi *et al.,* 2013; Lagomarsino *et al.,* 2013]. In the present work, the possible deviations are studied in the results of pushover analysis due to the use of different hinge definitions in terms of mathematical expressions.

In order to choose the most efficient hinge definition, test results from six different masonry walls are taken into account. These data are from the test results on the behaviour of masonry walls under in plane static (monotonic and cyclic) lateral loads, conducted by the organization from the University of Kassel in part of the project "Enhanced Safety and Efficient Construction of Masonry Structures in Europe" (ESECMaSE) [Fehling *et al.,* 2003]. From the experiments, it was found that the diagonal cracking in masonry walls were seems to be crucial. As a result, analytically it was attempted to determine this failure mode by adjusting the parameters of the wall material. However, in some cases, the horizontal force values calculated from mathematical expressions depend only on the dimension properties and cannot be adjusted to the desired values from the experiments. Therefore, some force values are the same for each wall (Figure 9).

The horizontal load – deformation curve obtained experimentally from ESECMaSE is compared with the load – deformation curve obtained analytically from each method (Figure 10). In comparison, the analytical outcome from the formulation by [Bal *et al.,* 2008] almost correlates with the experimental results and hence it is found to be an appropriate choice for this particular model (Figure 9). Therefore, it was decided to apply this particular proposal to the 3D model. The diagonal shear strength 'f_{tb}' which has the principal impact on the value of ultimate shear force can be easily modified by this particular hinge definition method by [Bal *et al.,* 2008].
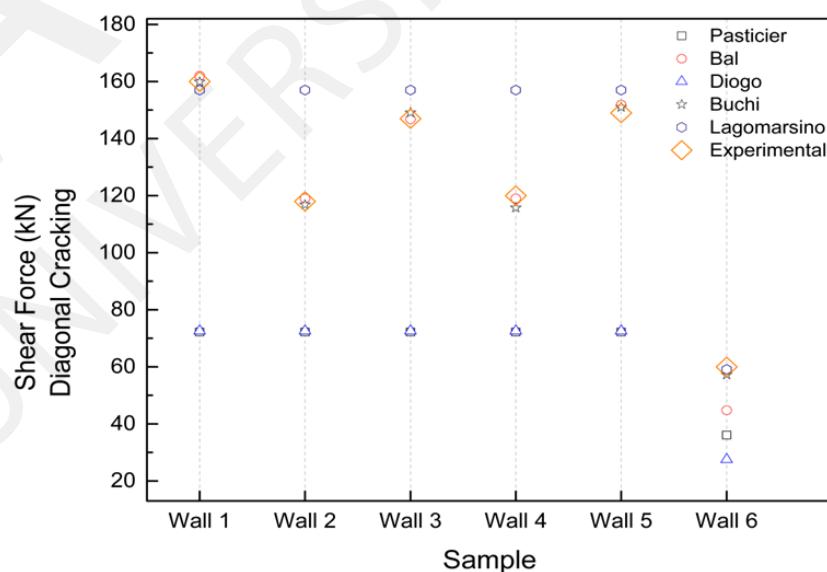

Figure 9. Simulation for the interior walls without openings.

32

Wall no. 5 - Test Enveloping Curve vs Numerical Model Capacity Curve
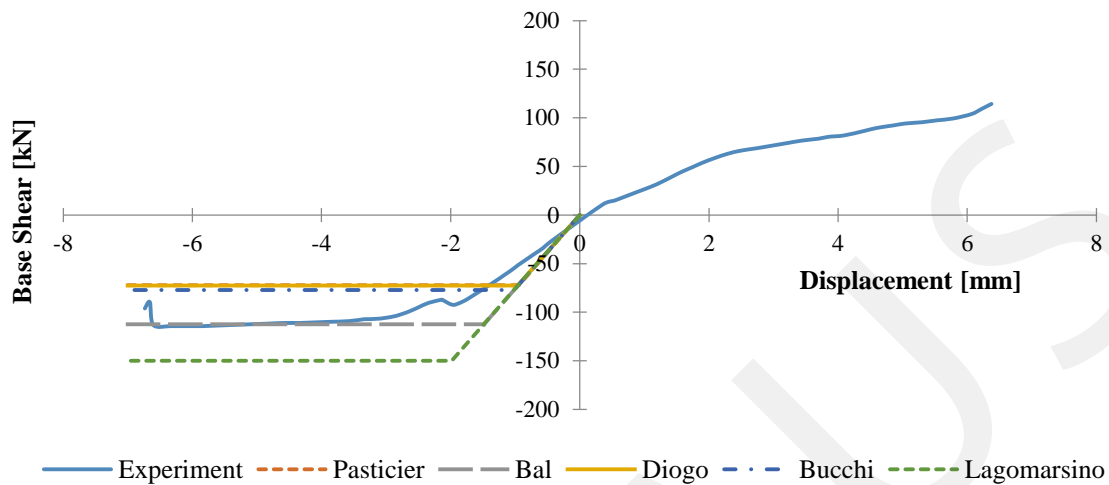

Figure 10. Comparison of analytical and experimental results for wall no. 5.

Ambient vibration measurement and processing

The building subjected to ambient vibration using an output-only identification technique has been used for the calibration of the linear elastic numerical model. The modal parameters of the building consist of natural frequencies, mode shapes and modal damping ratios. A number of mathematical models for output-only identification have been developed and roughly classified by parametric time domain methods and non-parametric frequency domain methods [Le *et al.,* 2009]. In the present work, it has been tried to calibrate the material property used in the numerical model with the modal frequencies of the building. In order to do so, the non-parametric frequency domain decomposition (FDD) method has been used to extract the principle mode of the building from the ambient vibration data. Among all non-parametric methods in frequency domain, FDD has been widely used due to its reliability and effectiveness.
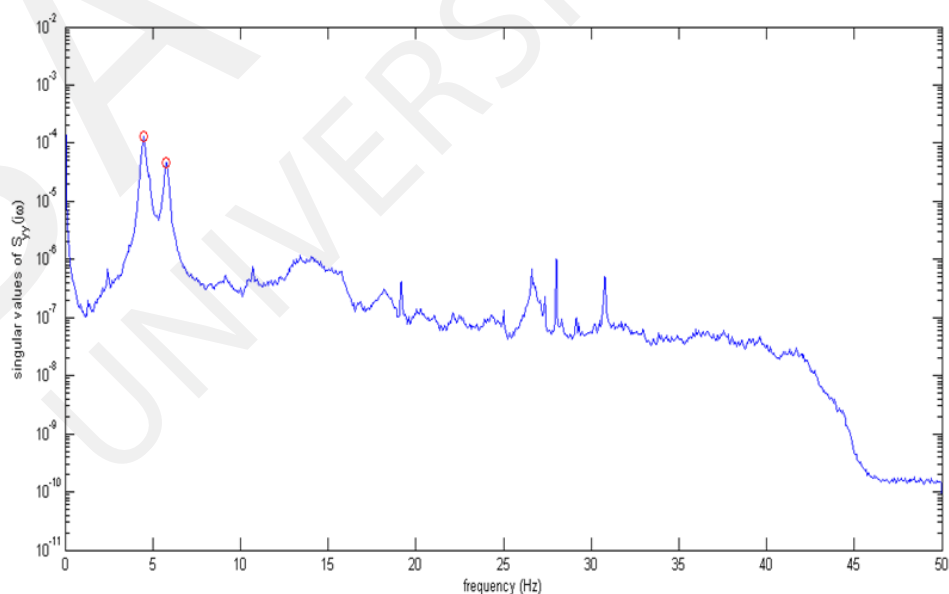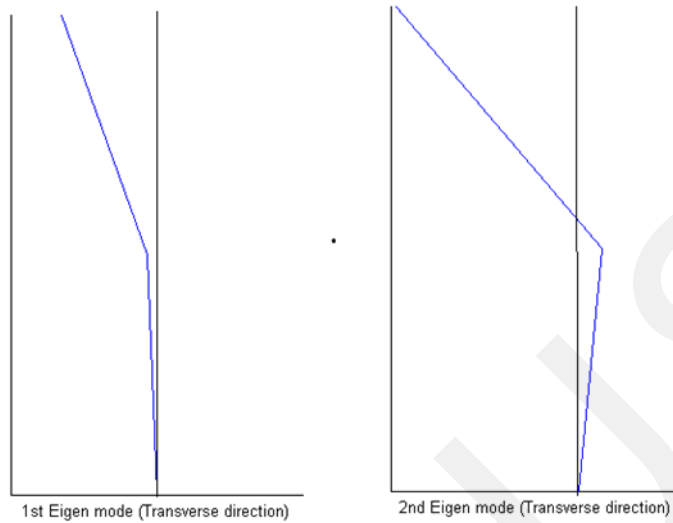

Figure 11. Manual peak-picking of singular value data in the frequency domain.

33

Figure 12. First two Eigen modes in the transverse direction of the building.

The FDD technique and a manual peak-picking algorithm have been implemented into Matlab to detect the first natural frequency in the longitudinal and transverse direction. The two significant peaks in the singular values of the correlation matrix as well as the first two Eigen modes corresponding to the Eigen frequencies of 4.49 Hz and 5.76 Hz are shown in Figure 11.

The first Eigen frequency of 4.49 Hz has been used to calibrate the effective modulus of elasticity of the brick masonry. The calibration curve is shown in Figure 13 and using a linear interpolation scheme, the effective value of the modulus of elasticity corresponding to the first Eigen frequency of the building has been found to be 1.26 GPa.
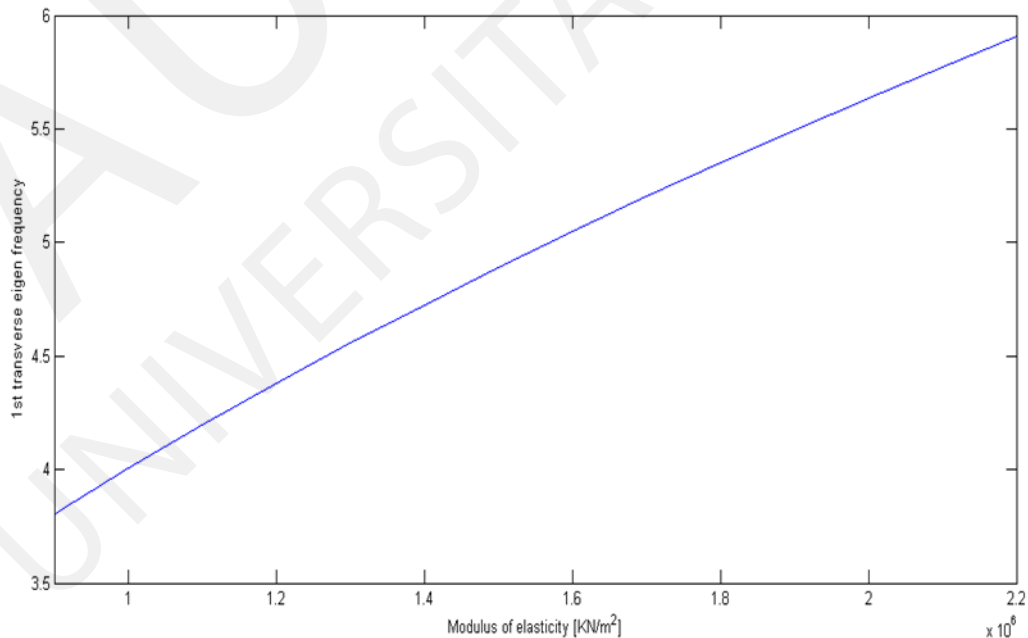
Figure 13. Variation of the first Eigen frequency corresponding to the effective modulus of elasticity of brick masonry.

Non-linear and damage analysis

After the inelastic characteristics of the building are modeled, a non-linear analysis can be performed in order to assess the building's performance under seismic excitation. In this case, an aftershock following main event is also considered for a more detailed damage prognosis. The analysis method to be used is the non-linear static analysis, also known as pushover analysis. Due to its simplicity in executing as well as the fact that the building's first mode is translational in the YZ plane, it makes an acceptable analysis method for the demands of this project.
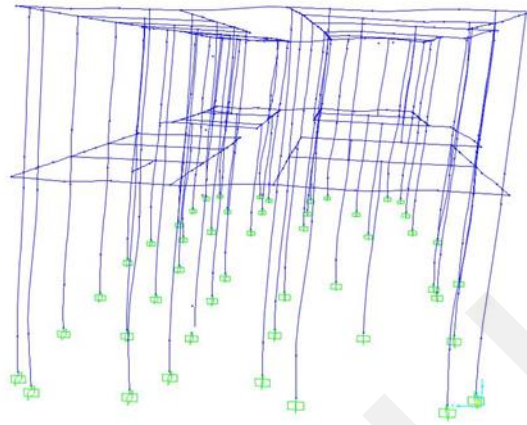
More specifically, the ATC - 40 capacity spectrum method is used to calculate the performance point between capacity and demand. The demand curves correspond to a specific response spectrum. In this case, the elastic design spectrum specified in the Turkish seismic code [TMPS, 1998] is used. This spectrum defines the expected spectral acceleration values that have a 10% probability of exceedance in 50 years. The examined building belongs to seismic zone 1, for which an effective ground acceleration coefficient (A_o) of 0.4 is used. This value corresponds to 0.4g of peak ground acceleration expected for the design earthquake. Furthermore, the building has an importance factor of '1' and the local soil conditions are used to specify the characteristic periods of the design spectrum. The design spectrum that was previously specified is shown in Figure 14.

In order to perform a non-linear analysis, it was necessary to include all the different hinges due to the different capacity of elements. And so, a total of 624 hinges, such as; flexural and shear hinges was assigned to the elements for the analysis. This was performed by an interactive procedure between Excel, Matlab and SAP2000.

A modal pushover analysis was performed by the following steps: at first, the dynamic analysis of the building showed that the principal mode was in the YZ direction; secondly, a displacement control method was selected, for which a monitored displacement of node 630 was checked; and thirdly, a modal force distribution following the first mode and scaled by the mass was applied to the building. In this way, the forces were able to resemble the principal mode shape (Figure 15).
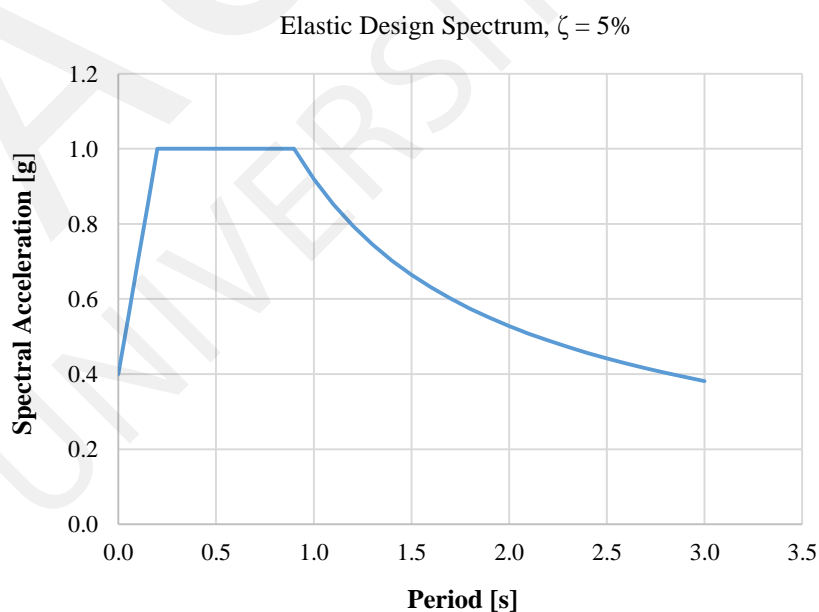
Figure 14. Elastic design spectrum for the highest seismic zone according to [TMPS, 1998].

Figure 15. Principal mode shape.

For the first pushover analysis the performance point was obtained using the ATC – 40 capacity spectrum method implemented in SAP2000. The spectral displacement using the Turkey design spectrum was introduced in the program. The spectrum for different values of damping ratios were assigned in order to obtain the performance point and the top story displacement (node 630) using equation 1.

The value of the roof displacement obtained is 0.036 m and for this value, the building is no longer in the elastic region because a reduced stiffness are obtained due to the presence of hinges. This stiffness are used for an aftershock response, for which the period of the building is 1.33 Hz. The aftershock is simulated as a new pushover analysis (Figure 16). A new capacity curve (Figure 17) is obtained by following the same procedure, in which, a performance point of 0.032 m and a roof displacement of 0.04 m were obtained.

$$D = \frac{u_n}{\Gamma_n \Phi_{ni}}$$ [1]
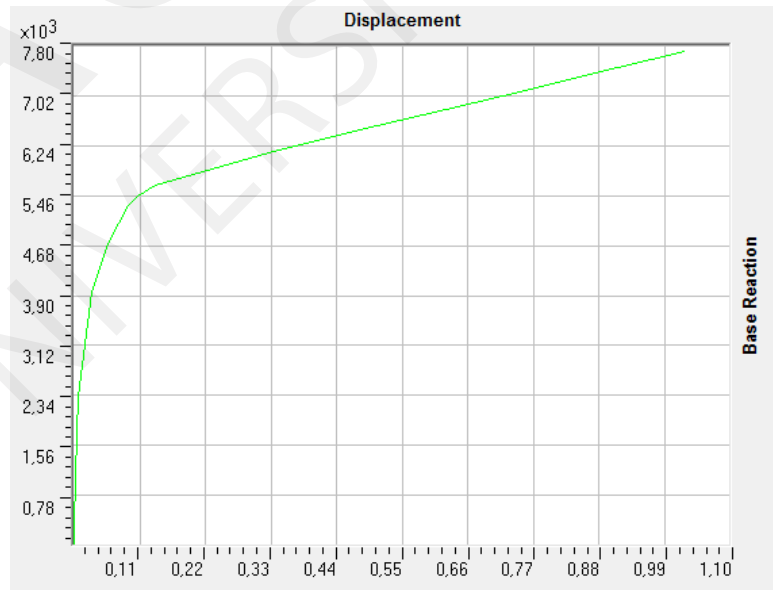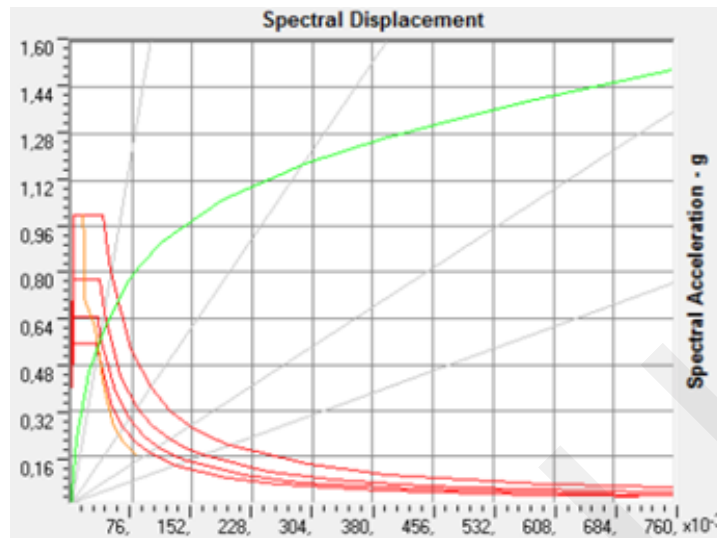

Figure 16. Pushover curve.

Figure 17. Performance point.

From the pushover curves, it is observed that the building is capable to withstand the design ground motion and an aftershock. It is obtained by comparing the results with the drift limit ratios for masonry buildings [Alcocer *et al.,* 2004] for which a value of 0.5% was obtained. It is also important to note that the behaviour of the building is highly nonlinear; which was expected from the type of the material. From the pushover curve, it is also possible to observe that the non-linear behaviour of the top storey starts at the displacement of 0.02 m.

Conclusions

From the completion of the analysis and the tasks of the current study, the main conclusions that can be derived are as follows:
- The simulation of the building through the equivalent frame method was found to be efficient, because the modal behaviour of the analytical model reflects adequately with the results obtained from the ambient vibration measurements.
- After the calibration of the model by considering different plastic hinge properties between six experimental specimens, the hinge definition by [Bal *et al.,* 2008] was decided to be the most efficient one by comparing the analytical results to the experimental ones.
- The final value selected for the modulus of elasticity 'E' of the wall approaches the one used in the experimental tests.
- The sensitivity analysis, which was conducted regarding the rigid zone angle variation, presents no significant deviations as showed from the values of the modal frequencies.
- The first plastic hinge appears at a displacement of 0.02 m.
- The respective building in Antakya can sustain the design ground motion and an aftershock loading, without any collapse.

References

Abrahamczyk, L., Schwarz, J., Shetty, N. [2014]. "Seismic damage prognosis of masonry structures using nonlinear hinges". Natural Hazards and Risks in Structural Engineering. Bauhaus University Weimar.

Abrahamczyk, L., Schwarz, J., Langhammer, T., Genes, M. C., Bikce, M., Kacin, S., Yakut, A., Erberik, A. M., Gülkan, P. [2012]. "Empirical and analytical vulnerability assessment of the masonry building stock in Antakya (Hatay / Turkey)". 15th World Conference on Earthquake Engineering, LISBOA 2012.

Abrahamczyk, L., Schwarz, J., Lang, D. H., Leipold, M., Golbs, Ch., Genes, M. C., Bikce, M., Kacin, S., Gülkan, P. [2008]. "Building monitoring for seismic risk assessment (I): Instrumentation of RC frame structures as a part of the SERAMAR project". The 14th World Conference on Earthquake Engineering, October 12 – 17, 2008, Beijing, China.

Alcocer, S. M., Arias, J. G., Vazquez, A. [2004]. "Response assessment of Mexican confined masonry structures through shaking table tests". 13th World Conference on Earthquake Engineering, Vancouver, 1 – 6 August 2004, 13 pages.

Arangio, S., Bucchi, F., Bontempi, F. [2013]. "Pushover seismic analysis of masonry buildings with different commercial codes". In: Built Heritage 2013 Monitoring Conservation Management, 18-20 November 2013, Milan, Italy. pp. 733-780.

Bal, I. E., Crowley, H., Pinho, R. [2008]. "Displacement based earthquake loss assessment of Turkish masonry structures". The 14th World Conference on Earthquake Engineering, Beijing, China.

Belmouden, Y., Lestuzzi, P. [2009]. "An equivalent frame model for seismic analysis of masonry and reinforced concrete buildings". Construction and Building Materials, Vol. 23, pp. 40 – 53.

Bucchi, F., Arangio, S., Bontempi, F. [2013]. "Seismic Assessment of an historical masonry building using nonlinear static analysis". Proceedings of the Fourteenth International Conference on Civil, Structural and Environmental Engineering Computing, 2013, Stirlingshire, Scotland. Paper No. 72, 14 pp., Civil-Comp Press.

DIN [2010] EN 1996-1-1: 2010-12: Eurocode 6: Part 1-1: General rules for reinforced and unreinforced masonry structures. DIN Deutsches Institut für Normung.

Diogo Filipe de Sousa Micael Pereira [2009]. "Nonlinear seismic analysis of ancient buildings – structural characterization for successful seismic retrofit". Extended Abstract of the Master's Dissertation. Department of Civil Engineering and Architecture – Instituto Superior Técnico – Universidade Técnica de Lisboa.

Dolce, M. [1989]. "Schematizzazione e Modellazione per Azioni nel Piano delle Pareti", Corso sul Consolidamento Degli Edifici in Muratura in Zona Sismica, Ordine degli Ingegneri, Potenza.

Erberik, M. A., Yakut, A., Genes, M. C., Abrahamczyk, L., Bikçe, M., Kacin, S., Langhammer, T., Gülkan, P., Schwarz, J. [2013]. "Characteristics of unreinforced masonry buildings in Antakya through field survey". 2nd Turkish Conference on Earthquake Engineering and Seismology – TDMSK – 2013. September 25 – 27, 2013, Antakya, Hatay/Turkey.

Fehling, E., Stuerz, J., Emami, A. [2003]. "Test results on the behaviour of masonry under static (monotonic and cyclic) in plane lateral loads". Enhanced Safety and Efficient Construction of Masonry Structures in Europe, Project No. Coll – Ct - 2003 – 500291, Work Package No. 7.1a.

Genes, M. C., Erberik, M. A., Abrahamczyk, L., Gülkan, P., Bikçe, M., Kacin, S., Yakut, A., Schwarz, J. [2012]. "Vulnerability Assessment of two instrumented masonry buildings in Antakya (Hatay, Turkey)". 10th International Congress on Advances in Civil Engineering, 17 – 19 October 2012, Middle East Technical University, Ankara, Turkey.

Lagomarsino, S., Penna, A., Galasco A., Cattari, S. [2013]. "TREMURI program: An equivalent frame model for the nonlinear seismic analysis of masonry buildings". Engineering Structures, 56: 1787-1799.

Le, T., Tamura, Y. [2009]. "Modal identification of ambient vibration structure using frequency domain decomposition and wavelet transform". The Seventh Asia – Pacific Conference on Wind Engineering, November 8 – 12, 2009, Taipei, Taiwan.

Magenes, G., Morandi, P., Penna, A. [2003]. "Test results on the behaviour of masonry under static cyclic in plane lateral loads". Enhanced Safety and Efficient Construction of Masonry Structures in Europe, Project No. Coll – Ct - 2003 – 500291, Work Package No. 7.1c.

Pasticier, L., Amadio, C. Fragiacomo, M. [2008]. "Nonlinear seismic analysis and vulnerability evaluation of a masonry building by means of the SAP2000 v.10 code". Earthquake engineering and structural dynamics, 36: 467 – 485.

Pereira, D.F. [n.d.]. Nonlinear analysis of ancient buildings. Structural Characterization for Successful Seismic Retrofit. 11pp.

TMPS [1998]. Turkish Ministry of Public Works and Settlements. Specification for Structures to be built in Disaster Areas. Part III – Earthquake Disaster Prevention (Chapter 5 – 13). English Translation, 1998; 84 pp.,
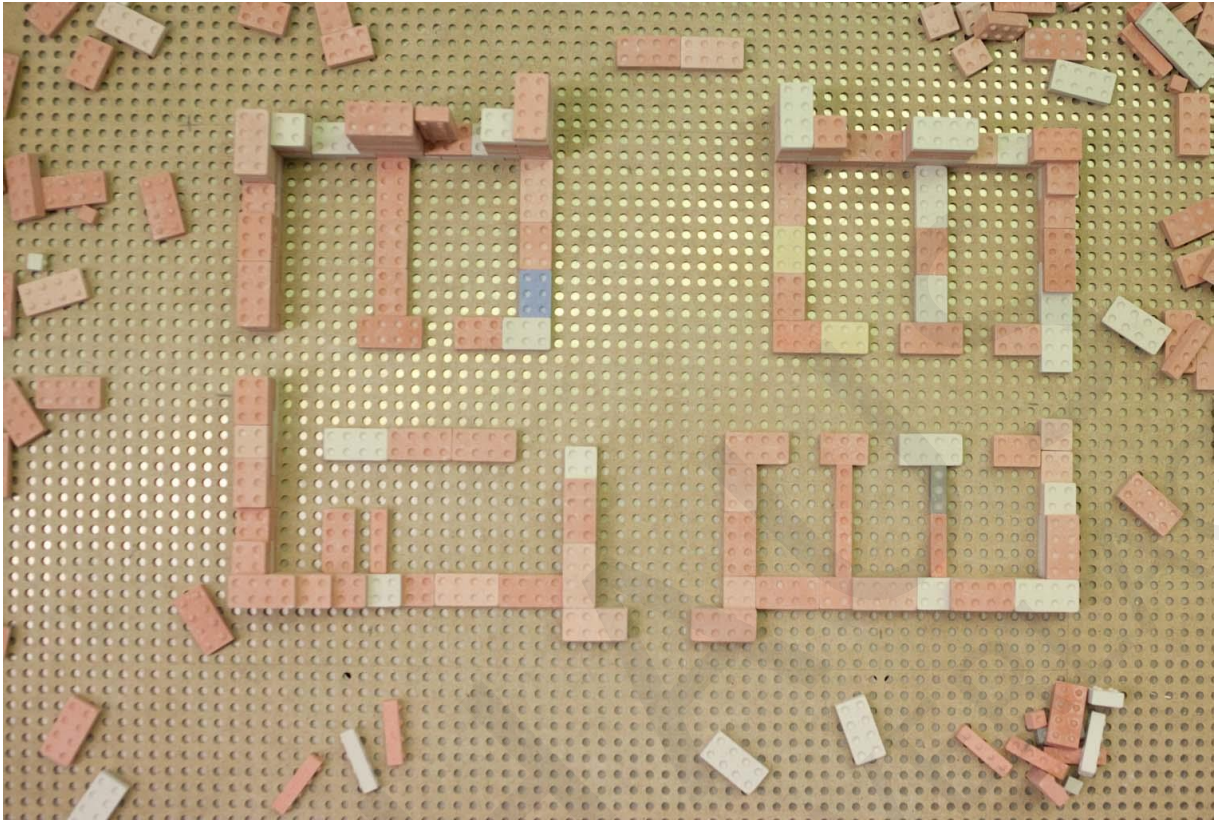
Special aspects of steel structures: case study RBS coupling beam

CRISAN Andrei Nicolae
CMMC Department, Politehnica University Timisoara

WITTOR Björn
Professorship Steel Construction, Bauhaus-Universität Weimar

HILDEBRAND Jörg
Junior Professorship Simulation and Experiment, Bauhaus-Universität Weimar

Abstract. The project is connected with the design of an 18-story office building, located in Bucharest, Romania. The building height is 94 m, and the plan dimensions are 43,3m x 31,3m. The building site is located in a high seismic area, which is characterized by a design peak ground acceleration 0.24g for a returning period of 100 years, and soft soil conditions, with TC=1.6 s. Lateral force-resisting system consists of exterior steel framing with closely spaced columns and short beams. The moment frame connections employee reduced beam section connections that are generally used for beams loaded mainly in bending. By using the FEM-simulation-program ANSYS$^©$ the experimental data could be verified. During the analysis different material law were compared for finding the best way to reflect the real behaviour of the construction. A parameter analysis at the end of the project gives a perfect overview about the different influences of the geometry- and material properties.

General description of the research project

Introduction

The complexity of numerical and FE models has advanced to the point where human understanding is of little use as a validation tool. Moreover, the interdisciplinary use of finite element methods to solve different complex models rise the need of accurate and reliable rules for the quantification of principal model parameters, the evaluation of individual partial models, their coupling as well as the overall model. In order to produce reliable results, any given model has to be verified and validated. In practice, validation is often blended with verification, especially when measurement data is available for the system being modelled.

In order to achieve a high quality FE model, there are a series of parameters to be considered and monitored. For the case of homogeneous models, the validation and calibration can be done relatively easy and a high quality model is usually obtained. For the case of complex models, composed of multiple sub models with different requirements regarding the geometric detail, mesh density and overall quality, the correct evaluation can become a cumbersome procedure.

Model verification is intended to ensure that the model does what it is intended to do. In general, techniques that can help to develop, debug or maintain a large computer programs are useful for models. Antibugging (adding supplementary output in order to check for eventual hidden errors), structured walk-through (step-by-step analysis of the model), the use of simplified models, use of deterministic models, degeneracy testing (testing for extreme values) or consistency testing are few of the model verification techniques that can be used to asses complex models.

41

Validation is the task of demonstrating that the model is a reasonable representation of the actual structural system and it reproduces the system behaviour with enough fidelity to satisfy analysis objectives. A complex model is usually composed of more sub models representing different parts of the system at different levels of abstraction. As a result, the complex model may have different levels of validity for different sub models, parts of the system across the full spectrum of system behaviour.

During the validation process, the different attributes are usually included i.e. Selectivity/specificity, accuracy and precision, repeatability, reproducibility, limit of quantification, curve fitting and its range.

General data

The project is connected with the design of a 18-story office building, located in Bucharest, Romania. The building height is 94 m, and the plan dimensions are 43,3m x 31,3m, see Figure 1. The building site is located in a high seismic area, which is characterized by a design peak ground acceleration 0.24g for a returning period of 100 years, and soft soil conditions, with TC=1,6 s.

Lateral force-resisting system consists of exterior steel framing with closely spaced columns and short beams. The central core is also made of steel framing with closely spaced columns and short beams. The ratio of beam length-to-beam height, L/h, varies from 3.2 to 7.4, which results in seven different types of beams. Some beams are below the general accepted inferior limit (L/h=4). The 82 moment frame connections employee reduced beam section connections that are generally used for beams loaded mainly in bending (Figure 2). Circular radius cuts in both top and bottom flanges of the beam were used to reduce the flange area. For current experimental program, two types of beams, which have the shortest L/h ratio, have been selected. The first beam, denoted as RBS-S, has a clear length of 1450 mm, and the lowest span over height ratio, L/h=3.2. The second type, denoted as RBS L, has a clear length of 2210 mm, and a corresponding span over height ratio L/h of 4.9. The columns have a cruciform cross-section made from two hot-rolled profiles of HEA800 and HEA400 section (Dinu et. al., 2013).

Figure 1. Plan layout and elevation of the building.
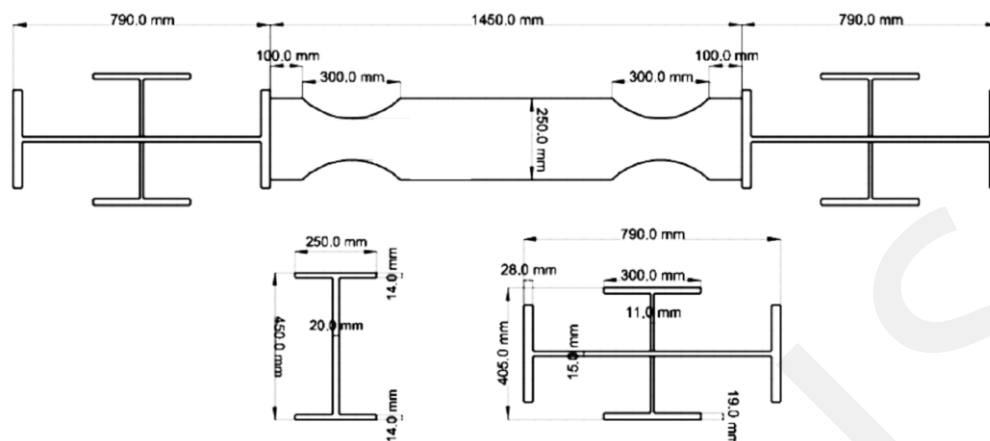
Figure 2. Moment frame with short beam – beam and column details

Beams with span-to-depth ratio shorter than four are not very common in the design of moment resisting frames. For such beams, the shear stresses may become a controlling factor in the design, as the moment capacity is influenced by the presence of the shear. This is an important matter when such a beam is part of the seismic lateral force resisting system that is designed according to the dissipative concept. In this case, the contribution from the shear force affects the dissipation capacity and plastic mechanism. Both beams and columns are made from S355 grade steel.

Experimental test setup and test protocol

Specimens were tested under cyclic loading. The cyclic loading sequence was taken from the ECCS Recommendations. The yielding displacement is then used for establishing the cyclic loading. In order to reduce the number of tests, the monotonic test was replaced by the push-over curve obtained numerically using the general-purpose finite element analysis program ABAQUS. For the FE model, the measured material properties were used.

In Table 1 and Table 2 are presented the experimental results for uniaxial tension tests for the hot rolled profiles and flat steel plates.

Table 1. Material properties of rolled profiles (Columns) – Dinu et. al., 2013

Section	Steel grade	Element	f_y [N/mm²]	f_u [N/mm²]	A_u [%]
HEA800	S355	Flange	410.5	618.5	15.0
		Web	479.0	671.2	13.0
HEA400	S355	Flange	428.0	592.0	15.1
		Web	461.0	614.0	12.8

**Table 2.** Material properties of flat steel (Beam) – Dinu et. al., 2013

Section	Steel grade	Element	f_y [N/mm²]	f_u [N/mm²]	A_u [%]
14mm	S355	Beam flange	373.0	643.0	17.0
20mm	S355	Beam web	403.0	599.0	16.5
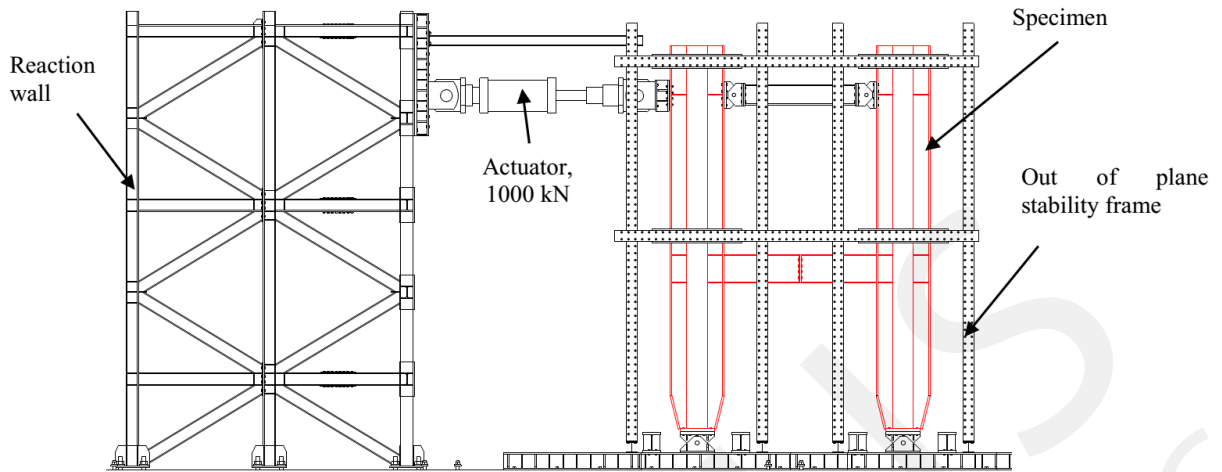
Figure 3. Experimental test setup (Dinu et. al., 2013).

It can be observed that the experimentally measured yield strength and tensile stress of the plates and profiles were larger than the nominal values. The highest increase has been recorded for the hot rolled sections, being lower for plates. In Figure 3 is presented the experimental setup.

Further, in Figure 4 is presented the loading protocol. Due to physical limitations, an asymmetric loading protocol was selected.
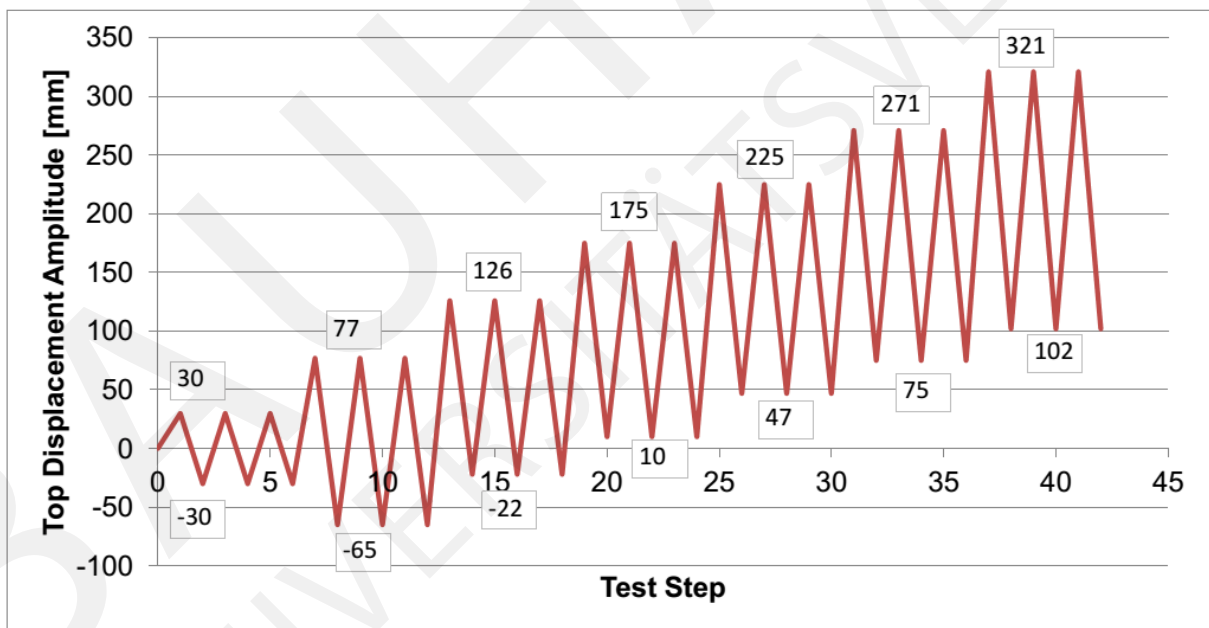
Figure 4. Experimental test loading protocol

Experimental test results

In Figure 5 are presented the experimental test results for the RSB-S3 coupling beam and the observed failure mode (Dinu et. al., 2013).
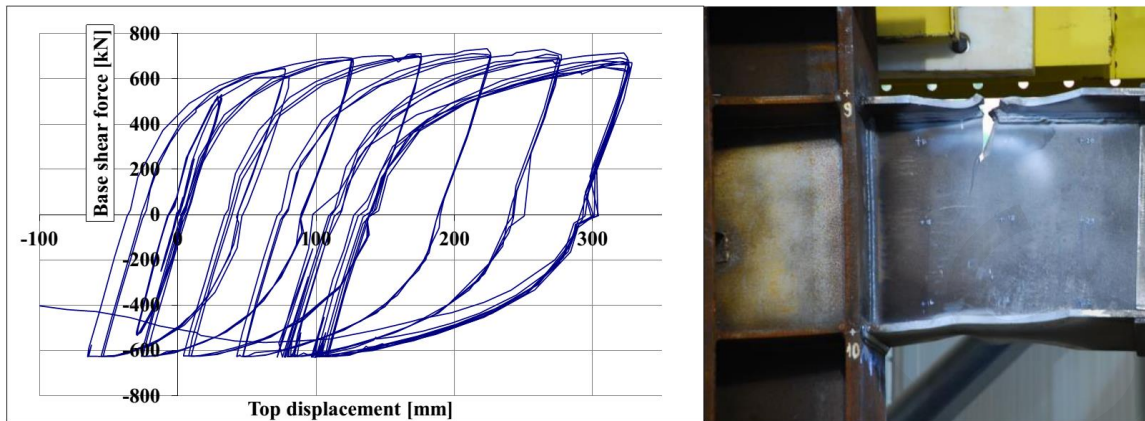
Figure 5. Experimental test results and failure mode

Numerical model calibration and validation

Based on the experimental test results presented in previous chapter, Ansys WorkBench (Ansys, 2012) commercial finite element software package was used to create a calibrated and validated numerical model for conducting an extended sensitivity analysis.

In order to be able to conduct a successful sensitivity analysis, the numerical model has to have the following characteristics:

- Successfully replicate the experimental test results with high accuracy;
- Increased robustness in order to reduce the sensitivity to eventual external noise;
- Simple model in order to better control the input parameters, but complex enough in order to model the observed structural behavior.

Initial FE model

For this model, the calibration consists, in fact, in finding the suitable material behavior law to be used in analysis. In a first attempt, a complete model was created using solid elements, as presented in Figure 6.
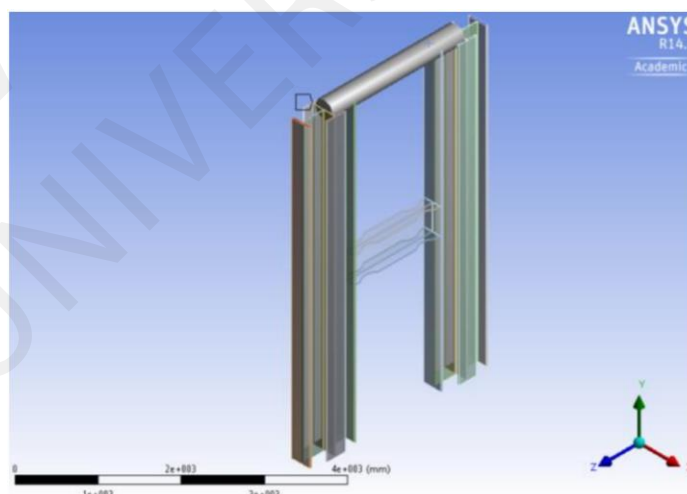

Figure 6. Initial FE model

At the bottom, the supports were modelled using Remote Displacement constraints. The translation was blocked on X, Y and Z together with the rotation about Y and Z, while the rotation about the X axis was left free in order to simulate a pinned connection.

The connection beam at the top was considered using a Beam Body-Body connection. The displacement was applied at the top left column and it was introduced using a 42 steps static analysis. The material behaviour was considered as Elastic-Perfect plastic, in accordance with EN1993-1-5 specifications. Using this approach to simulate the experimental tests, the analysis was timed at more than 10 hours.

Simplified FE model

Due to the fact that a sensitivity analysis was supposed to be performed, the computational time had to be reduced. In order to simplify the numerical model, the symmetry and anti-symmetry properties can be used. It can be observed that the geometry is doubly symmetric. A symmetry plane defined by the mid cross-section of the beam (Figure 7a), while the other is defined by the centroids of the columns (Figure 7b).

Using these approximations, a new model was created in order to reduce the computation time. The reduced numerical model is presented in Figure 8a, together with the symmetry (Figure 8b) and anti-symmetry constraints (Figure 8c).

Since for usual structural steel elements the stresses do not largely varies through the thickness. Shell elements were used instead of solid elements. Using the simplified model, the computational time was reduced to approximately 20 minutes.

a. Symmetry plane   b. Anti-symmetry plane
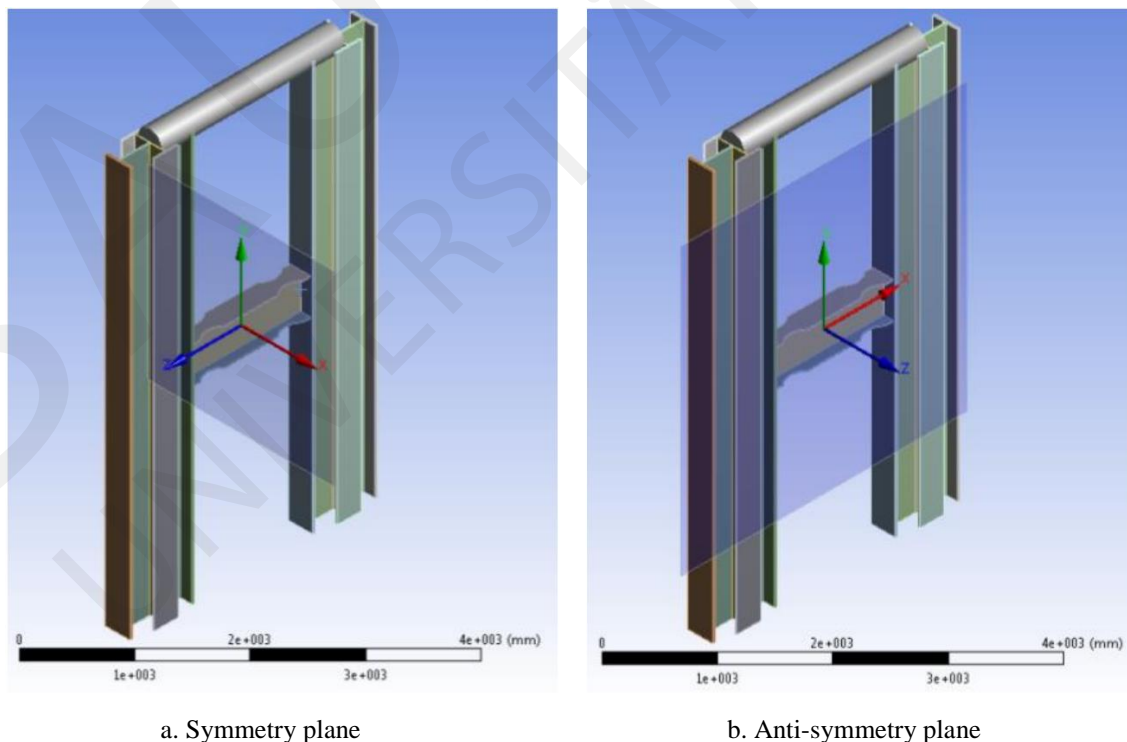
Figure 7. Symmetry and Anti-symmetry plane

| a. Reduced model | b. Symmetry constraint | c. Anti-symmetry constraint |
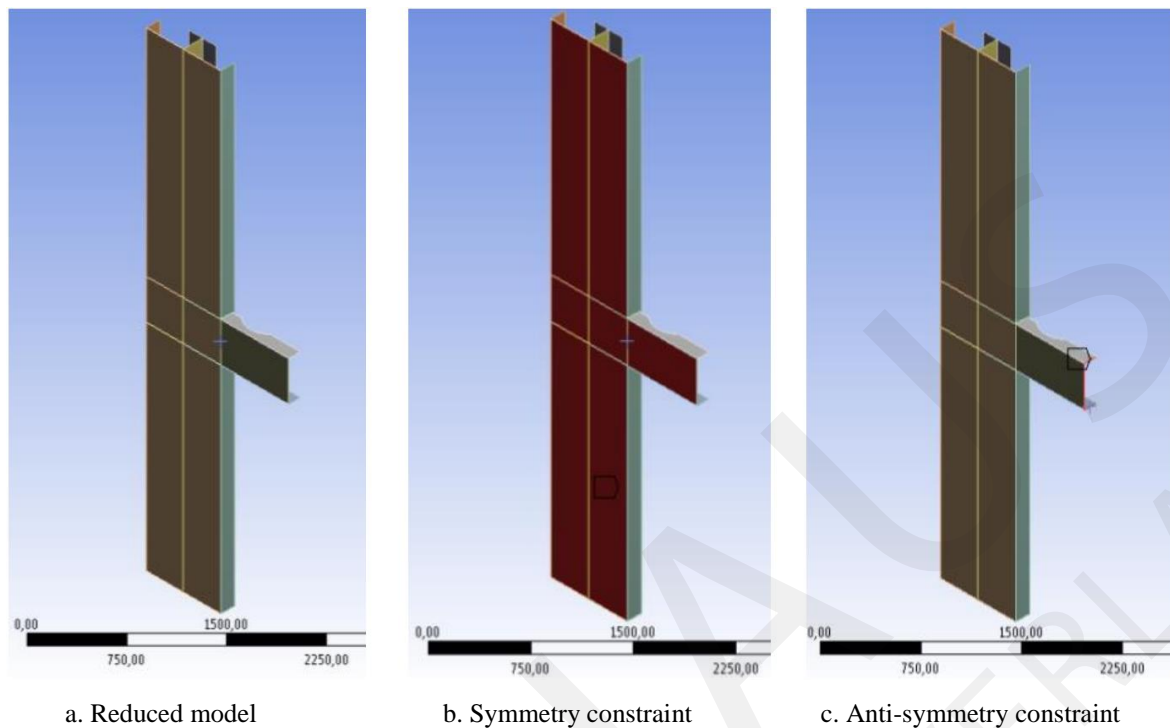
Figure 8. Reduced numerical model
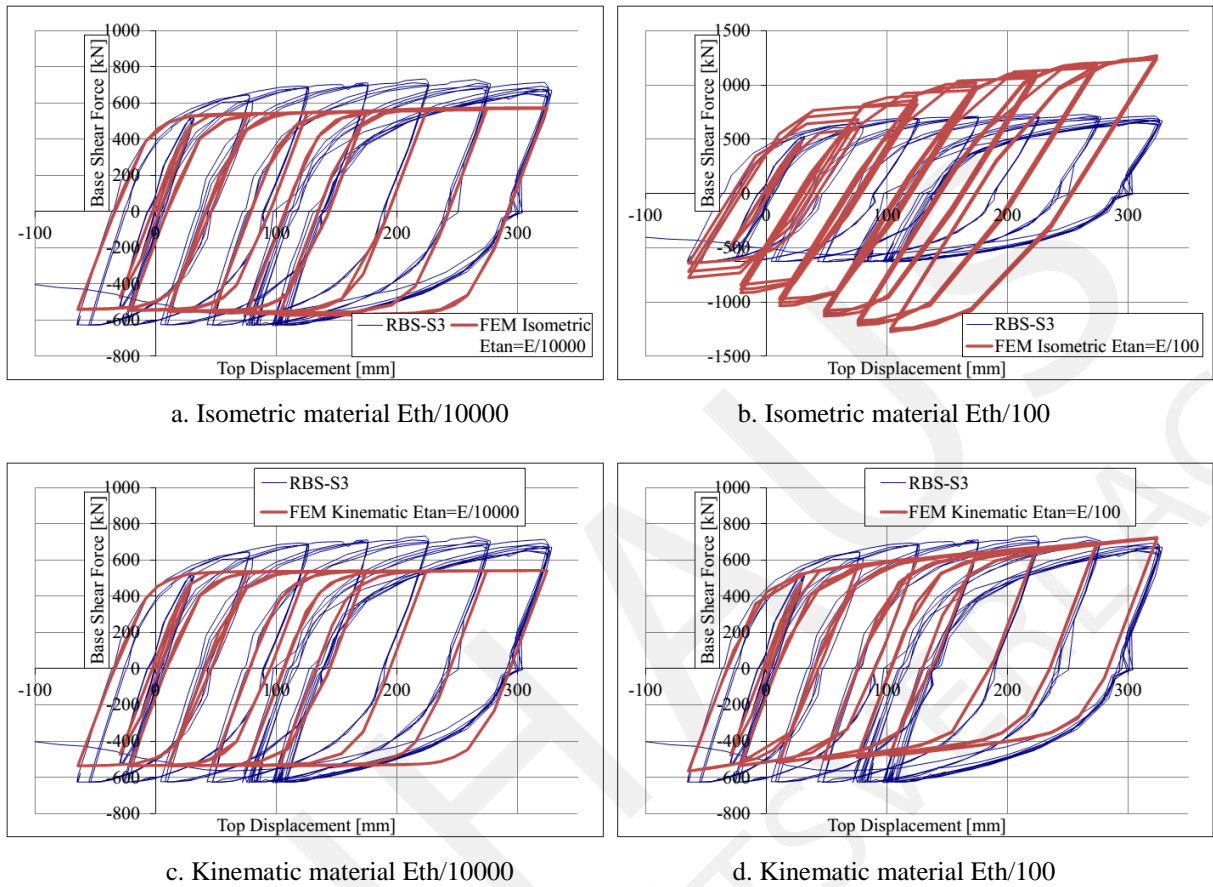
Material calibration

Following, using the reduced model, different types of material behaviour were considered, according to EN1993-1-5 provisions:

- Elastic – Perfect Plastic;
- Elastic – Plastic with a hardening modulus of E/10000;
- Elastic – Plastic with a hardening modulus of E/100;
- Elastic – Plastic with the experimentally determined true stress-strain curve.

It must be mentioned that, for monotonic loads, the isometric hardening models with above given properties offer a good approximation, while material models with kinematic hardening are the simplest way to model cyclic loadings. Using ANSYS WB (Ansys, 2012) capabilities, different material models were considered using ISOMETRIC or KYNEMATIC plasticity. The results of these analyses are presented in Figure 9a and Figure 9b for isometric hardening plasticity Figure 9c and Figure 9b for the kinematic plasticity models.

It can be observed that the case of cyclic loading none of these models is appropriate to simulate the behaviour obtained following the experimental tests. A combined Isotropic/Kinematic approach was considered, the Chaboche material model. For this material model, the parameters were taken from Budaházy and Dunai (2013). Following, using a trial and error approach, the material parameters were further modified in order to obtain the best fit.

The obtained von Misses stresses are plotted in Figure 10a, while the equivalent plastic strain plot is presented in Figure 10b for maximum displacement.

a. Isometric material Eth/10000   b. Isometric material Eth/100

c. Kinematic material Eth/10000   d. Kinematic material Eth/100

Figure 9. Plasticity models

It can be observed that the maximum stresses are concentrated in the reduced area of the beam. Furthermore, no plastic deformations were found in the column. These observations are in accordance with the test results. Using the calibrated material, a solid 3D model was created in order to compare the difference in the behaviour of solid and shell elements. No difference was observed for this application considering shell and solid elements (see Figure 11).
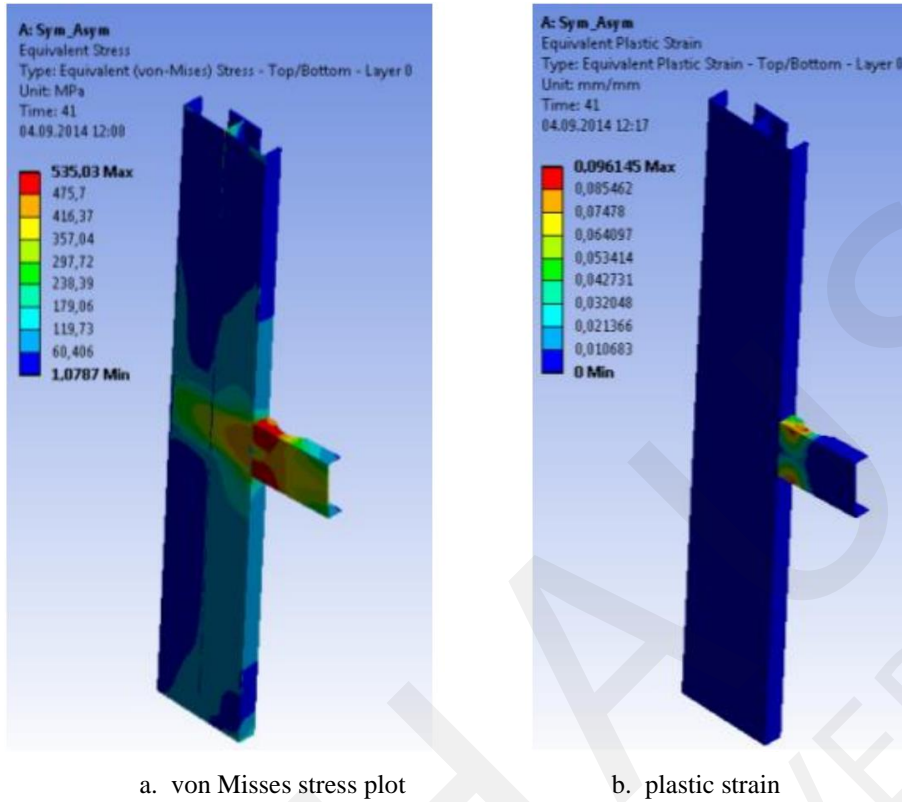
48

a. von Misses stress plot   b. plastic strain

Figure 10. Calibrated reduced model results

a. Solid elements – Chaboche material model   b. Shell elements – Chaboche material model
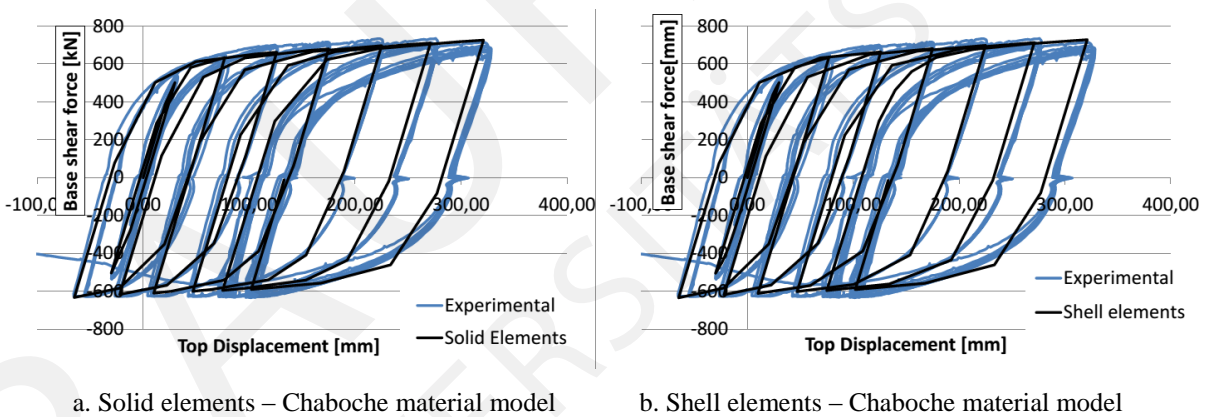
Figure 11. Reduced model

Sensitivity study

In order to be able to consider a higher number of samples for the sensitivity study, the computational time was reduced even more. For this, a monotonic analysis was defined. The results of this analysis were compared with the results of the cyclic analysis and the experimental test behaviour curves (see Figure 12). It can be observed that the monotonic analysis can successfully characterize the response of the structure.
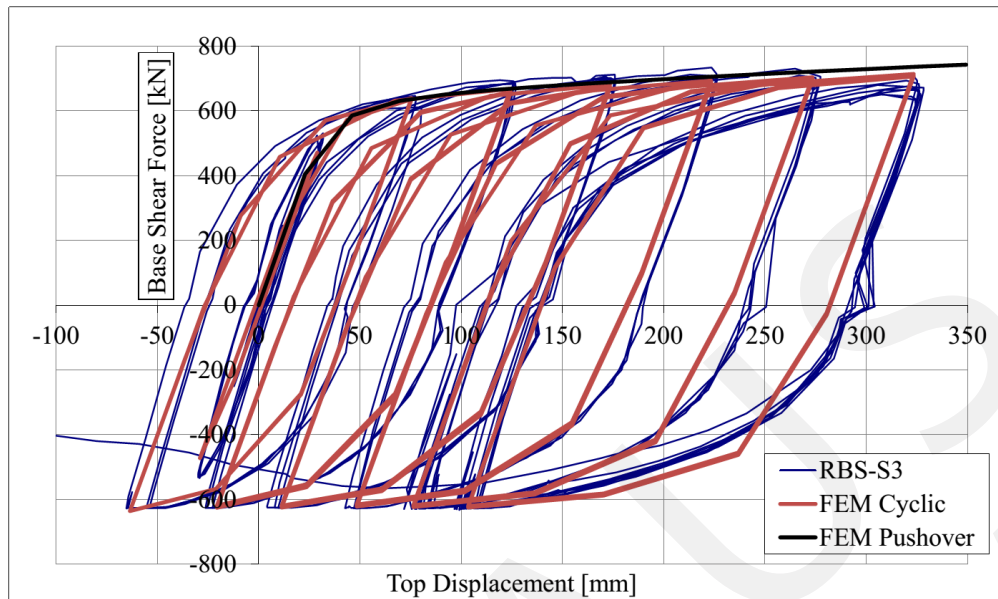
Figure 12. Experimental, numerical cyclic and monotonic behaviour curves

Parameters

For steel structures, the uncertainty for material behaviour and geometry is usually limited. Even so, considering the experimental test results for the material properties, the S355 steel used for beam web was found to have the yield stress of 403 MPa (+13.5%), while for steel properties used in the beam flanges, the yield stress was found to be 373 MPa (+5%). According to norms, the Young modulus for steel has different values in Europe, USA and Japan.

From the geometric point of view, the width and thickness of flat steel used to create the welded beam profile influence the normal to shear stress ratio. The dog bone dimensions (depth and length) can influence the overall behavior of the assembly.

On this line, using the calibrated reduced model, a sensitivity analysis was performed with respect to the following parameters:

1. Input parameters
    a. Beam Flange yield stress (range: 355 – 460 MPa)
    b. Beam web yield stress (range: 355 – 460 MPa)
    c. Young modulus in the flanges (range: 190 – 210 GPa)
    d. Young modulus in the flanges (range: 190 – 210 GPa)
    e. Beam web height (range: 350 – 500 mm)
    f. Beam web thickness range: 5 – 15 mm)
    g. Beam flange width (range: 200 – 300 mm)
    h. Beam flange thickness (range: 10 – 20 mm)
    i. Dog bone depth (range: 30 – 80 mm)
    j. Dog bone length (range: 350 – 460 mm)
2. Output parameters
    a. Maximum base shear force
    b. Maximum normal stress in the flanges of the beam
    c. Maximum shear stress in the web of the beam
    d. Equivalent maximum stress in the beam
    e. Maximum plastic strain

Sensitivity study results

Using this input and output parameters, deterministic + stochastic sensitivity analysis was carried out using the optiSLang (Optislang, 2013) for Ansys WB (Ansys, 2012). A dynamic sampling using Advanced Latin Hypercube Sampling (ALHS) was used with a population of 500 samples. In Figure 13 is presented the influence of input parameters on the output parameters.
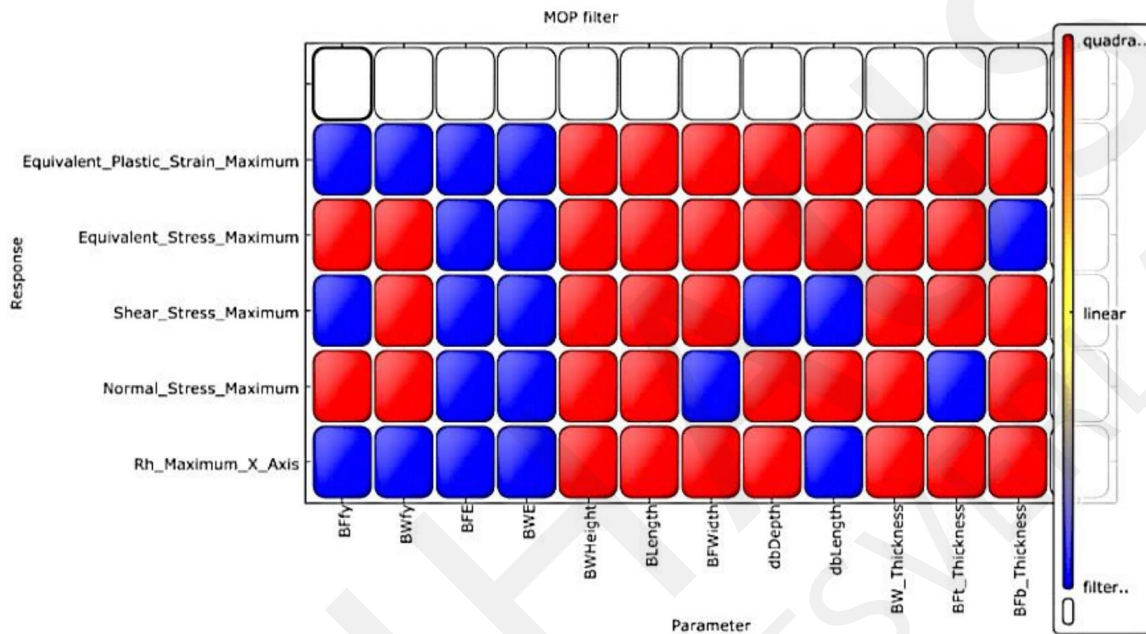

Figure 13. Filter model

Considering the output parameters, in Figure 14 to Figure 17 are presented the response surfaces for the most important input variables for each output parameter together with the coefficients of prognosis for the meta-model of optimal prognosis (MOP).
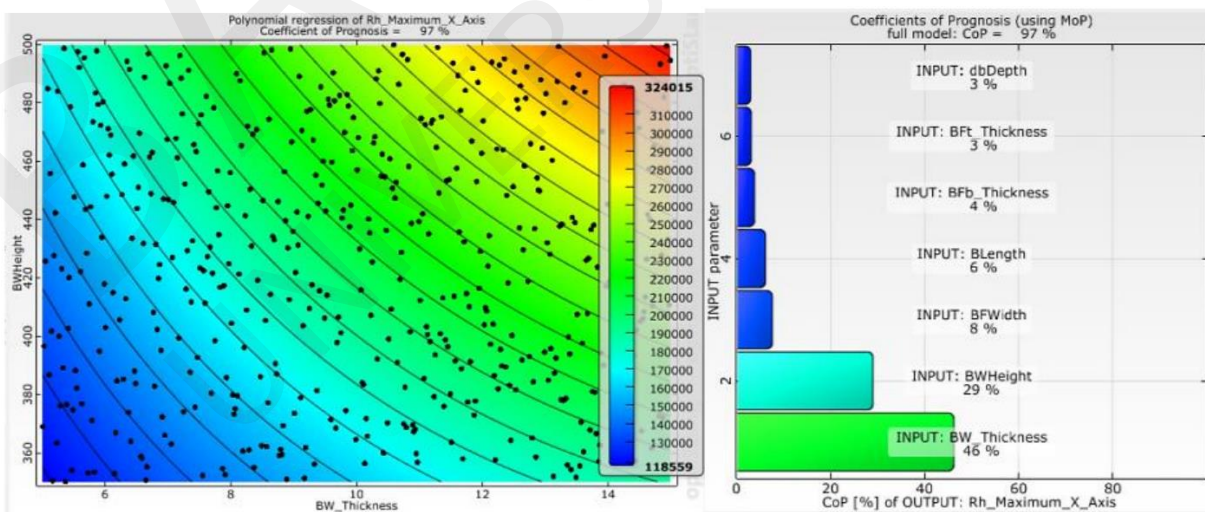

Figure 14. Response surface and coefficients of prognosis for base shear force
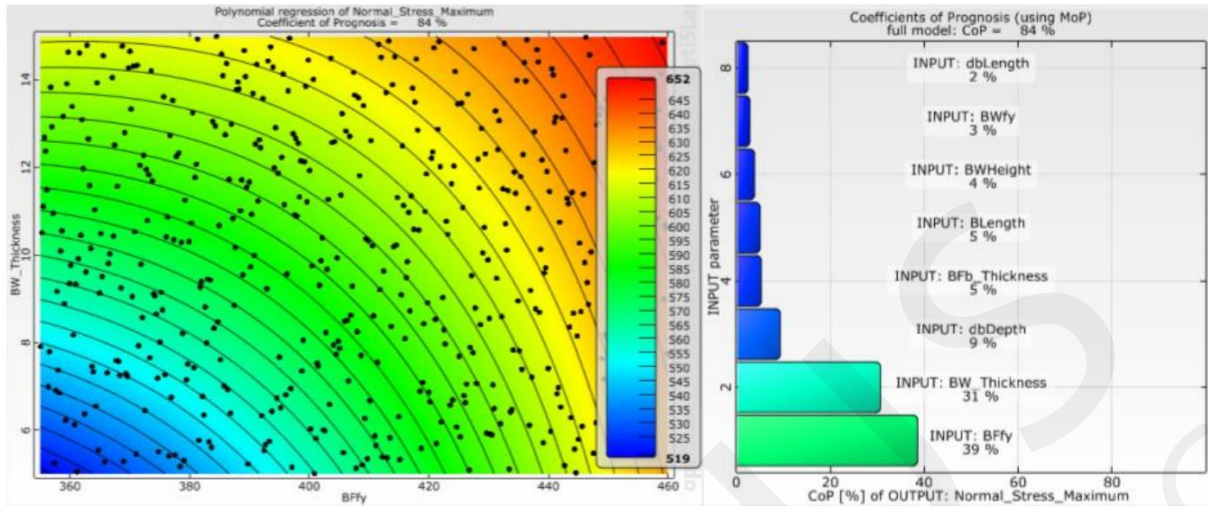
Figure 15. Response surface and coefficients of prognosis for maximum normal stress in the flanges
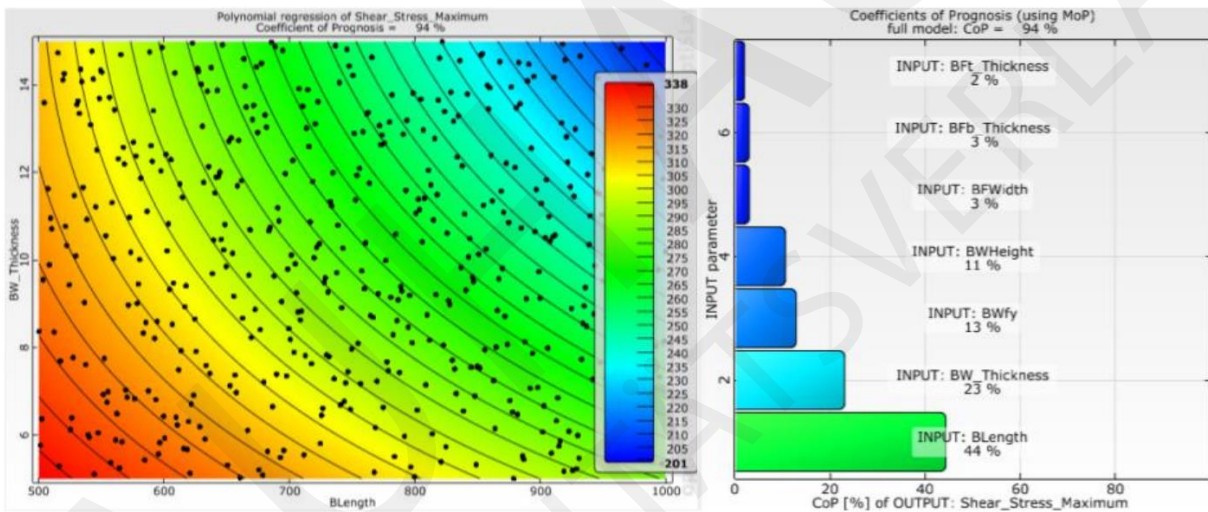

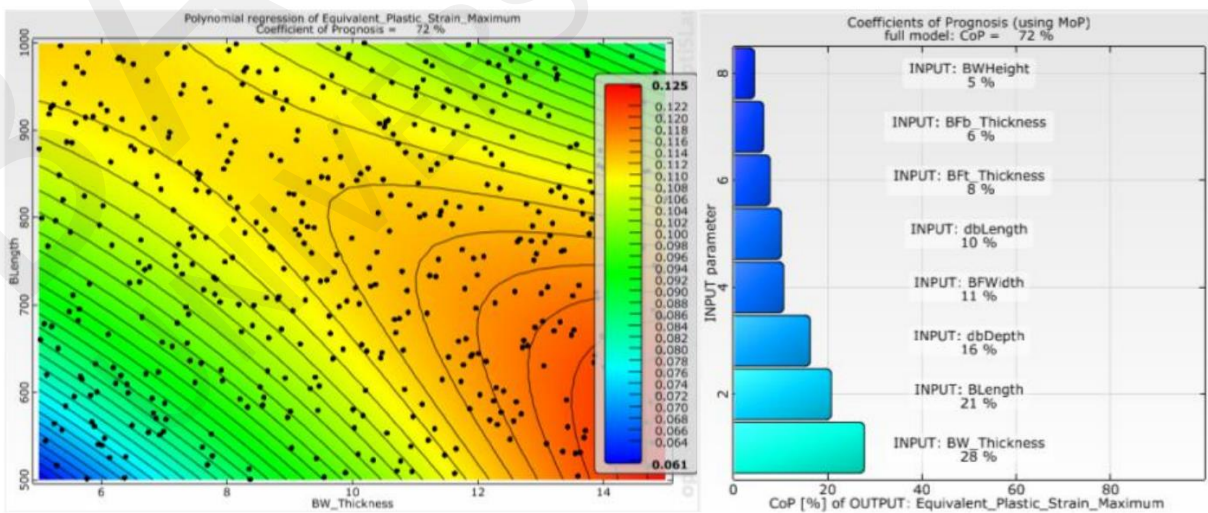**Figure 16.** Response surface and coefficients of prognosis for maximum shear stress in the web

Figure 17. Response surface and coefficients of prognosis for maximum plastic strain

52

Concluding remarks

Considering the results of the sensitivity study the following remarks can be made:

The value of the yield stress in the flanges influences only the maximum value of the normal stresses in the flanges. Since the design of seismic resistant steel structures is done in the plastic domain, it can be said that the influence of the yield stress is limited, having a limited influence on base shear force and plastic strain.

The Young moduli have limited or no influence on all output parameters and in the subsequent sensitivity analyses they should not be considered.

Due to the fact that the beam flange width was reduced to change the location of the plastic hinge, the geometry of the dog bone have become more important than the beam overall dimensions. The role of initial beam dimensions is to ensure the over-strength for the beam to column connection in accordance with the P100 (or EUROCODE 8) provisions.

The beam web thickness is an important parameter to be considered in design of short coupling beams. Even if, for the case of maximum shear stress, the beam length is more important, in Figure 17 it can be observed that, for the case of plastic deformations, the web thickness is the most important parameter.

References

ANSYS Release 14.5 documentation, Theory reference for ANSYS and ANSYS Workbench 14.5, ANSYS Inc., Canonsburg, Pennsylvania, USA, 2012

Budaházy V., Dunai L. (2013). "Parameter-refreshed Chaboche model for mild steel cyclic plasticity behaviour", Periodica Polytechnica, Civil Engineering 57/2 p.139–155.

Dinu F., Dubina D., Neagu C., Vulcu C., Both I, Herban S., Marcu D. (2013). "Experimental and numerical evaluation of an RBS coupling beam for moment-resisting steel frames in seismic areas", Steel Construction, Vol. 6 (1), p. 27–33.

Optislang 4.1.0, Dynardo GmbH, Steubenstraße 25, 99423 Weimar, Germany

Calibration of engineering and climate models

JAOUADI Zouhour, JORGE Pedro, KAMAN Csaba, KIAN Rozita, KOCAMAN Bülent, KURTOGLU Ahmet Emin, FLORICEL Andra-Daniela

LAHMER, Tom

Abstract. This work aims to apply some optimization methods for the calibration of engineering and climate model. Gradient based methods and gradient free method (Nelder-Mead method) are selected as optimization strategies for a 1D climate model. The model considers temperature varying only in latitudes. In this paper, several measured temperatures for water and land are regarded to make applicable the optimization process. Some of the parameters of the climate model are used as optimization variables. Some results and conclusions are presented.

Introduction

Today's highly capitalized societies require maximum benefit with minimum cost. In order to find a low cost design in practice, experienced engineers have traditionally used trial-and-error methods based on their intuitive engineering sense. However, their approaches have not guaranteed optimal or near-optimal designs, therefore researchers have been interested in optimization methods [1]. The ability of engineers to produce better designs has been severely limited by the techniques available for design optimization.

There are many methods to apply in optimization solutions, two of them which are suitable for convex functions are discussed in this project; gradient based methods and direct search methods (gradient free): Nelder-Mead method. Gradient free methods are applied mostly when the analytical gradient cannot be computed or when the values of function are contaminated with noise [2].

In this article an application of the two optimization methods on a 1D climate model was made based on the research work of Jonathan Fivelsdal [3]. This model considers the temperature varying only in the latitudes. For calibration purposes, measured temperature data were used. It was considered different measured temperatures for water and land and selected different parameters to be the variables of the optimization process. Some results and conclusions are presented.

Optimization methods

Nelder-Mead method

Nelder-Mead Method as a gradient free method and heuristic search method is a pattern search method for use on unconstrained nonlinear models. It is also known as the downhill simplex method or the flexible polyhedron method. The Nelder-Mead simplex algorithm finds a minimum of a function of several variables without differentiation. It is easy to use and will converge for a large class of problems [4].

The Nelder–Mead technique was proposed by John Nelder & Roger Mead (1965) [5]. This method uses the concept of a simplex which is a special polynomium type with $N + 1$ vertices in N dimensions.

The method approximates a local optimum of a problem with N variables when the objective function varies smoothly and is unimodal. In general the performance of the Nelder-Mead algorithm is good in practice. Also when the iteration stagnates, a restart with the same best point and a different set of directions can help. But this algorithm is not guaranteed to converge and the failure mode is stagnation at a non-optimal point. Nelder-Mead in a MATLAB program seeks to minimize a scalar function of several variables, by Jeff Borggaard [6].

The Nelder-Mead algorithm starts with a simplex in domain of the function to be minimized, then modifies the simplex five different ways until the simplex is very flat (function value is almost the same at all the vertices), at which point the minimum is the vertex with the smallest function value. Usually when the minimum is found the simplex is very small. The five transformations of the simplex are: reflection, expansion, outward and inward contraction, as well as shrink [7].

Extended gradient-based method

Deterministic methods are mostly gradient-based. Since these methods use gradient information and the objective functions in many engineering optimization problems are not differentiable, they cannot be applied to problems where the objective function is discrete or discontinuous or the variables are discrete. On contrary, in problems where the derivative information is easily available, gradient-based methods are very efficient. However, the concept of gradients in understanding the working principle of the optimization algorithm is so intricate that gradient-based methods are mostly used in engineering design problems by calculating the derivatives numerically. Even when gradients are not available directly, various techniques for estimating their values can still make gradient-based search methods the best choice for many optimization problems [8]. Very common extensions for gradient-based parameter identification are the Newton method and Quasi-Newton method.

Many quasi-Newton methods are advantageous due to their fast convergence and absence of second-order derivative computation [9]. These methods begin the search along a gradient line and use gradient information to build a quadratic fit to the economic model. Consequently, to understand these methods it is helpful to apply the gradient search algorithm and Newton's method as background for the extension to the quasi-Newton algorithms [10].

Climate basics

Climate can be defined as a system in the atmosphere, which considers well known weather parameters, such as temperature, precipitation, humidity, air pressure, wind etc. in a short term or long term period. In this paper, long term climate analysis on a global level are considered.

The interpretation of climate change according to Wikipedia is the following: *"Climate change is a significant time variation in weather patterns occurring over periods ranging from decades to millions of years. Climate change may refer to a change in average weather conditions, or in the time variation of weather around longer-term average conditions...Certain human activities have also been identified as significant causes of recent climate change..."* [11].

The human induced change in weather patterns is often explained by the greenhouse effect. The sun emits short wavelength radiation, which is mostly absorbed by the earth, however some part is reflected in the form of long wavelength radiation.
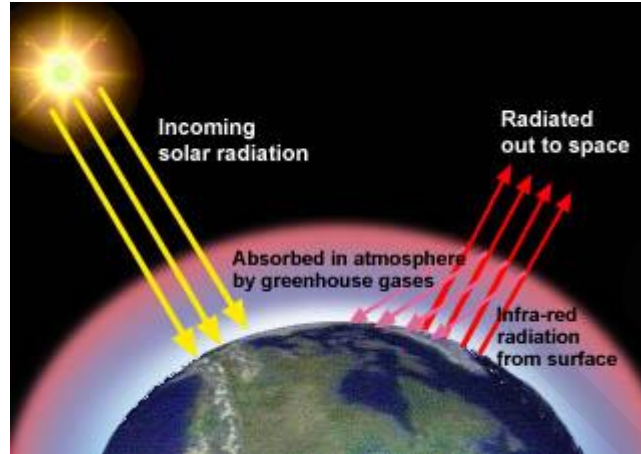
Figure 1. Greenhouse effect [11]

Some part of this long wavelength radiation is blocked by the atmosphere, and the remaining part passes through it (see Figure 1). The greenhouse effect refers to the atmosphere's ability to block this long wavelength radiation. The albedo of the surface is a ratio that represents the amount of radiation, what is reflected by a surface. Earth's average albedo is 30%, which means that the Earth absorbs most of the incoming solar radiation.

The total amount of solar radiation received by an average point on the earth is approximately 343 W/m², however the solar constant is about 1380 W/m². The difference between the average value and the solar constant can be explained with the spherical form and the fact, that at a given time only one half of the planet receives sunlight.

The atmosphere is a complex system which includes several feedback loops. It consists negative feedbacks (self correcting effect: increase in consequence generates decrease in cause), and positive feedbacks (self reinforcing effect: increase in consequence generates increase in cause). The most important loops are the water vapour feedback, ice albedo feedback and the ocean feedback. These effects cannot be considered in the one-dimensional model, like the one was applied.

Climate modeling

If considering the complexity of a system like the climate, a wide range of models can be used. Generally four types of models are distinguished: 0, 1, 2, and 3 dimensional models. The most important parameter of the climate is it's temperature. So if only that parameter are considered, the Earth's temperature can be examined in one point (0 dim.). It's also possible to make it along a line, considering the latitudes (1 dim.), or similarly in 2 dimensions, considering latitudes and longitudes. For a more advanced model also a 3rd dimension is applicable, the altitude.

In the project a one dimensional model was applied, with the following governing equation (1):

$$\frac{\partial T(t,y)}{\partial t} = \frac{1}{\rho c_p h} \times \left[Qs(y)(1-\alpha) - I + D \right] \qquad (1)$$

where $T(t,y)$ is the average temperature of a given altitude (y) in a given time (t). ρ is the average density of the surface on a latitude, c is the specific heat of the surface.

Q is the average solar radiation (343W/m²), α is the albedo, I is the outgoing long wave radiation, calculated from Sefan-Boltzmann law, s(y) is the latitude distribution of heat and D is the diffusion.

In the 1D climate model, which is based on the research work of Jonathan Fivelsdal [3] four fictive land configurations were used. Type 1 represents a model, where land is on the poles only, with an overall land ratio of 39%. Type 2 represents a case, where land is on the poles and on the tropics (land ratio of 65%). Type 3 considers land on the tropics only (land ratio of 26%). And type 4 considers land mostly in northern hemisphere (land ratio of 39%).

Applications and results

For the climate model the parameters shown on the Table 1 are considered. In Figure 2 both measured and calculated temperatures are presented. The blue and green curves are the model solutions with the initial guessed parameters and represent the temperature on the rock and on the water, in each grid of the earth. Both red and blue point plots represent the measured temperature on the rock and on the water, respectively.

Table 1. Initial parameters for the climate model

Bolzman constant		5,6686E-8	K⁴m²
Global mean solar flux		343	W/m²
Rock	Specific heat capacity	850	J/(K Kg)
	Density	2400	Kg/m³
	thickness of thermally active layer	3	m
Water	Specific heat capacity	4200	J/(K Kg)
	Density	750	Kg/m³
	thickness of thermally active layer	50	m
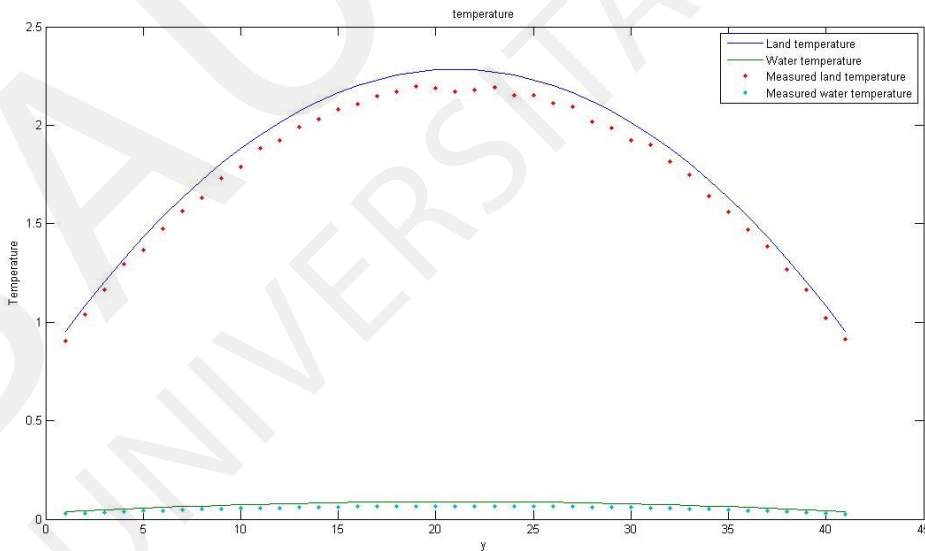
**Figure 2.** Measured and calculated temperatures

In the Figure 2 exist a difference between the numerical model and the measured data. This difference explains the necessity of a calibration of the numerical model. Two parameters were selected for this process: the density of the rock and the density of the water.

a) bi-dimensional   b) tri-dimensional
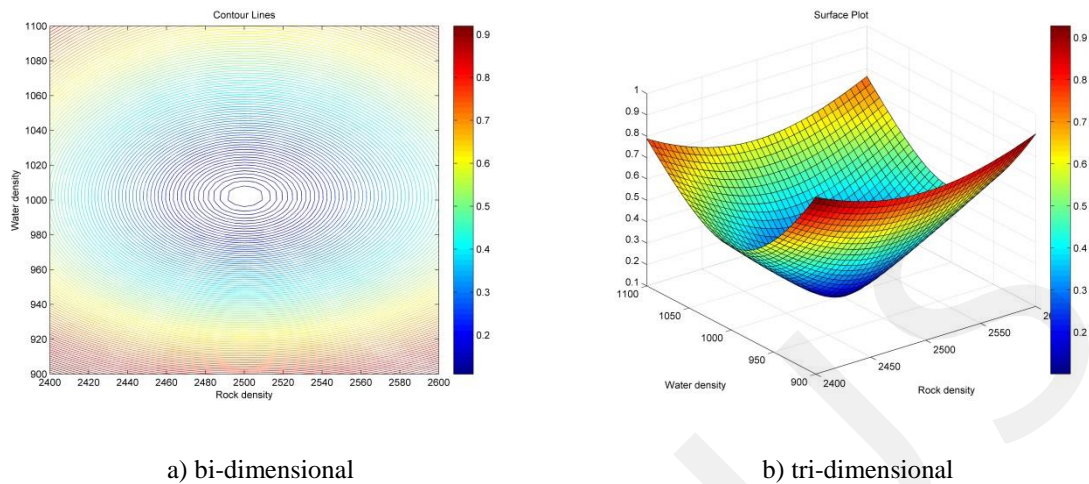
Figure 3. Contour lines for the density of the rock and the water

Independing of the land type and the initial temperature, the temperature registered in the land is higher than the temperature of the water. That can be analyzed as the earth is a blackbody since it absorbs most of the incident solar radiation. However, for the water and according to its character, it transfers the solar radiation.

The initial model has some issues because only the parameters of the rock of the land type 1 on the calibration process were considered. Some improvements are required to consider all the land types and to take into account the temperature of the water and the rock for the optimization. The results obtained by the contour lines for this optimization problem with two variables, the water density and the rock density, shows a global minimum for these boundaries and the two parameters have both a great influence on the optimization process. This is an example of a convex optimization process. In the Figure 3 the contour lines are illustrated.
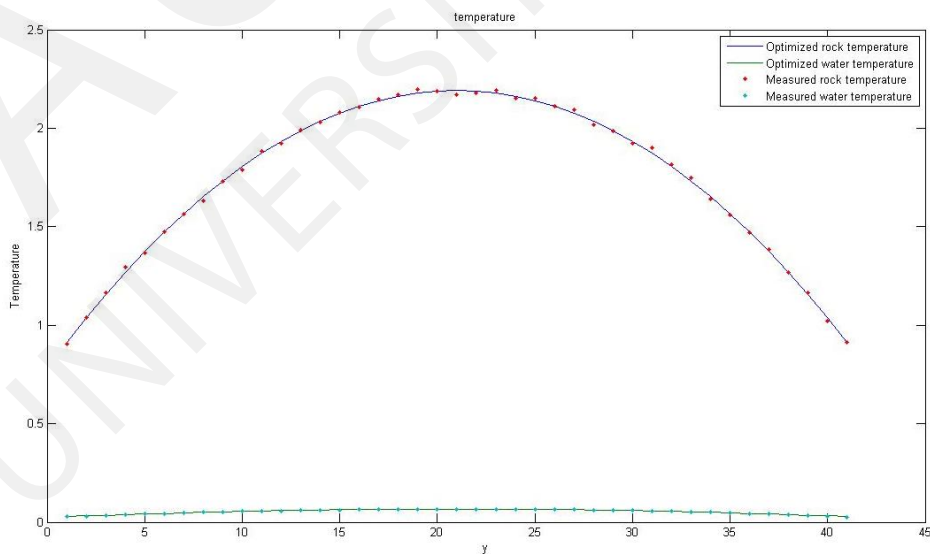
Figure 4. Temperatures for the model with the calibrated values

Applying the Nelder-Mead Method or the extended gradient based method, it is possible to find with less than 100 iterations the new values of the density of the rock and the water. The Nelder-Mead Method is faster than the extended gradient based method. The optimum values for the two densities are 2500 for the rock and 1000 for the water. After running the model with these new parameters, new curves are obtained (see Figure 4). The results gathered reveal good coherence between the two measured and calculated values of the temperature.

To see the effect of the other parameters on the optimization process, different parameters were considered. Not all parameters should be considered on the calibration because some of them are related and their influence didn't appear. For example, the density and the thickness of the rock were considered. The influence of the thickness was almost null, as shown in the Figure 4.

The conclusion made in the Figure 4 can be extended to the other parameters. In the case of the rock, the three parameters: the specific heat capacity, the density and the thickness are related, because they are used to calculate the heat capacity. The same conclusion can be made for the water.

Trying to make an optimization of the example shown in Figure 4, new optimized values of these parameters are obtained. This solution didn't reflect the correct results, because it is only a mathematical solution with no physical significance. This is a common mistake in the optimization problems when the user hasn't a sufficient knowledge of the numerical model.

Conclusion

In this work, two optimization methods were applied: the gradient based method and the Nelder-Mead method which are implemented in Matlab. The two methods gave good results, however, the Nelder-Mead method was faster in the considered model. The choice of the best optimization method depends on the problem.
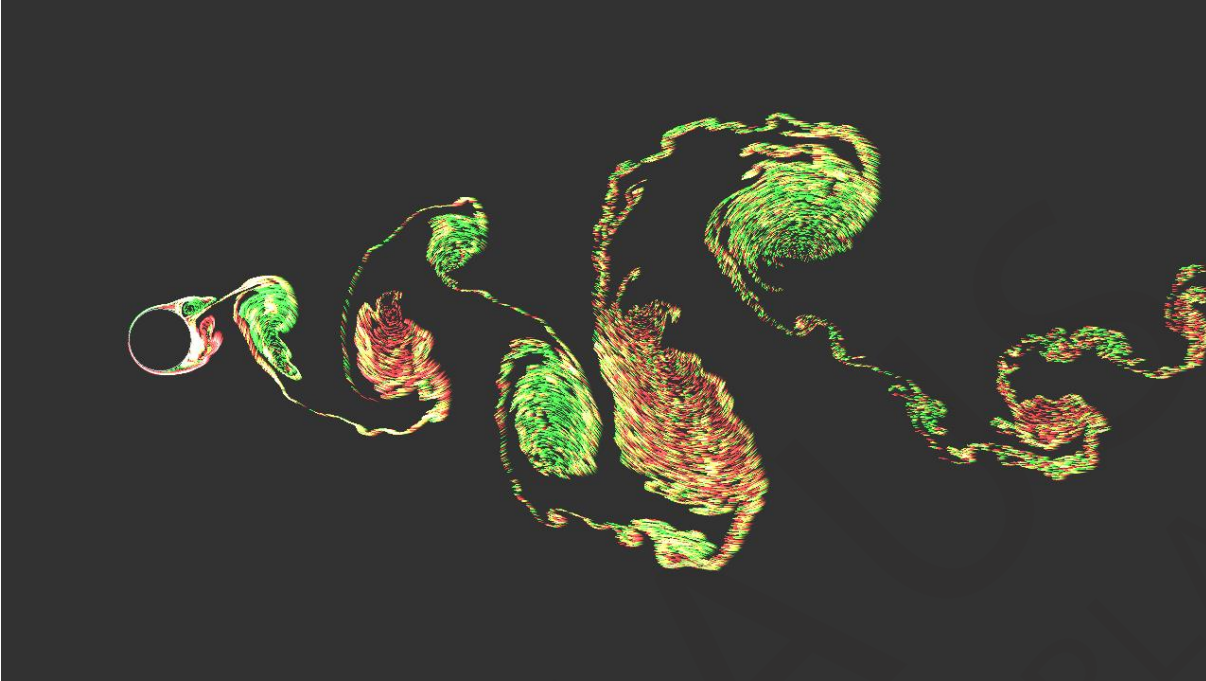
In this paper, only the 1D climate model was applied. This work can be extended to the 3D model were many other parameters should be considered and the work then will reflect the real behaviour of the climate. To control the optimization process, the user should have a good knowledge of the model in order to choose the best parameters that have a significant effect on the response of the model.

a) bi-dimensional   b) tri-dimensional
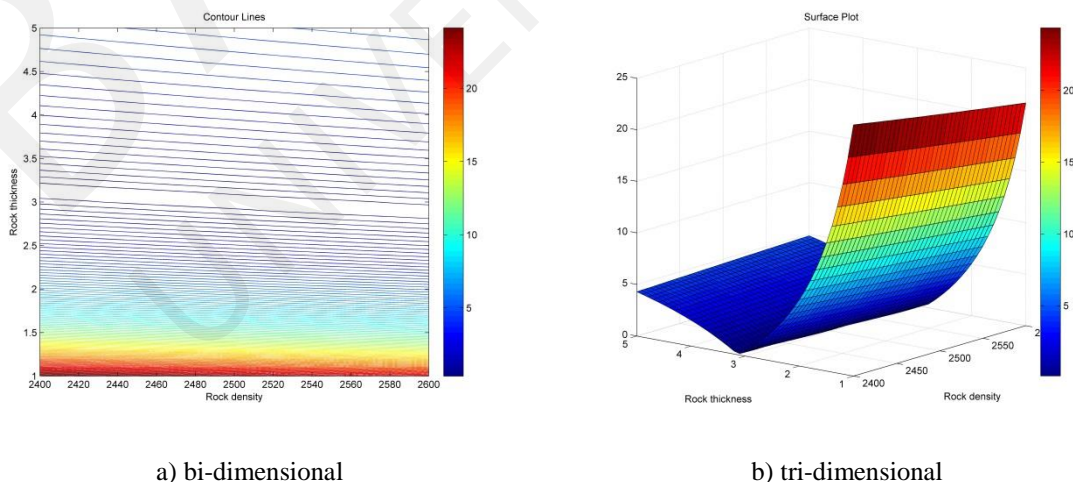
Figure 5. Contour lines for the thickness and the density of the rock

References

1. Geem, Z.W., Optimization in Civil & Environmental Engineering. 2012.

2. Lahmer, T., Calibration of Enginering and Climate Models. Lecture Notes, 2014.

3. Fivelsdal, J., Simulating Global Climate Using A Simple Model. A Senior Project submitted to The Division of Science, Mathematics, and Computing of Bard College, 2010: p. 39.

4. http://optlab-server.sce.carleton.ca/POAnimations2007/NonLinear7.html. August, 2014.

5. Nedler, J.A., Mead, R., A simplex method for function minimization. The computer Journal, 1965.

6. http://people.sc.fsu.edu/~jburkardt/m_src/nelder_mead/nelder_mead.html. August, 2014.

7. http://online.sfsu.edu/meredith/Numerical_Analysis/nelder-mead.pdf. August, 2014.

8. Deb, K., Optimization for Engineering Design; Algorithms and Examples. Second Edition. 2012.

9. http://people.sc.fsu.edu/~inavon/5420a/qn.pdf

10. http://www.mpri.lsu.edu/textbook/Chapter6-a.htm#quasi

11. http://en.wikipedia.org/wiki/Climate_change. August, 2014.

12. http://www.weather-climate.org.uk/15.php. August, 2014.

Wind-induced vibrations of long-span bridges

MORGENTHAL Guido
Chair of Modelling and Simulation of Structures, Bauhaus-Universität Weimar, Germany

The project deals with the structural modelling and dynamic analysis of long-span cable-supported bridges under wind excitation. In 4 sub-groups the participants of the project are trained within the:

- Numerical modelling techniques for long-span cable-supported bridges;
- Simulation of dynamic structural behaviour;
- Models for Predicting Wind-induced Vibrations of Long-span Bridges;
- Numerical (CFD) analysis of bridge aerodynamics and dynamic response to wind;
- Optimising aerodynamic performance.

In the course the participants first looked at methods of modelling the structural behaviour of such bridges, specifically cable-stayed and suspension bridges, in commercial Finite Element software. The specific focus was on determining the dynamic properties, like natural frequencies and corresponding mode shapes. In the next step, various phenomena of dynamic wind excitation were introduced. These include turbulence-induced buffeting, vortex-induced vibrations and instabilities like flutter. A Computational Fluid Dynamics (CFD) software was introduced and applied to determine the aerodynamic properties of bridge decks. These results were used to assess the wind excitation phenomena using various analytical and numerical methods. Also fully coupled numerical fluid-structure interaction analyses were performed.

Buffeting response of the Mersey Gateway Bridge Main Crossing

ABERLE Markus, KIM DaeYoung, LOPEZ TORO Carolina

Abstract. The displacement response due to an incoming turbulent wind was obtained for a cable stayed bridge spanning 998 m over the Mersey River (United Kingdom). Using the commercial software SOFiSTiK, the wind-time histories of the wind fluctuations were calculated, as well as the dynamic response of the bridge (Eigen modes). Afterwards, the static wind coefficients, needed for buffeting analysis, were obtained from VXflow, a vortex particle based Computational Fluid Dynamics (CFD) code. Further computations need to be performed in order to get the dragging and lifting forces, as well as the section moments.

Introduction

The Mersey Gateway is a cable-stayed bridge that will connect the towns of Runcorn and Widnes, in the United Kingdom. The main crossing of the bridge, spanning over the Mersey River, has a length of 998 m as shown in Figure 1.
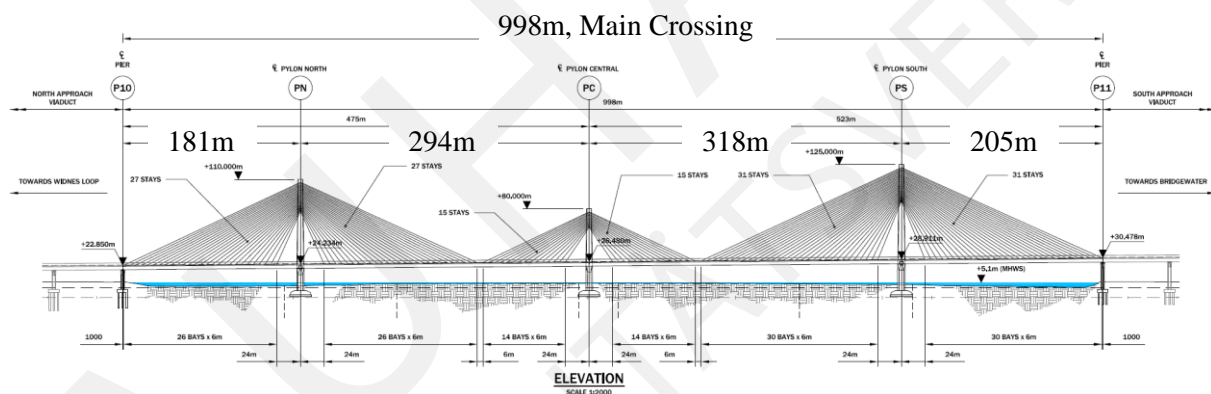

**Figure 1.** Mersey Gateway Bridge main crossing: Structural drawings.

Being a cable-stayed bridge, this structure is under the influence of various wind induced phenomena such as vortex induced vibrations, buffeting, and wake induced vibration. Wind loads can also produce instabilities like galloping, flutter or divergence in flexible structures like bridges supported by cables. For this project the aerodynamic phenomenon of buffeting was chosen as main topic. The following paragraphs give more information about such phenomenon and its influence in the study case.

Buffeting definition

For structural engineering purposes, buffeting can be defined as the movement of a structure caused by turbulent air flow, in other words, displacements caused by wind flow with randomly changing properties.

For this project, the buffeting analysis was performed based on the static wind coefficients of the deck section. Such coefficients can be obtained from a CFD simulation. A vortex-particle-based CFD code named VXFlow was used to calculate the coefficients of the deck section.
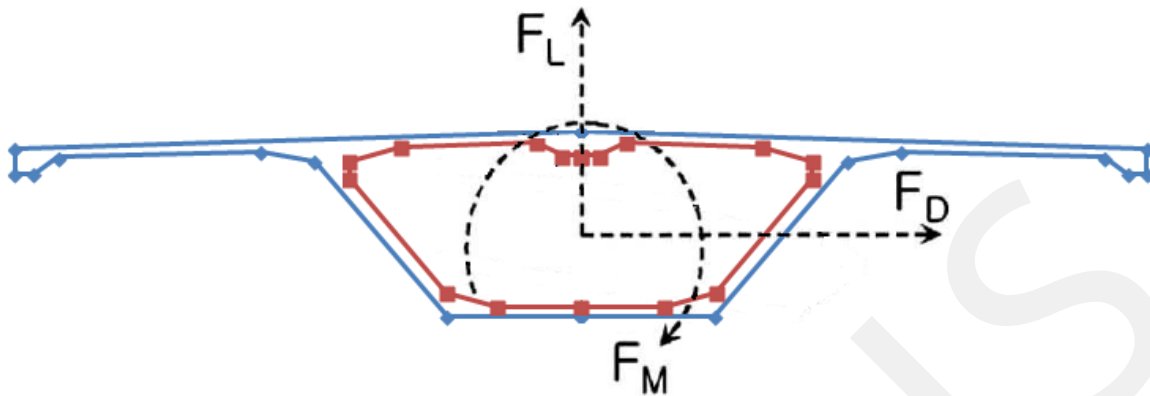
Figure 2. Degrees of freedom for buffeting.

There are three wind coefficients needed for the analysis: drag coefficient, lift coefficient and pitching moment coefficient.

These coefficients can be expressed as:

$$C_D = \frac{F_D}{\frac{1}{2}\rho U^2 D}, \quad C_L = \frac{F_L}{\frac{1}{2}\rho U^2 B}, \quad C_M = \frac{F_M}{\frac{1}{2}\rho U^2 B^2} \tag{1}$$

Where:
ρ = 1.20 kg/m3, density of the fluid (air)
B = 33 m, deck width
D = 4.60 m deck depth
U = 25 m/s2, mean wind speed

Wind time histories

In order to do the buffeting analysis, it was first necessary to model the wind-time histories of the wind fluctuations. This task was performed using a commercial finite element package called SOFiSTiK, which can simulate correlated wind-time histories for a given wind profile and a specified wind-spectrum (Figure 3). Hence, wind-time histories were generated on two 50m×475m reference planes perpendicular to the mean wind direction (Figure 4). The spacing of the two reference planes, as well as grid spacing within each plane was 0.5 m. This resulted in a total 2×96051 numerically generated time histories.
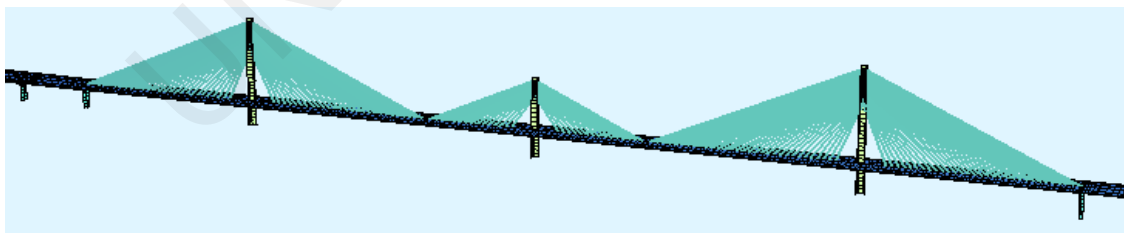
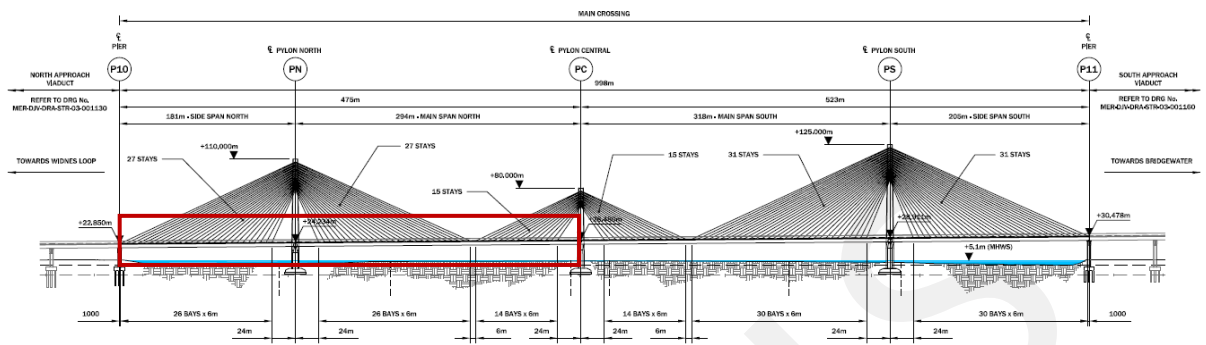**Figure 3.** Mersey cable-stayed bridge (FEM-Model)

Figure 4. Mersey cable-stayed bridge (reference plane)

The numerically simulated time history of the turbulent wind, which had a time length of 600s and time steps of 0.2s, was based on the Karman spectrum as shown in Figure 5. However, to consider the unstable state at the beginning of the analysis, a total time length of 620s was chosen. The mean wind speed at the height of the deck (27 m) was 27.36 m/s. The turbulence intensity at the deck level was 15.6%. The effective longitudinal wave length is 269 m. The parameters describing the turbulence of the wind were taken from an available wind report.
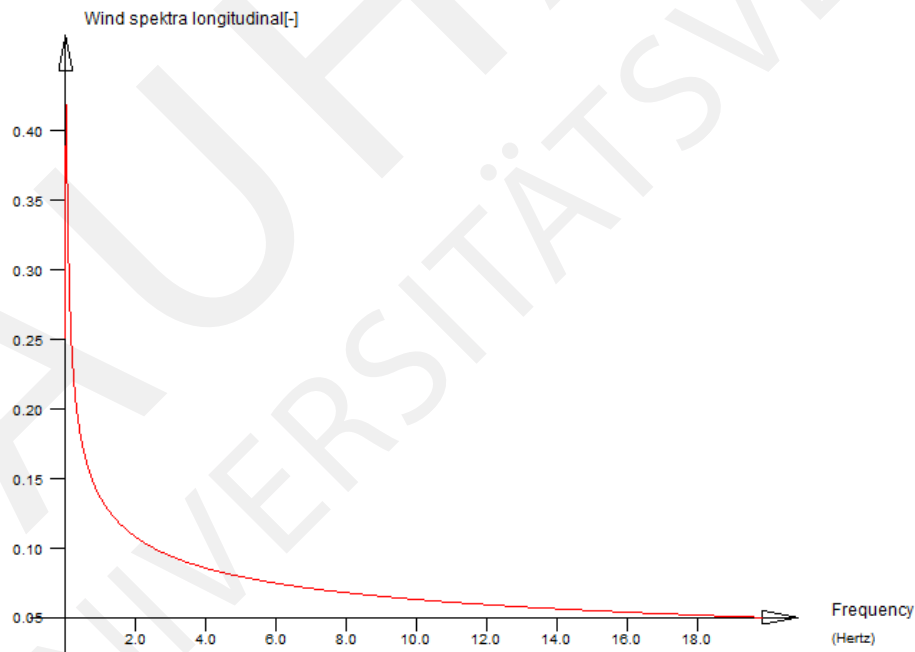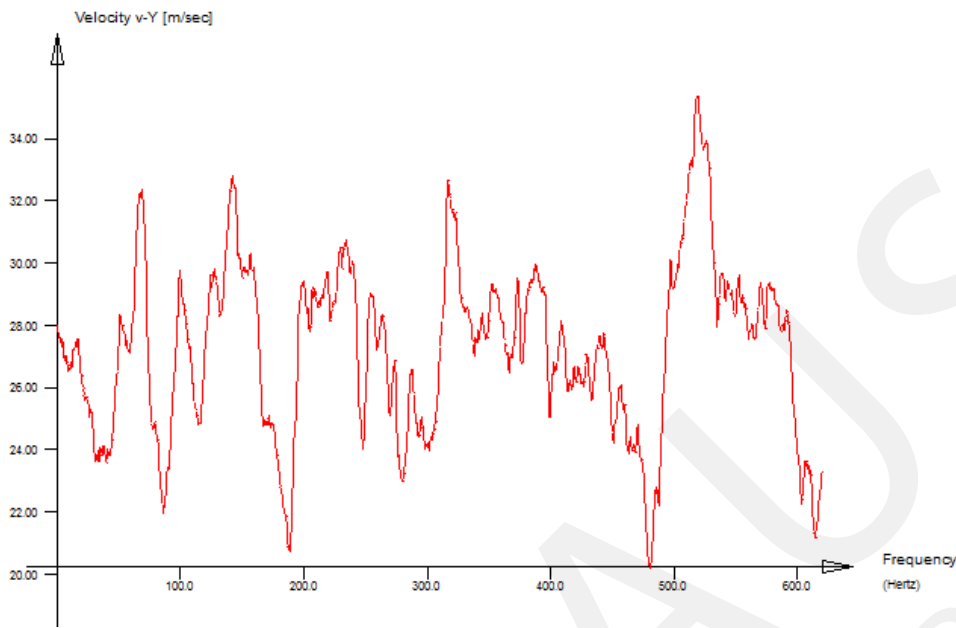

Figure 5. Karman wind spectrum

An example of such numerically generated time history is shown on Figure 6 for a point at the middle of the main span.

Figure 6. Generated time history of wind turbulence

The generated wind-time histories were then converted into vortex-time histories using a Matlab routine and used as input for VXflow buffeting analysis.

Dynamic response of the bridge

SOFiSTik was also used to obtain the dynamic response of the bridge. Many modes of vibration were generated, but it was concluded that only two vertical modes, two horizontal modes and one torsional mode were needed to capture the behaviour of the structure.

The following table and Figures 7 through 9 present information about the chosen modes.

Table 1. Modal information

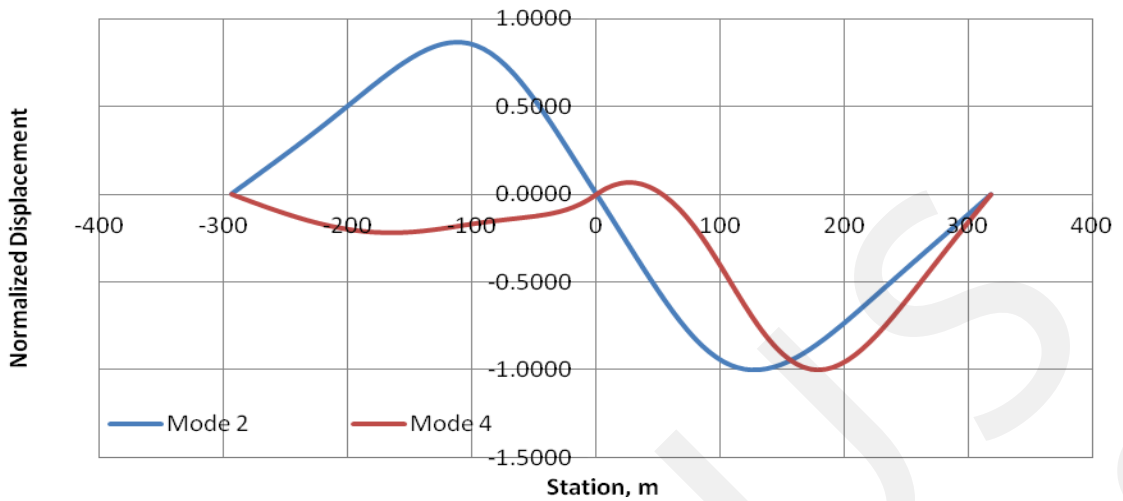| Mode Number	Mode Type	Frequency Hz	Modal Mass, Ton		Modal Damping ratio of critical damping
			North + South Span	South Span	
2	Vertical, Z	0.23	10902	6532	
4	Vertical, Z	0.32	5560	5229	
6	Horizontal, Y	0.45	8714	8395	0.005
7	Horizontal, Y	0.50	9430	1950	
18	Torsional, Rot-X	0.97	472726	464616	

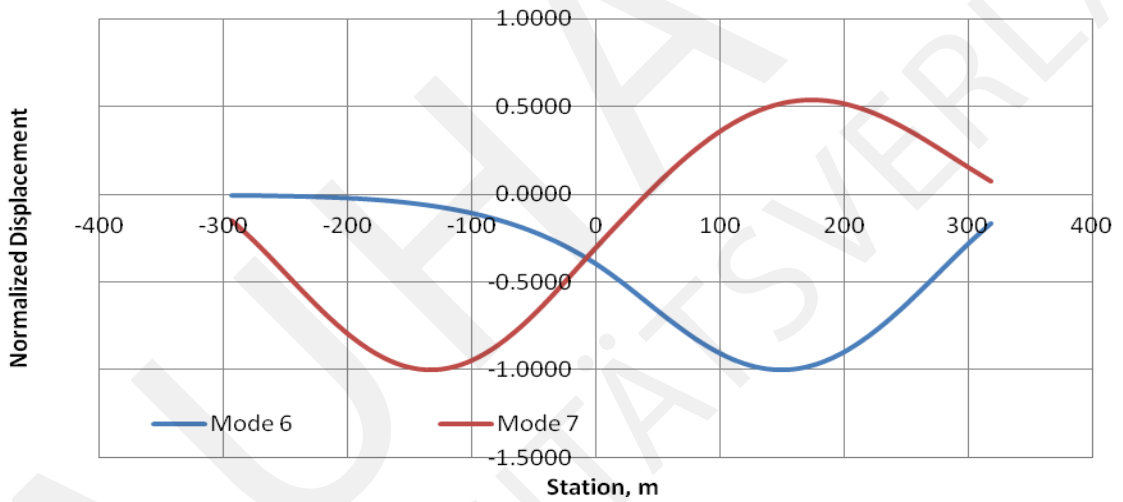**Figure 7.** Vertical Modes, Z.

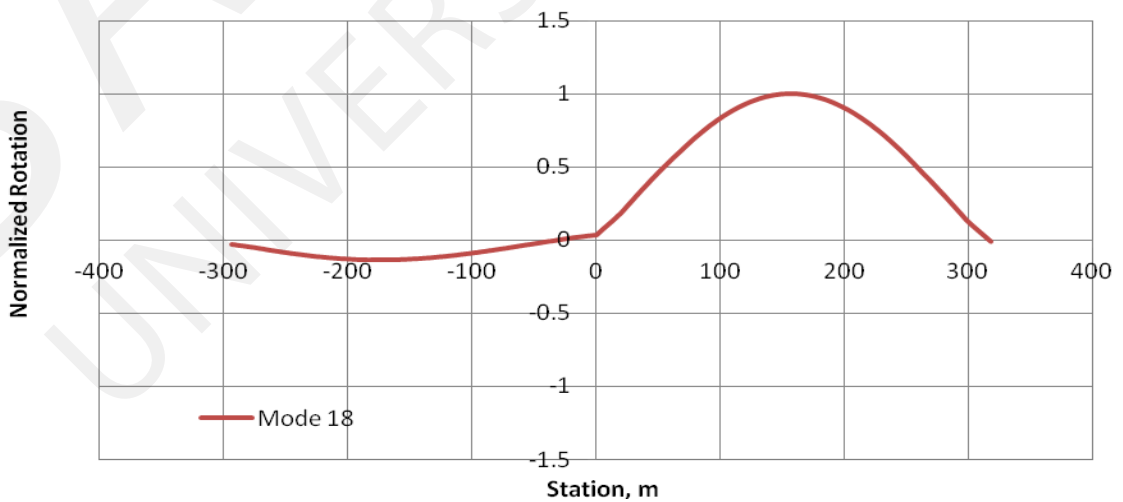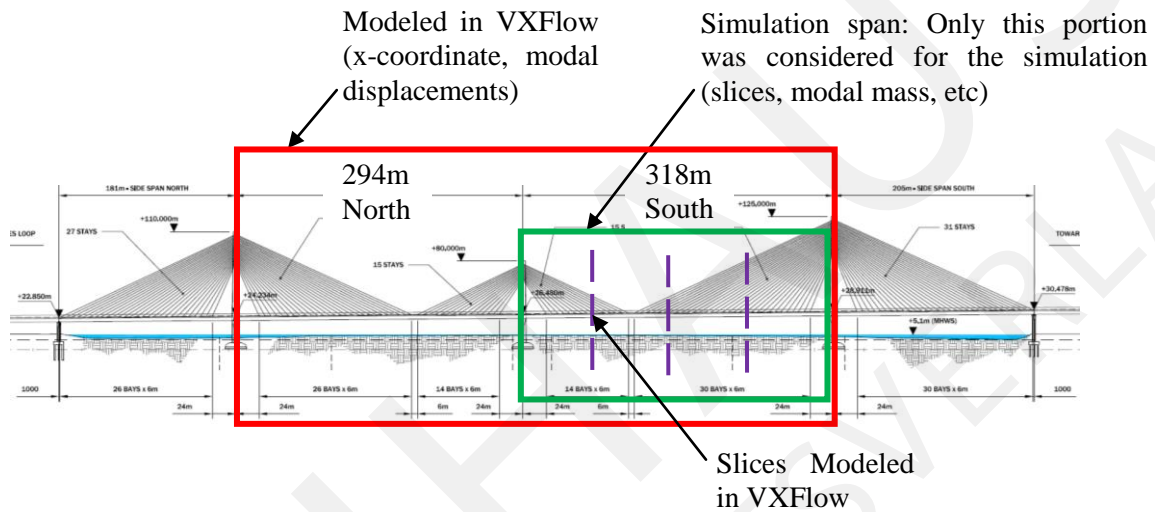**Figure 8.** Horizontal Modes, Y.

Figure 9. Torsional Mode, Rot-X.

VXFlow model definition

The following Figure 10 and Table 2 present information about the input information for VXFlow.

Table 2. VXFlow model information

Slice X- coordinate	Tributary Length, m
79.5	119.3
159	79.5
238.5	119.3

Modeled in VXFlow (x-coordinate, modal displacements)

Simulation span: Only this portion was considered for the simulation (slices, modal mass, etc)

294m North

318m South

Slices Modeled in VXFlow

Figure 10. VXFlow model definition.

Results

The following are the results obtained for the input data described previously. After running VXFlow, a total of 600 s of simulation were obtained. As illustrated in Figure 8, after second 300 there is a drop in the number of particles, this is due to the fact that the file with the turbulent particles was only generated for 300 s. For this reason all the figures shown as results were shorten to a time of 300 s.
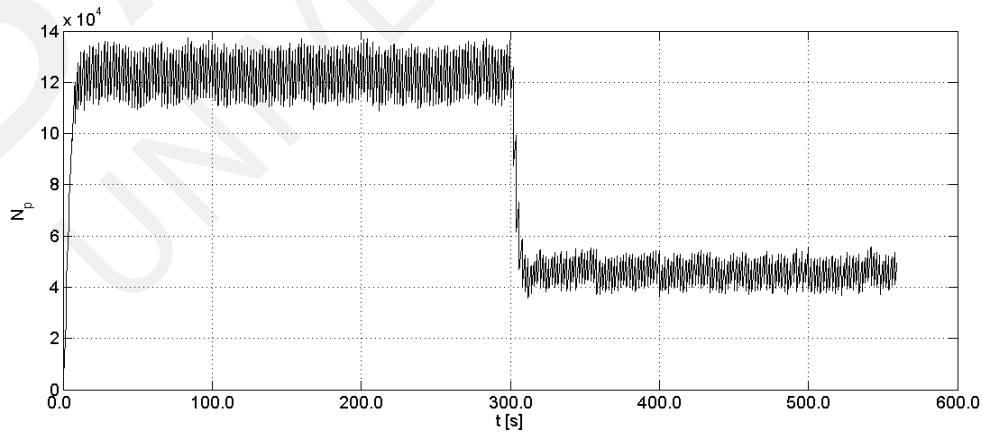
Figure 11. Number of particles for 600 seconds of simulation.

Static wind coefficients
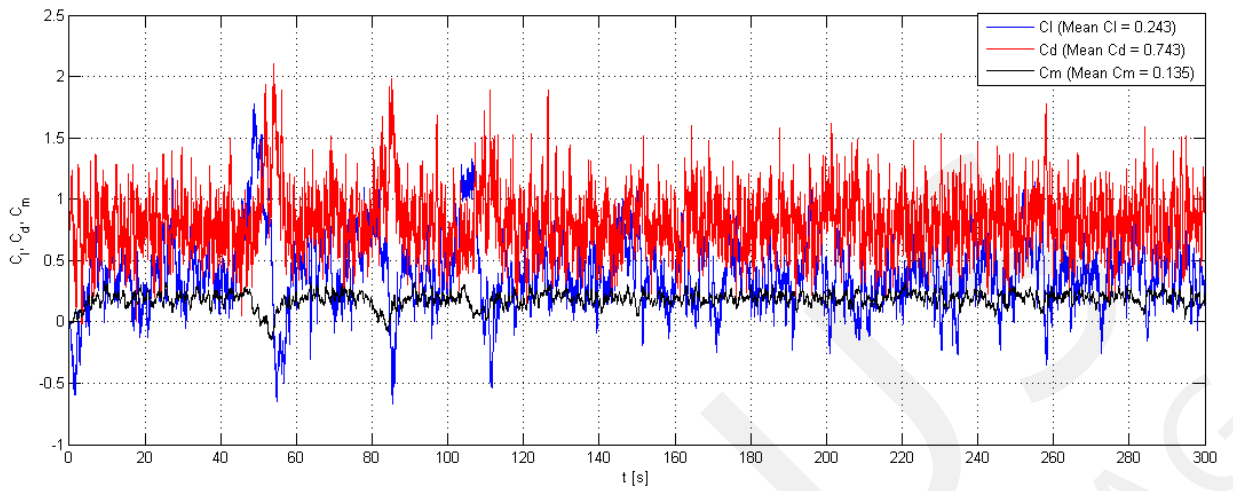
Figure 12. Static Wind Coefficient: Section 79.5 m.
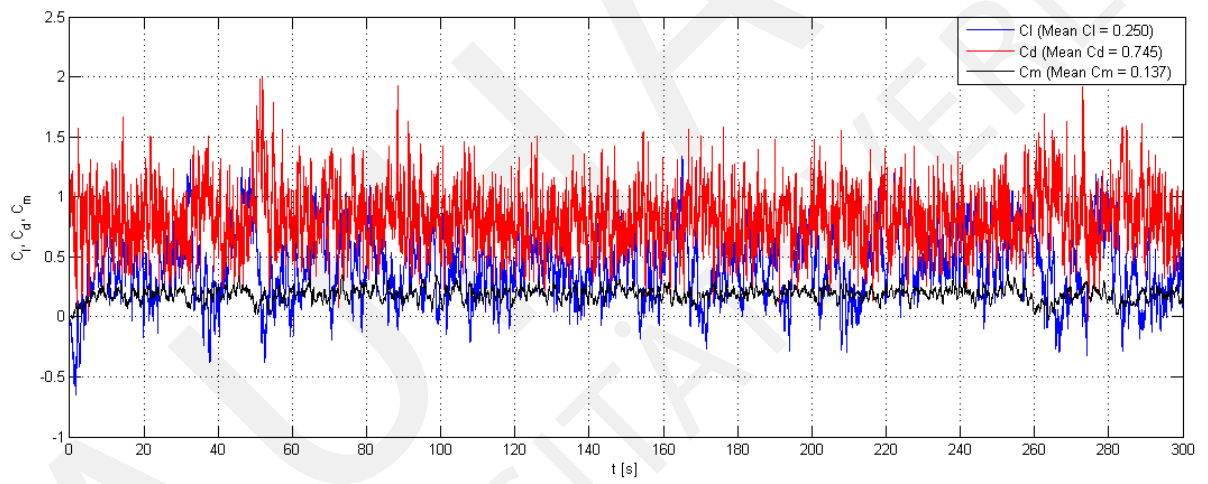
Figure 13. Static Wind Coefficient: Section 159 m.
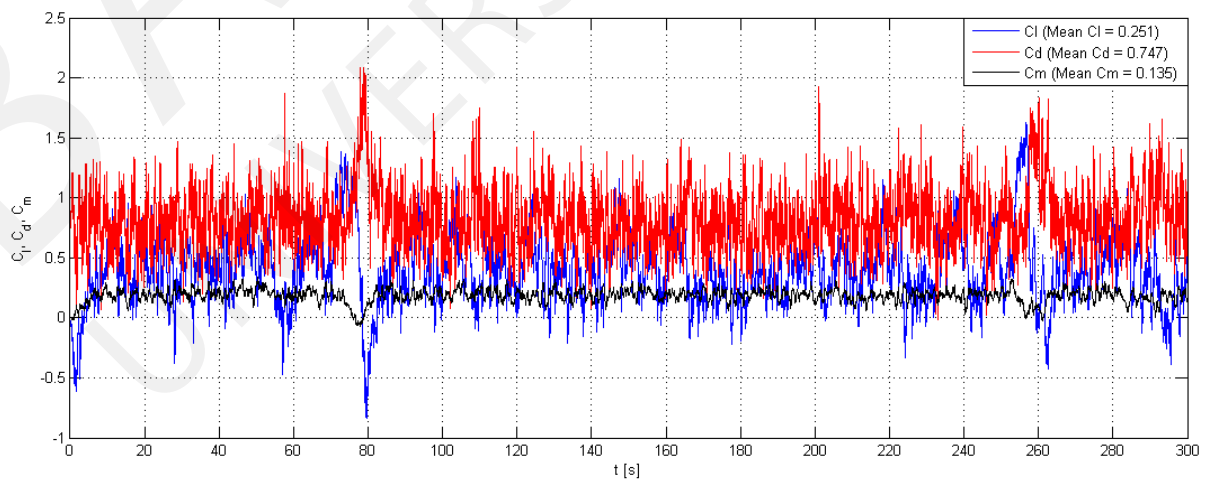
Figure 14. Static Wind Coefficient: Section 238.5 m.

Mean force coefficients on slice 79.5 m:

$$Cl=0.24344$$
$$Cd=0.74293$$
$$Cm=0.13502$$

Mean force coefficients on slice 159 m:

$$Cl=0.24969$$
$$Cd=0.74507$$
$$Cm=0.13696$$

Mean force coefficients on slice 238.5 m:

$$Cl=0.25072$$
$$Cd=0.74685$$
$$Cm=0.1354$$

Displacements
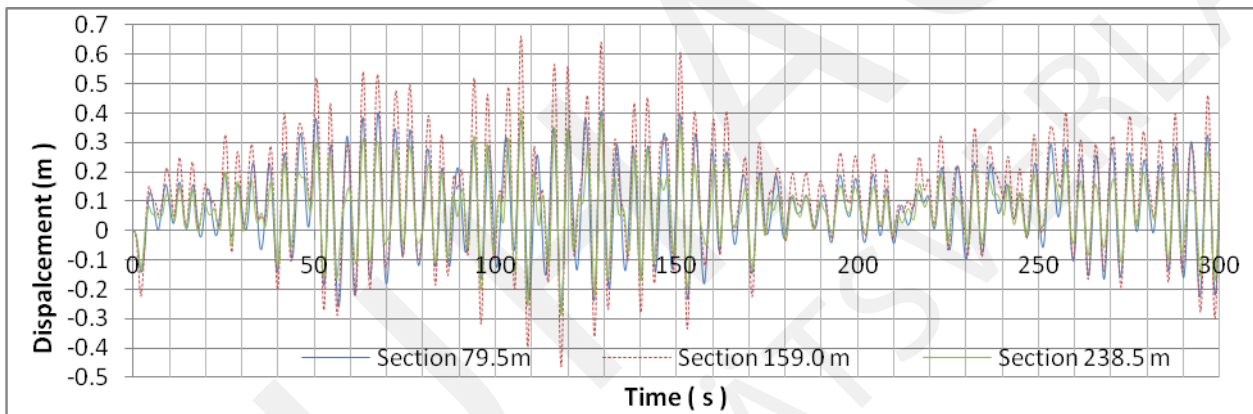
Figure 15. Vertical Displacements, Z.
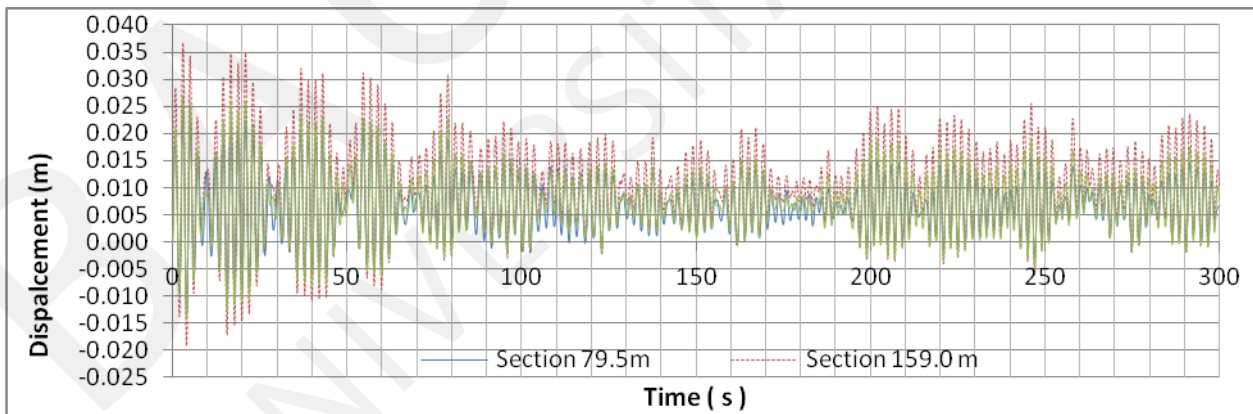
Figure 16. Horizontal Displacements, Y.
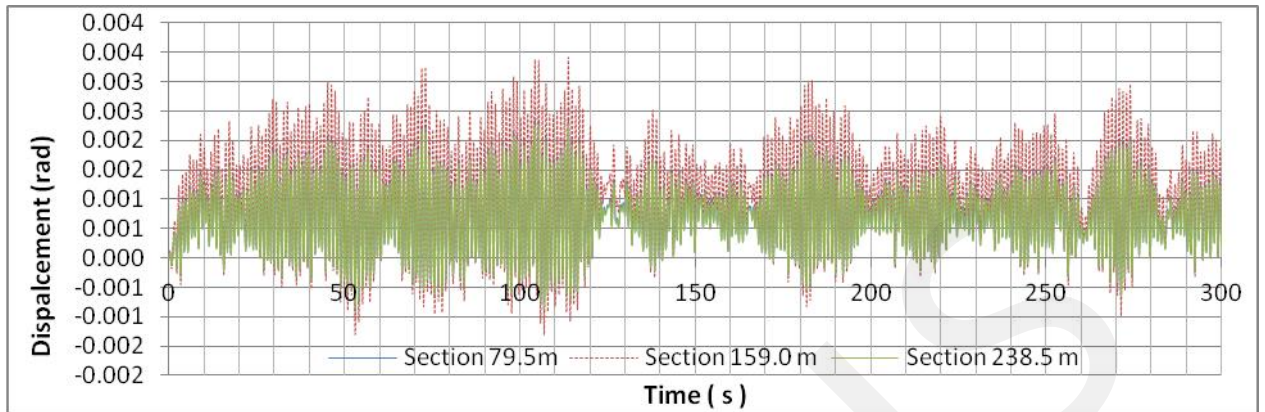
Figure 17. Rotations, Rot-X

Comments and conclusions

The previous exercise has been very educational for the authors of this report. Further analysis needs to be done in order to obtain the dragging and lifting forces, as well as the moments, based on the mean static wind coefficients and the equations (1). After obtaining the forces, structural checks need to be performed in order to ensure safety.

References

Goodrum, K. (2010). *Real planes, people and places.* Xlibris.

Kim, H.K., Choi, S.W., Kim, Y.H. (2006). Parametric Study on Buffeting Response for a Cable-Stayed Bridge. *Korean Society of Civil Engineers*, **26**: 371 – 382.

Morgenthal, G. (2013). VXflow Primer version 0.995, Weimar, Germany.

Flutter stability analysis of the Lillebaelt suspension bridge Denmark

ANAGNOSTOPULOS Danai Iris, KLASANOVIC Ivana, KAVRAKOV, Igor

Abstract. In the frame of the Project Work 6 our task was to analyse the flutter phenomenon for the Lillebaelt suspension bridge by using Sofistik, Matlab and VXflow software. The task was to determine the critical wind speed with a fully coupled CFD analysis and using hybrid model in order to understand the flutter and how it can be used for a practical problem. Visualisation was performed in VXviz and Matlab.

Figure 1. Lillebaelt suspension bridge, Denmark [http://www.phosee.dk]

Introduction

The Little Belt (Danish: Lillebælt) is a strait between the Danish island of Funen and the Jutland Peninsula. The belt is about 50 km long and 800m to 28 km wide, the maximum depth is approximately 75 m, and contains numerous small Danish Island. The main towers are made of steel. For this bridge it will be done analytical and numerical model in order to study the fluttering effect.

Flutter is an aeroelastic phenomenon associated with the modification of stiffness and damping of structure. It is a dynamic instability that takes into consideration two degrees of freedom: the vertical displacement to the wind direction and the torsional rotation. Classical flutter is critical for cable-stayed and suspension bridges where the rotational and bending frequencies are close. Generally, flutter takes place for modes that have close frequencies and similar modal forms [CNR-DT 207/2008].This is the reason why flutter is considered for the study of the bridge.
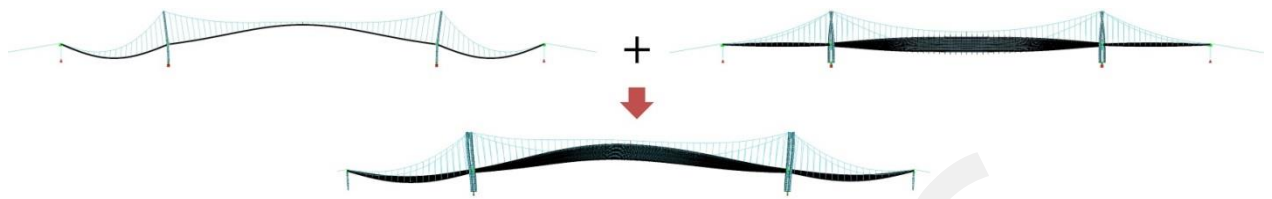
Figure 2. Flutter phenomenon

There were three proposals for a deck of this bridge. They are shown in picture below. The first one is better in order to spend less material than the other two but has some disadvantages in terms of construction. On the other hand, the second proposal is more like flat body so the wind has most directly way in comparison with others proposals. Third proposal is a middle solution.
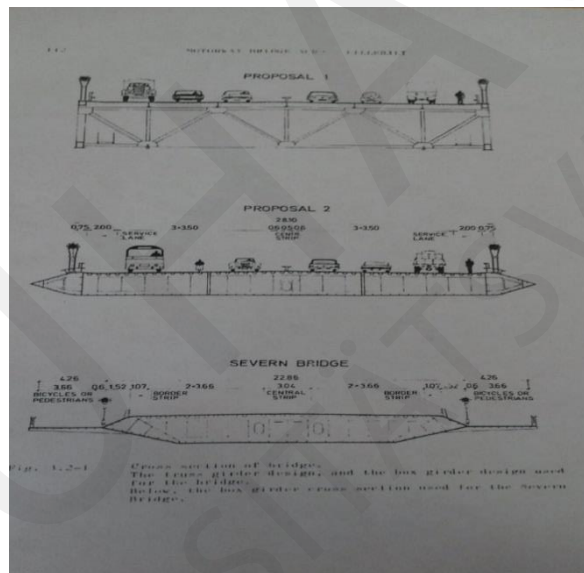
Figure 3. Proposals for a deck sections [4]

Equations of motion

Analytical methods (Theodorsen)

Theodorsen investigated the flutter phenomenon for aircraft wings and gave approach for the flutter analysis. His approach is independent of the shape of the cross section. He gave the simplifications for a flat plate.

Figure 4. Definition of degrees of freedom (h-heave, α – pitch) for flutter analysis

The equation of motion for two degrees of freedom is presented:

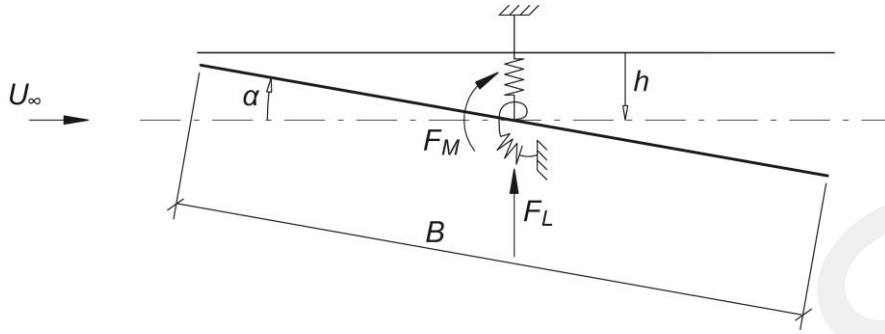$$F_L = m\ddot{h} + 2m\xi_h\omega_h\dot{h} + m\omega_h^2 h$$

$$F_M = I\ddot{\alpha} + 2I\xi_\alpha\omega_\alpha\dot{\alpha} + I\omega_\alpha^2\alpha$$

where, m and I are the mass and mass moment of inertia, ξ_h and ξ_α are the damping ratios and ω_h and $\omega\alpha$ are the natural circular frequencies for heave and pitch direction, h and α are the vertical displacement and rotation, F_L and F_M are the lift force and moment respectively.

The theoretical expressions on a flate plate airfoil for sinusoidal oscillating lift and moment:

$$F_L = -\rho b^2 U_\infty\pi\dot{\alpha} - \rho b^2\pi\ddot{h} - 2\pi\rho C U_\infty^2 b\alpha - 2\pi\rho C U_\infty b\dot{h} - 2\pi\rho C U_\infty b^2\frac{1}{2}\dot{\alpha}$$

$$F_M = -\rho b^2\pi\frac{1}{2}U_\infty b\dot{\alpha} - \rho b^4\pi\frac{1}{8}\ddot{\alpha} + 2\rho U_\infty b^2\pi\frac{1}{2}C U_\infty\alpha + 2\rho U_\infty b^2\pi C\dot{h} + 2\rho\frac{1}{2}U_\infty b^3\pi C\dot{\alpha}$$

$$k = \frac{b\omega}{U} = \frac{K}{2}$$

where ρ is the air density, C is the Theodorsens circulation function and b is a half of B. The system of different equations can be written in matrix:

$$\begin{bmatrix}\dot{h}\\\ddot{h}\\\dot{\alpha}\\\ddot{\alpha}\end{bmatrix} = \begin{bmatrix}0 & 1 & 0 & 0\\a_{21} & a_{22} & a_{23} & a_{24}\\0 & 0 & 0 & 1\\a_{41} & a_{42} & a_{43} & a_{44}\end{bmatrix}\begin{bmatrix}h\\\dot{h}\\\alpha\\\dot{\alpha}\end{bmatrix}$$

or in other form:

$$X = R.e^{\lambda t}$$

where **R** is real. This is a simplification for Eigenvalue problem if it is equal to zero. The solution for h(t) and α(t) is an exponential form and the λi of the matrix A characterize the response of the system in next three tips:

- Positive real part – increasing response,
- Negative real part – decaying response and
- Imaginary part – oscillating response.

The system is going to be unstable when the Eigenvalue has a positive real part or when the imaginary part goes towards zero [1].

Meta model

Meta model by Scanlan is the combination of analytical (Theodorsen), experimental (wind tunnel) and numerical simulation (CFD).
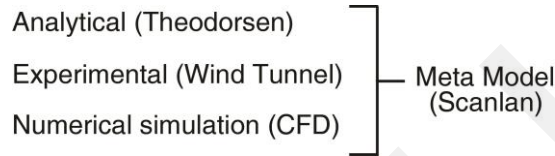
Figure 5. Meta model

Meta model is a mathematical framework for expressing the motion-induced aerodynamic forces on a cross section. It assumes that the self-excited lift FL and moment FM for a bluff body may be treated as linear in displacement h and rotation L and their first derivatives in a linearized from:

$$F_L = \frac{1}{2}\rho U_\infty^2 B\left[KH_1^*\frac{\dot{h}}{U_\infty} + KH_2^*\frac{B\dot{\alpha}}{U_\infty} + K^2H_3^*\alpha + K^2H_4^*\frac{h}{B}\right]$$

$$F_M = \frac{1}{2}\rho U_\infty^2 B^2\left[KA_1^*\frac{\dot{h}}{U_\infty} + KA_2^*\frac{B\dot{\alpha}}{U_\infty} + K^2A_3^*\alpha + K^2A_4^*\frac{h}{B}\right]$$

$$v_r = \frac{2\pi U_\infty}{\omega B} = \frac{2\pi}{K},$$

where B is the wide of the section, U_∞ is oncoming wind speed, h is vertical displacement, α is rotation and $H_i^*(\omega)$, $A_i^*(\omega)$ are aerodynamic derivatives.

The aerodynamic derivatives are non-dimensional functions of the reduced frequency K, which depends of the frequency of oscillation. These could be obtained ether by CFD analysis or wind tunnel tests. [Abbas T., Morgenthal G., 2014.]

Forced vibrations simulations

One way of obtaining the aerodynamic derivatives is by exciting the structure, with a force with a certain magnitude, to oscillate with its two fundamental modes, decoupled. Then, the response and forcing are known, and from the equation of motion the aerodynamic derivatives could be obtained [1]. Results of derivatives are shown in Table below and they are achieved by changing the wind velocity Vr from 2-16.

Table 1. Flutter derivatives in Scanlan expressions

Normalized wind speed	Flutter derivatives in Scanlan expression							
	Vertical forced vibration				Torsional forced vibration			
Vr	H1	H4	A1	A4	H2	H3	A2	A3
2	-0.5	1.5	0.3	0.0	-0.3	-0.5	-0.1	0.1
4	-1.4	0.0	0.6	0.1	-0.9	-1.8	-0.2	0.3
6	-3.7	-0.8	0.7	0.0	-1.1	-3.7	-0.3	0.7
8	-5.6	-0.8	1.0	0.2	-1.0	-6.8	-0.6	1.3
10	-6.0	-0.8	1.6	0.3	0.0	-10.9	-0.7	2.2
12	-8.1	-3.3	1.8	0.0	-2.6	-16.4	-1.0	3.5
14	-8.6	-4.3	2.2	0.2	-3.1	-23.4	-1.4	4.8
16	-20.2	-2.5	2.3	0.8	-2.3	-26.8	-1.4	6.4
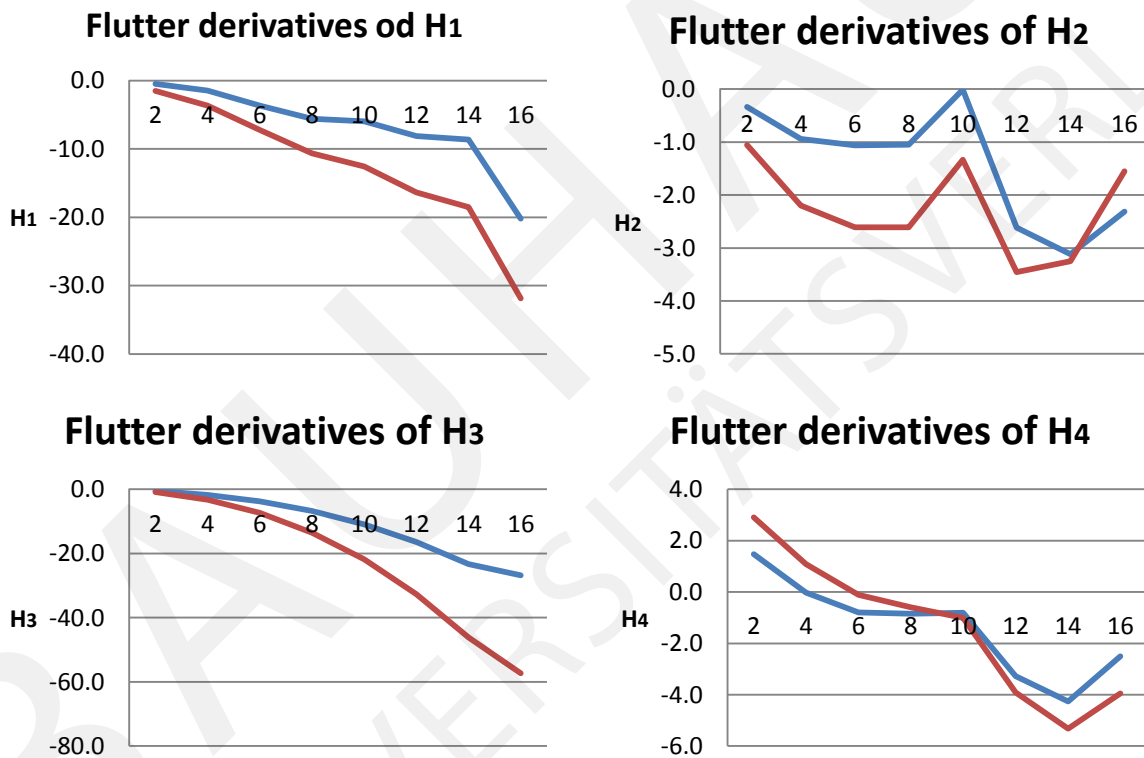
Figure 6. Aerodynamic derivatives H_1, H_2, H_3, H_4

The motion induced forces are the one of three main types of forces which are acting on a structure. The other two are steady wind and buffeting forces but in this report it will be described only motion induced forces which are related to the interaction between wind and the motion of the oscillating structure.

Those forces are central to the flutter stability analysis which involves the coupling of aerodynamic and inertial forces with the elastic structure such that the aerodynamic forces inject energy into the oscillating structure. Exactly at the boundary the sum of structural damping and aerodynamic damping

is zero. When that happens, the structural vibrations are in a harmonic motion with constant amplitude. These motion induced forces can be expressed in the form of indicial functions suggested by Scanlan.

There are three main types of analysis to deal with aerodynamic problems: experimental, analytical and numerical methods. The last two methods have been used in this research. [3]
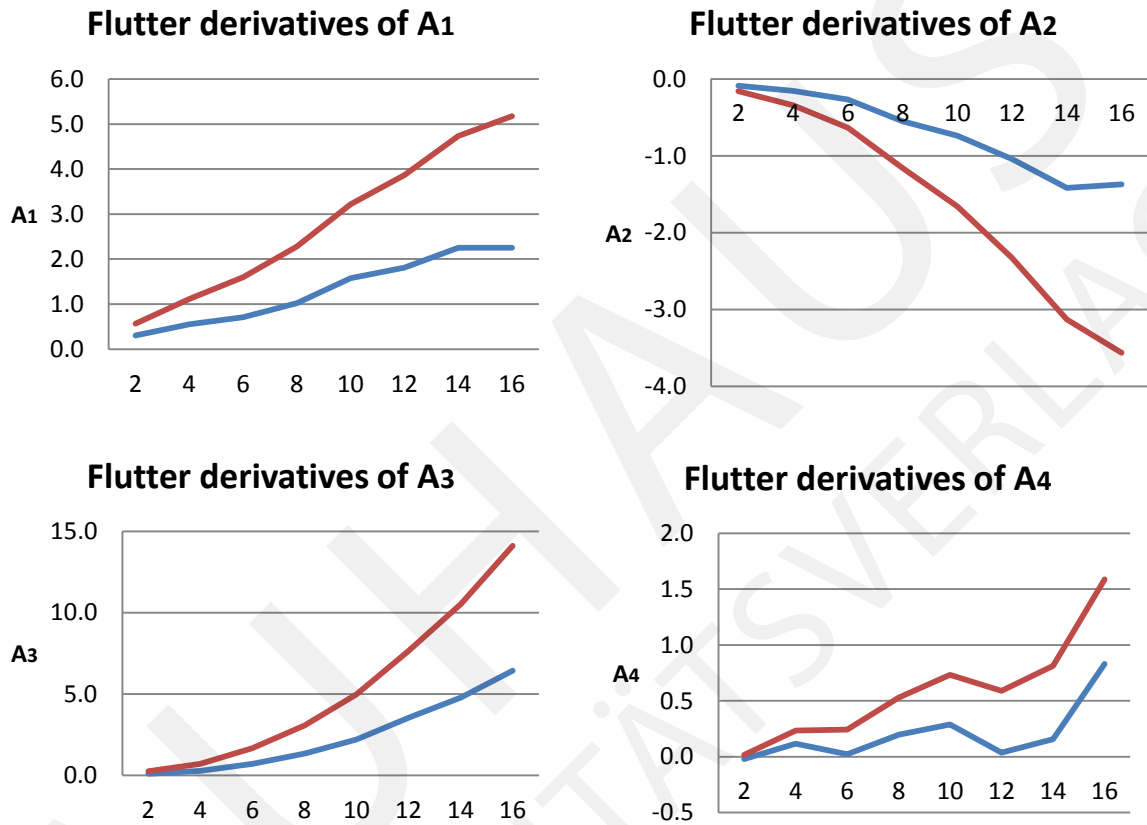
Figure 7. Aerodynamic derivatives A_1, A_2, A_3, A_4
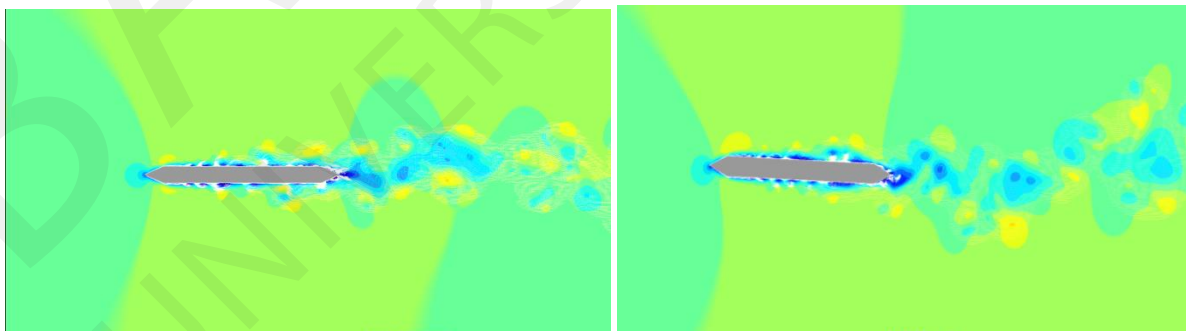
Figure 8. Presentation of forced CFD analysis, heave (left), pitch (right)

Figure 9. 3D scaled experimental model

Numerical model

A Finite Element analysis with the commercial software Sofistik was performed, from which were extracted the frequencies and it has been possible to evaluate the modal forms that are showed in the pictures below.
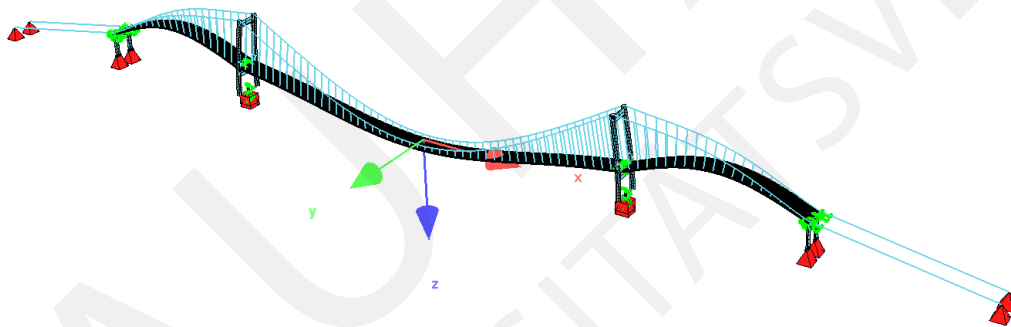
Figure 10. Visualization of first bending mode
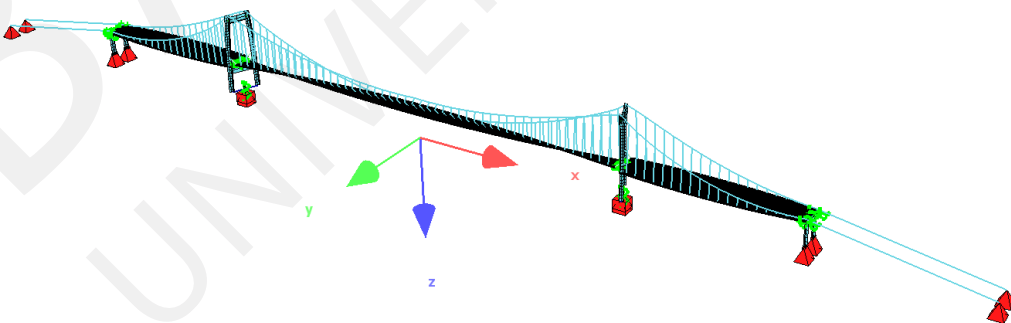
Figure 11. Visualization of torsional mode

In the Table 2 are compared the values of the frequencies from 3D model in wind tunnel and from the program Sofistik.

With calibration of the post tensioning force in the cables and comparison with the experimentally obtained results, comparable natural frequencies were obtained. The flutter frequency is between 0.156 and 0.50.

Table 2. Frequencies of 3D model and Sofistik

	Bending Frequency		Torsional Frequency	
	Mode 1	Mode 2	Mode 1	Mode 2
Measured(3D model)	0.156	0.153	0.5	-
Sofistik	0.156	0.161	0.5	-

Results

With the advanced computer modelling and processing power it's easier to work with Navier Stokes equations and by using the principles of CFD, it is now possible to study wind effects of structures in relatively less time. Those methods are also efficient, repeatable and economical.

Numerical simulations can be used in place of wind tunnel investigation for the fundamental studies only. However there are many limitations with the 3D modelling, so can be used the Vortex particle Method which is a common approach to simulate to the wind flow over a cross section allowing the vortex shedding process to interact with the structural motion. Traditional numerical solvers operate with a uniform incident flow.

The main task of this report was to compare the velocities calculated on a hybrid model and the one calculated from CFD. To achieve the critical velocity with CFD model it was necessary to vary the values from 90-110 in steps of 4. The results are presented in Table 3.
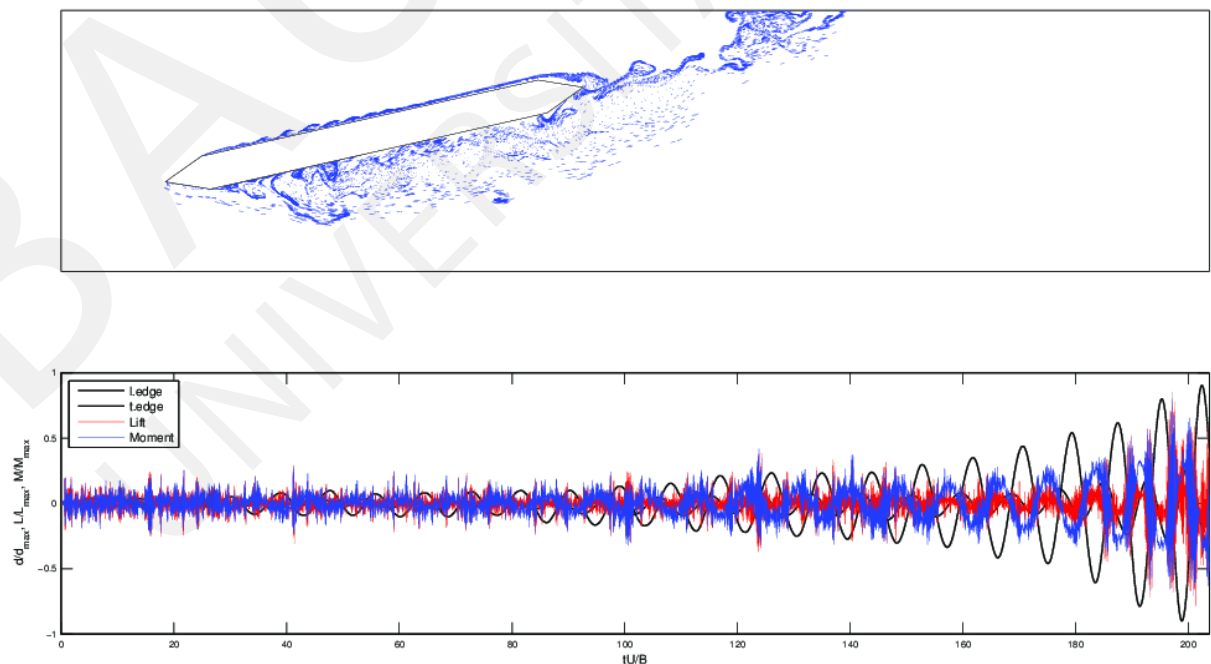
Figure 12. Coupling model from Matlab Software

Table 3. Critical flutter wind speed (m/s)

$V_{cr}\ CFD$	98
$V_{cr}\ Hybrid$	100.9
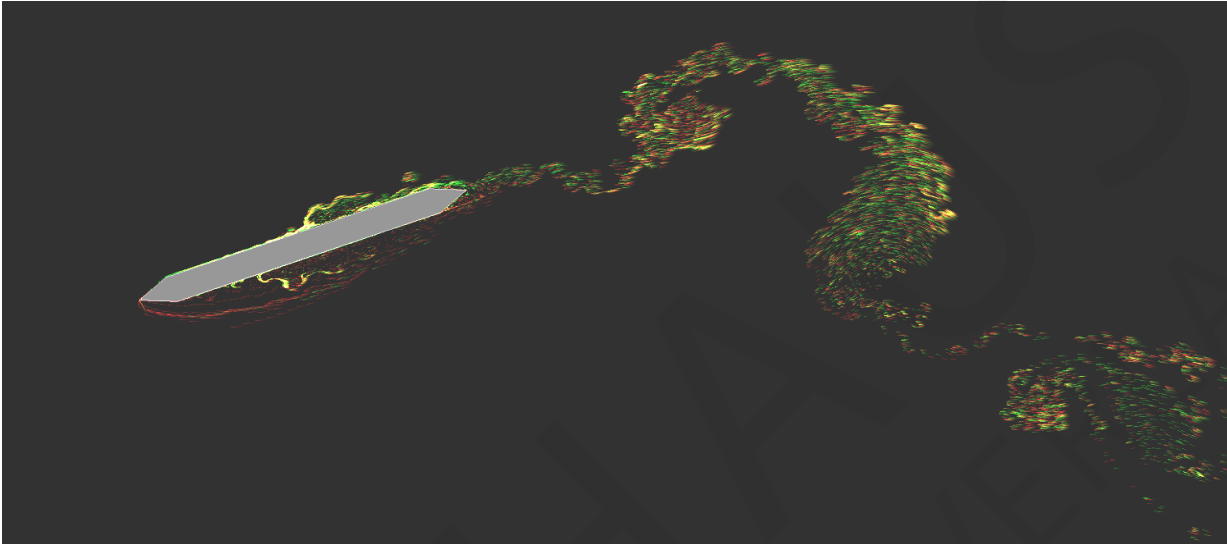
Figure 13. Coupling model from VXflow Software

Conclusion

A flutter instability analysis was performed using coupled hybrid model and a full CFD analysis in order to obtain the critical velocity. The results compared from both models were satisfactory since the difference is insignificant. The cross section of the bridge is aerodynamic and therefore the critical velocity is high.

References

[1] Abbas T., Morgenthal G. Numerical models for flutter analysis. Proceedings of Computational Wind Engineering, Hamburg, 2014.

[2] CNR-DT 207/2008. Istruzioni per la valutazione delle azioni e degli effettidel vento sulle costruzioni (translated from Italian).

[3] Abbas T., Morgenthal G. Hybrid models for assessing the flutter stability of suspension bridges; Proceedings of Bluff Body Aerodynamics 7, Shanghai 2013.

[4] Franden A.G., Hass G, Jessen J.J, Ostenfeld Chr. Motorway bridge across Lillebaelt; publication III. Design and construction of the bridge, Report, 1970,

Multi-objective optimization of bridge piers under wind-induced forces

MALHERBE Jan Stephanus, RHOMBERG Matthieu Benoît, SCHREUDER Jan-Hendrik Michiel

Abstract. The main topic of this project is the optimization. With the use of various optimization software it is possible to "optimize" various problems with a variety of constraints. By regarding different optimization possibilities the simulations were applied on a bridge structure that is exposed to wind induced vibration.

Introduction

The bridge structure is a two lane suspension-bridge, in the construction phase. In the simulation the optimum distance between the two main columns, under the influence of the worst wind scenarios, are being computed. By designing the optimum distance between the columns the safety risks during the construction phase are minimized. The execution of the construction is also simplified by this exercise.

Literature

Multi-objective optimization are done by creating an area of multiple criteria decision making, that is concerned with mathematical optimization problems involving more than one objective functions to be solved simultaneously. The purpose is to find a non-dominated/Pareto optimal. This is a point where none of the objective functions can be improved without degrading some of the other objective values.

The main methods are based on a deterministic approach, or a probabilistic approach, the probabilistic approaches is also known as heuristic approaches. Numerous methods exist under each class and algorithms are freely available, but our focus will be on Newton's Method, Method of Steepest Descent and the Genetic Algorithm which is based on the Evolutionary algorithms.

Newton's Method

Newton's method and methods based on this approach like quasi-Newton methods are usually used for small to medium scale CONSTRAINED problems. Although some versions can handle large-dimensional problems, other methods are much better suited for these problems. Figure 1 provides a high-level illustration of how the algorithm works.

The algorithm searches for the minimum or maximum points through the use of derivatives. Thus, a point in the domain where $f'(x) = 0$ will be a point of interest that will be compared with other local minima/maxima.

Although Newton's Method can converge very fast and with high accuracy, there are certain limitations that have to be considered. These are listed below:

- The algorithm can present difficulties at inflection points on a domain, since it is based on derivatives.
- The method needs to compute the Hessian, $H(x)$, at each iteration.
- $H(x)$ needs to be positive definite for the general cases.

Steepest Descent Method

This method is a (slow) method of mostly historical and theoretical interest. Interest in this method has been renewed for finding approximate solutions for enormous problems. This method basically looks for the steepest path (there where the contours of the projected function would be closest to one another) and then follows this towards the local minima. This method is illustrated below in Figure 1.

This method also poses certain problems, some of which are listed below:

- The method can be slow, otherwise stated, its asymptotic rate of convergence is inferior to many other methods.
- The algorithm might stall at flat domains, or appear to 'zigzag'.
- Non-smooth curves can present problems since the derivative is not defined at this position.

Genetic Algorithm

Unlike the previous two methods, this method is a heuristic method, based on the theory of evolution. This algorithm mimics the process of natural selection. In this algorithm, the biological evolution candidate solutions to the optimization problem, plays the role of individuals in the population. A fitness function is used to determine the quality of the solution (as specified by the objective function).
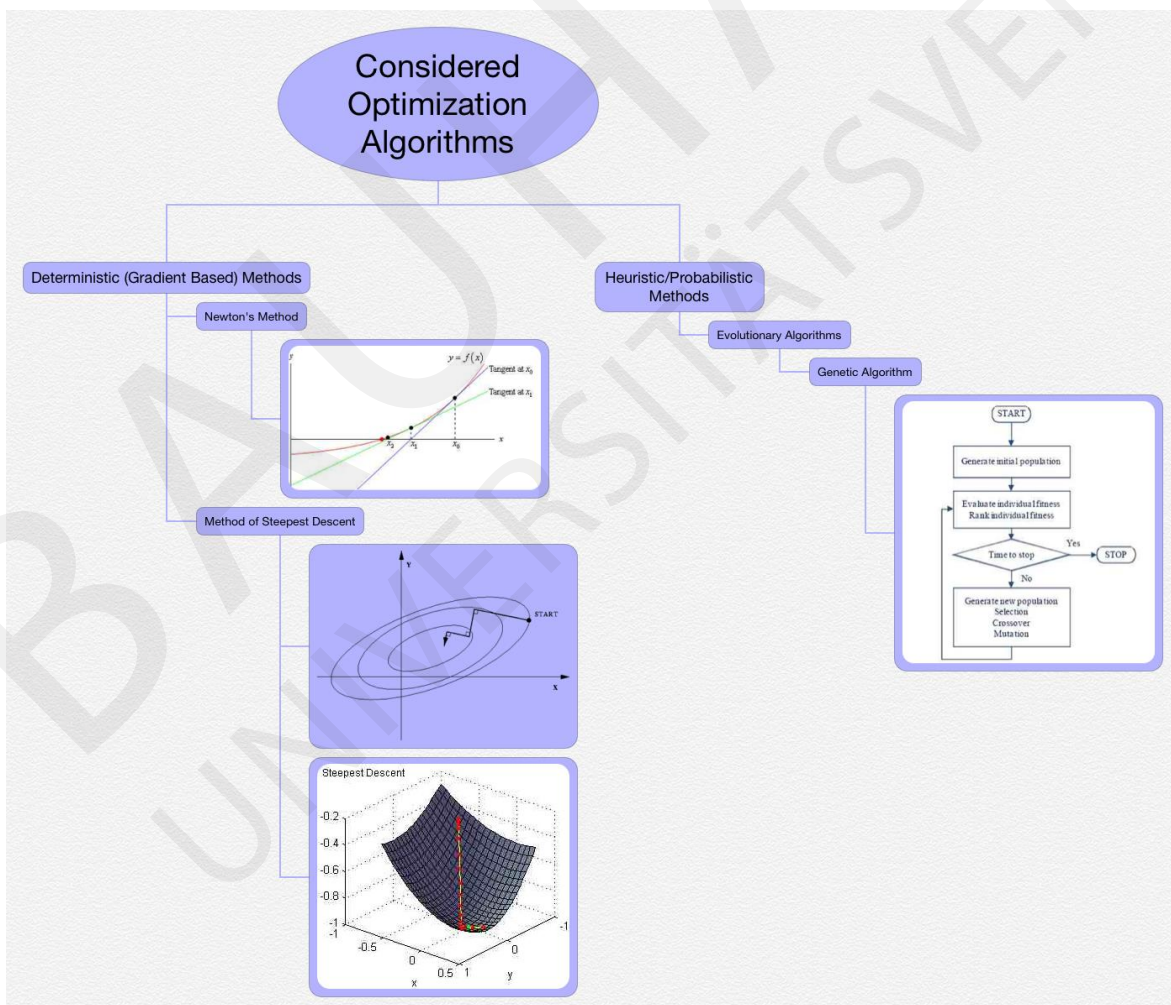
Figure 1. Considered Algorithms

The wide application of the genetic algorithm, due to the absence of assumptions on the range, or fitness landscape, is one of its great advantages. Another advantage is that the algorithm can operate on a totally random domain.

Figure 1 illustrates the working of this algorithm. One possible problem might be that this algorithm cannot simulate a clear genotype-phenotype distinction. This is natures way of stopping infeasible solutions before they realize.

This method is usually used for multi-objective optimization, this was also the chosen method for this particular example described in the report.

Problem description

Figure 2. Bridge example [1]

In the Introduction it was mentioned that the optimization project deals with a long span bridge. Figure 2 shows an example for a long span bridge with similar geometry of that which will be used in the simulation. The bridge will consist of two traffic lanes, one in each direction, with a pedestrian walkway on both sides. Dimensions were defined as follow:

- Width per traffic lane: 3,5 m
- Pedestrian walkway: 1,5 m
- Column radius: 1,0 m
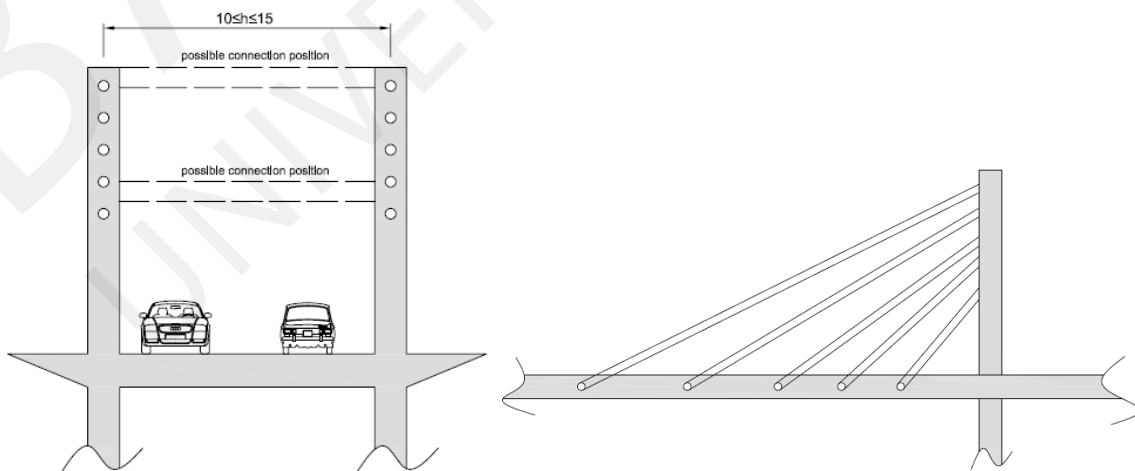
Figure 3. Bridge Sketch

Before the connection of the columns is constructed, high wind speeds can be a great risk for the structure. In this case, the columns will be at their most vulnerable point of their designed loading range. The distance between these two columns can influence the displacement of the columns' top ends due to wind loads. By optimizing the distance between the two columns higher safety is given to the structure as well as labourers on site (during the construction phase). In Figure 3, different views of the simulated case study are shown.

Methodology

The defined model was done using two circular sections to represent the two unconnected columns. By describing the two columns as two circles in the model, it represents the top view of the two piers. Figure 4 explains the cross-sections used in the optimization setup.
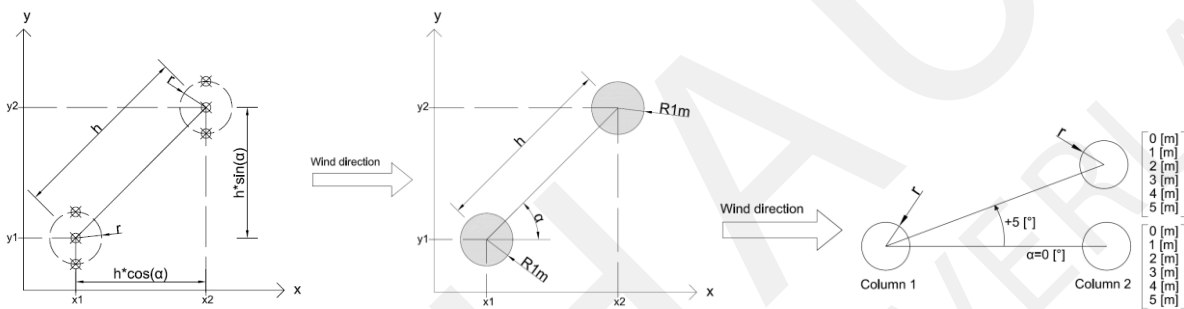
Figure 4. Problem Geometry

Mathematical problem description

The problem were first geometrically formulated as in Figure 4. The different force components were simulated as 'lift' and 'drag' in the simulation software. Although, for the specific problem these forces will be the x and y components of the resultant force, in a horizontal plane. This resultant force is our objective function which needs to be minimized, or for which the Pareto optimal has to be found. The following mathematical description applies to the problem.

Objective function

$$\min(F = \sqrt{[f_1(\alpha, h)]^2 + [f_2(\alpha, h)]^2}) \tag{1}$$

Where:

F = Resultant force on system
α = Approach angle of oncoming wind [°]
h = Distance between freestanding columns [m]
f_1 = x-component of resultant force (Drag)
f_2 = y-component of resultant force (Lift)

Constraints

Referring to Figure 4 the distance between the centroids of the two columns was limited to:

$$10 \text{ m} \leq h \leq 15 \text{ m}$$

The reason for this constraint was to allow the bridge deck to have a width clearance of 10m. To find the worst case wind direction, the angle α of the wind direction has been changed during the simulation in the following range:

$$0° \leq α \leq 45°$$

This range reflects the assumption that the suspended bridge is in a valley where the oncoming wind direction is limited to a maximum offset of 45°. These constraints were also based on the assumption that the bridge is perpendicular to the valley. The wind speed was set to 10m/s.

Concluding, these constraints were developed to find the optimum distance between the columns for the worst wind direction.

Modelling and simulation

The simulation defenition was done in an Input file where the geometry and variables specifications, as discussed in the Problem Description, was defined. Before the Input file was implemented in Matlab the domain was defined within Optiflow. During the simulation Optiflow is changing the distance between the center of the columns in steps of 1 metre, for various wind directions ranging from 0° to 45°, in steps of 5°. These steps are executed within the domain as defined by the constraints in the Mathematical problem description. Figure 3 and Figure 4 shows the procedure discussed above. Furthermore Figure 5 shows the software application.
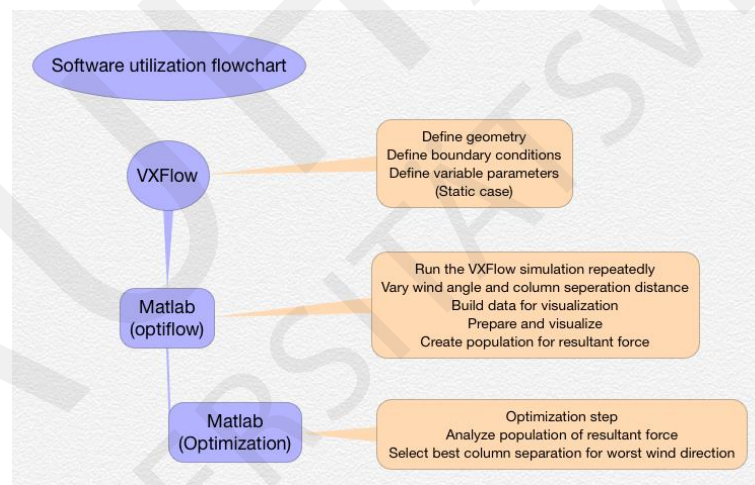
Figure 5. Software application

Results

In Figure 6 the 3 dimensional plot of the simulation population is showed. This population is the result of the optimizing process described in Figure 5. The two components, α and h, are in the same plane. The axis named «Multi» is the combined targets of the optimizing process. «Multi» is a combination of the x and y components as given in Equation 1 (MULTI = F(x)). Figure 6 thus represents all the possible resultant forces for various α and h within the given domain. In Table 1 results of interest are listed.
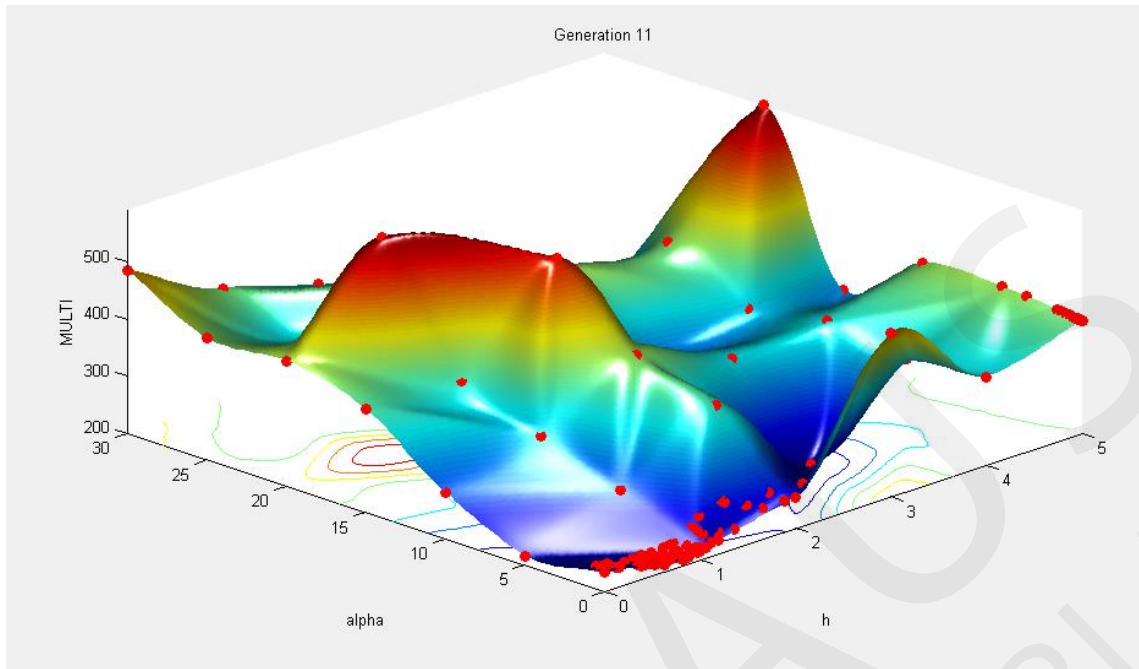
Figure 6. 3D Plot

Table 1: Results

Setting	Components	
	h [m]	α [°]
Maximum Force	5	20
Minimum Force at 20[°]	3	20
Ideal distance	0,73	0,34

The listed h in Table 1 represents the difference that has to be added to the minimum clearance distance, h_{min}= 10m of the two columns. By using the optimization program the maximum force exerted on the structure can be found. Concluding from Figure 6 and Table 1 the worst wind direction is at α=20°. The optimum distance between the two columns for an angle of α=20° is 3 metres. Adding this length to the minimum distance of 10 metres, results to a total column seperation of 13 metres.

For the ideal distance with the lowest acting force on the structure, an h of 0,73m with a wind direction angle α of 0,34° has been computed, this corresponds to the trivial solution where both parameters are zero.

References

[1]   http://www.pellfrischmann.com/sectors/longspanbridge/secondbosphorus.php

Vortex-induced vibration analysis on the Alconétar Bridge in construction stage

ALRAYES Omar, DONG Haotian, MALEZANOV Lazar, KASAPOVA Krumka

Abstract. In the frame of the Project Work our task was to analyse the vortex shedding effect on the Alconétar Bridge in construction stage by using the specific software **VXFlow**. The main problem of this topic is that during the construction stage, when the arches were implemented without any vertical pillars on it, the second Eigen mode was observed as vibration of the arches caused by a certain wind speed.
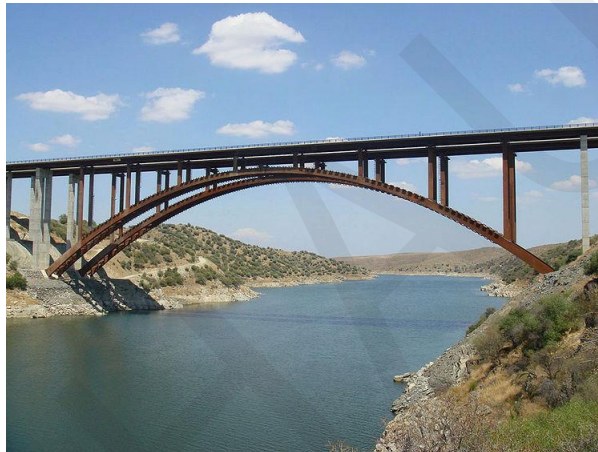
Figure 1. Alconétar Bridge [http://www.highestbridges.com/].

The aim of this study is to determine the specific wind velocity in which this vibration mode occurs. For the determination of the wind velocity related to this oscillation we have used a numerical method called **Vortex Particle Method**.

The effect of the deflectors, which were performed on the structure aiming to reduce the oscillations, will be analyzed after the determination of this certain wind speed. Using numerical evaluation we can compare the results from these two numerical models and also we can compare the results with the measured values.

Introduction

Arcos de Alconétar is a bridge over the river Tagus located at a region of Spain called Alcantara Reservoir. It represents a steel deck arch bridge with 220 meters span consisting of two parallel arches formed by longitudinal box sectioned parts connected with a X-formed horizontal bracing system.
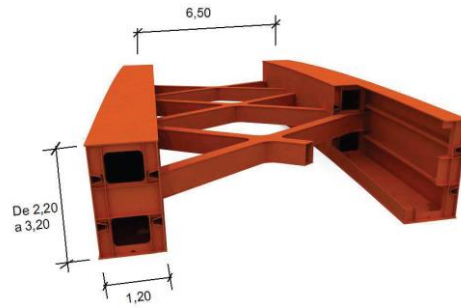
Figure 2. Cross section of the arch.

During the construction heavy harmonic oscillations occurred due to constant but low wind speed. The measured vertical displacement was about 40 centimetres.

Figure 3. Second vibration mode.

Subsequent examination showed that the vibration was caused by vortex shedding whose period coincided with the structure's second mode and thus driving it to resonance. To avoid such oscillation in the construction phase wind deflectors were applied on the steel structure to change the aerodynamic behaviour of the structure and therefore to influence the air flow's trajectory and suitably channel it to prevent vortex forming.

Figure 4. Deflectors on the Alconétar bridge [Corriols A., Morgenthal G. (2012)].

Figure 5. Detail of Deflectors [Corriols A., Morgenthal G. (2012)].

Vortex-shedding excitation

The natural vibration frequency of the bridge depends on several factors - mass, stiffness and damping. The vortex shedding phenomenon is influenced by the specifity of the structure. Its frequency is a function of the height of cross section (D) and wind speed (U_∞).

$$f_v = (0.8 - 1.2)\, f_n \qquad (1)$$

If the vortex shedding frequency is close to one of the natural frequencies of the structure then **'lock-in'** phenomenon can happen. This phenomenon can cause resonance in a narrow range of wind speed. The Strouhal number is defined as follows:

$$St = \frac{fD}{U} \qquad (2)$$

It is a dimensionless characteristic which describes the oscillating flow mechanisms. The vortex vibration phenomenon is caused by eddies on the "leeward side" of the cross section. This phenomenon is a self-limited phenomenon because the amplitude of the resonance can reach a limited value which could be between D and D/2 where D is the depth of the cross-section but it can be very dangerous from serviceability and from fatigue points of view.

Numerical model

Vortex Particle Method is a *Lagrangian* Method and the program to perform the simulations is *VXFlow*. The program allows very efficient simulations of two-dimensional flows around bodies of arbitrarily complex geometry and arrangements.

Cross sections

The cross section examined does not include any braces. The 4 types of cross sections models are shown in the Figure 4 to 7. Among them, section B was applied in the bridge actually, however, the deflectors were not continous.
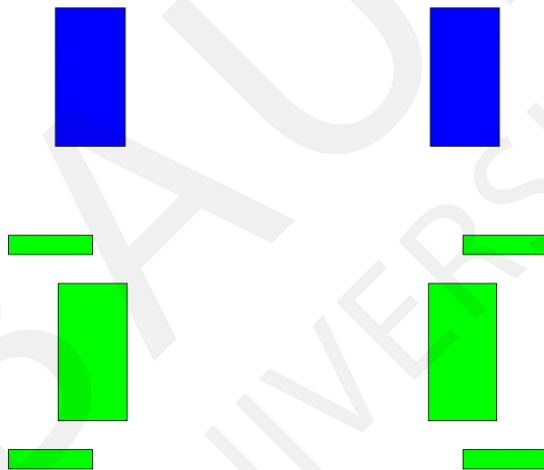
Figure 6. Cross section (A):
Cross section with rectangular deflectors (C).
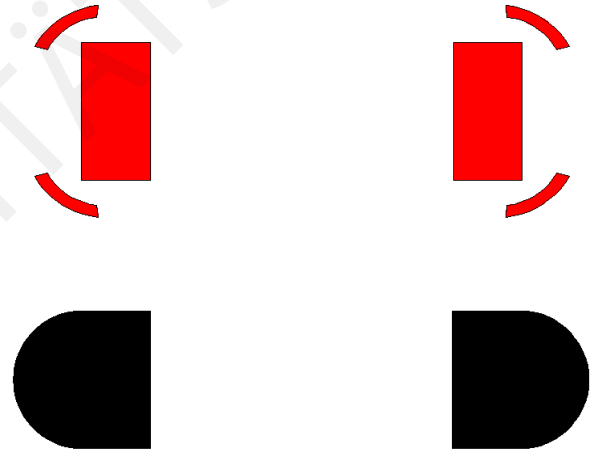
Figure 7. Cross section with curved deflectors (B):
Curved section (D).

Table 1. Cross section geometry and material properties

Width of rectangular (m)	Depth of rectangular (m)	Central distance S (m)
1.2	2.4	5.3
Mass (Kg/m)	fN (Hz)	Damping %
1130	0.7	0.3
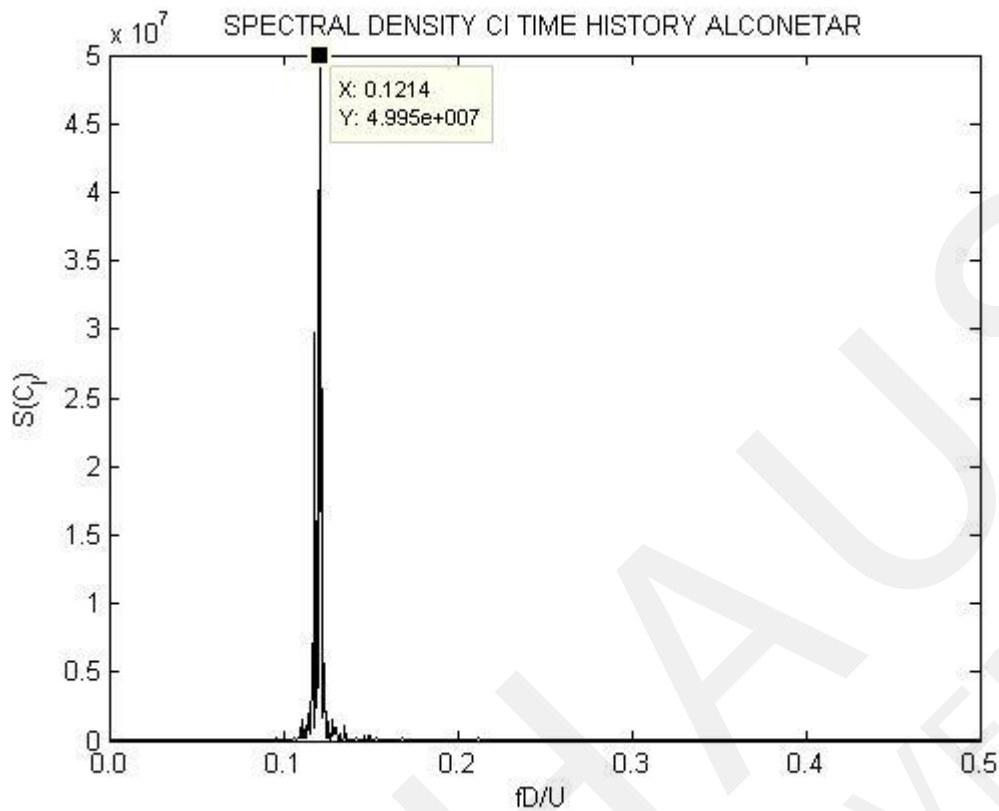
Figure 8. Spectral density of C_L for static simulation, cross section (A).

Analysis

Static simulations

Firstly the static simulation has been performed with cross section (A) in order to determine the dominant vortex shedding frequency. In this case the section is fixed. The flow impacts the structure and generates the vortex. The predominant vortex shedding frequency is to be identified in order to subsequently evaluate the critical wind speed for lock-in phenomenon. As shown in figure 8 the maximum lift coefficient C_L occurs with a Strouhal number of $S_t=0,1208$.

By using the definition of the Strouhal number the critical wind speed for the lock-in phenomenon can be calculated. Having determined the approximated critical wind speed dynamic analysis can be performed.

$$St = \frac{fD}{U} => 0,1208 = \frac{0,7 \cdot 2,41}{U} <=> U = 13,91 \, m/s \tag{4}$$

Dynamic simulations

For dynamic simulation the range of wind speed was set from 2 to 20 m/s. For each wind velocity parameters were calculated for cross section A to D. The Figure 9 shows the arrangement of vortex particles for a wind speed of 16 m/s (section A).
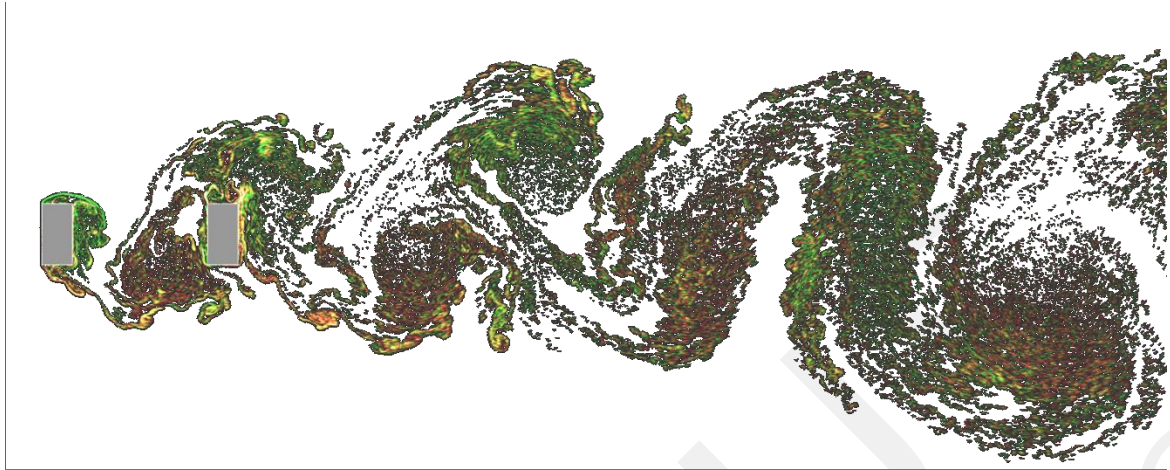
Figure 9. Vortex shedding, cross section (A), $U_\infty = 16$ m/s.
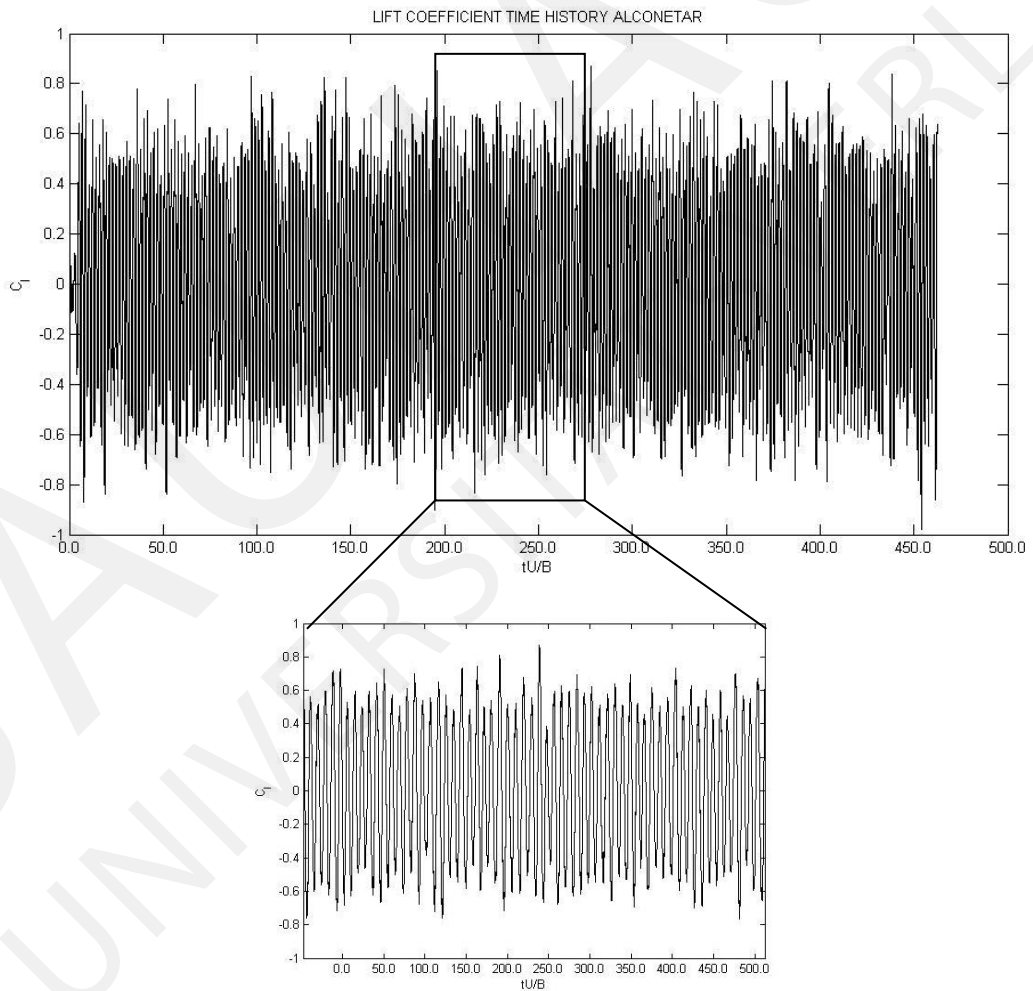
Figure 10. Lift coefficient, cross section (A).
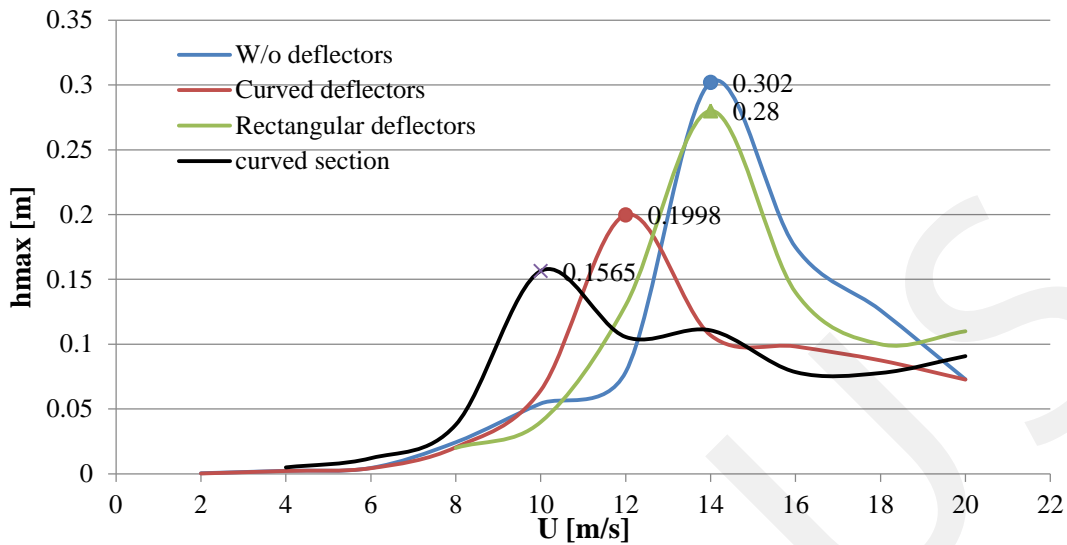
Figure 11. Max vertical displacement (m).

Figure 10 shows the lift coefficient of cross section (A) at the critical wind speed of 16 m/s. It can be concluded that the lift coefficient for the bare cross section is very regular and therefore the bridge can be easily excited due to low wind speed. The reason for this behaviour depends on the simple shape of the cross section.

Vortex lock-in wind speeds were: Cross section A: around 14m/s, B: around 12m/s, C: around 14m/s, D: around 10 m/s. Figure 11 shows the max vertical displacement of different wind speeds. Among the 4 sections, C didn't change the vortex wind speed and max displacement too much. B and D were much better.

Strouhal number remains the same with wind speed, except within the lock-in area, as is shown in Figure 12. Lock-in happens when frequency of flow becomes closed to the frequency of structure, and the frequency is supposed to remain the same in the lock-in area. However in Figure 13, this is not quite obvious, maybe more simulations should be done within the lock-in area.
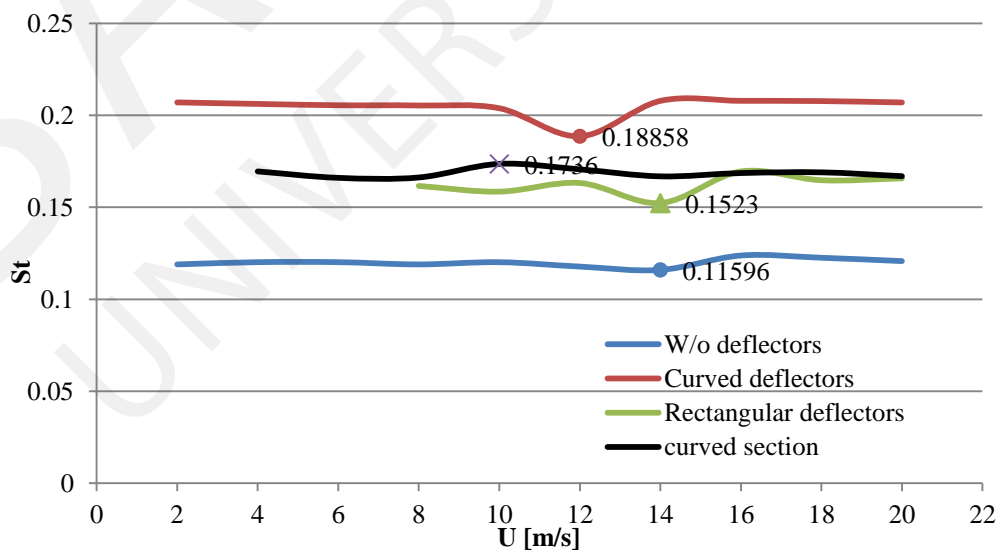
Figure 12. Strouhal numbers.
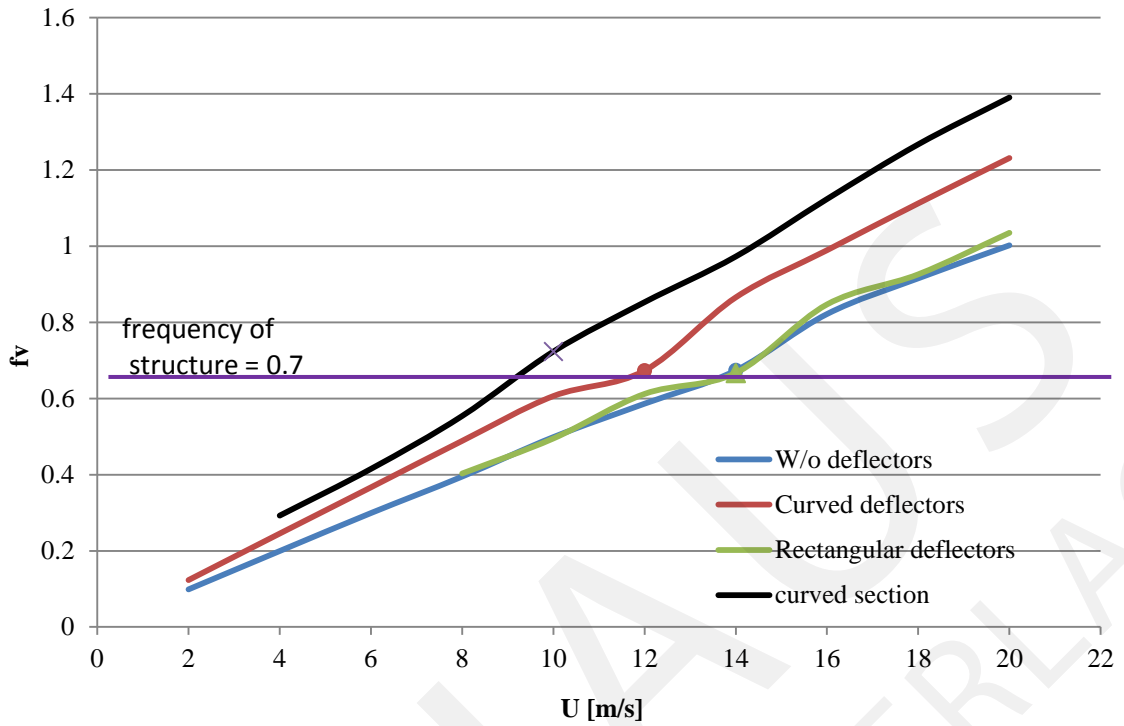
Figure 13. Frequency of vortex.

Figure 14 shows the vertical vibration history of cross section D at wind speed U = 10 m/s, which is within the lock-in area of VIV. Obviously, the amplitude of vibration kept oscillating. The spectrum (Fig. 15) has more than one peak.
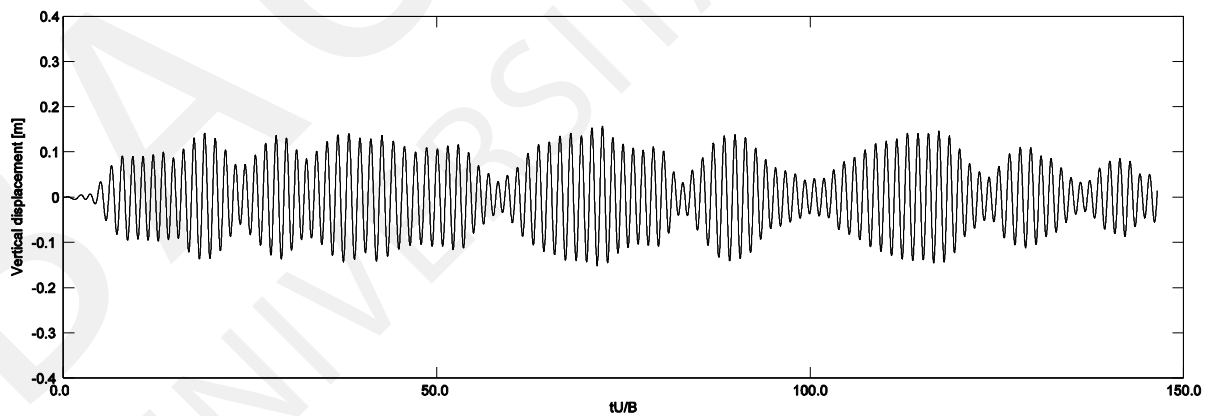
Figure 14. Time history of vertical displacement, cross section D, wind speed at U=10m/s.
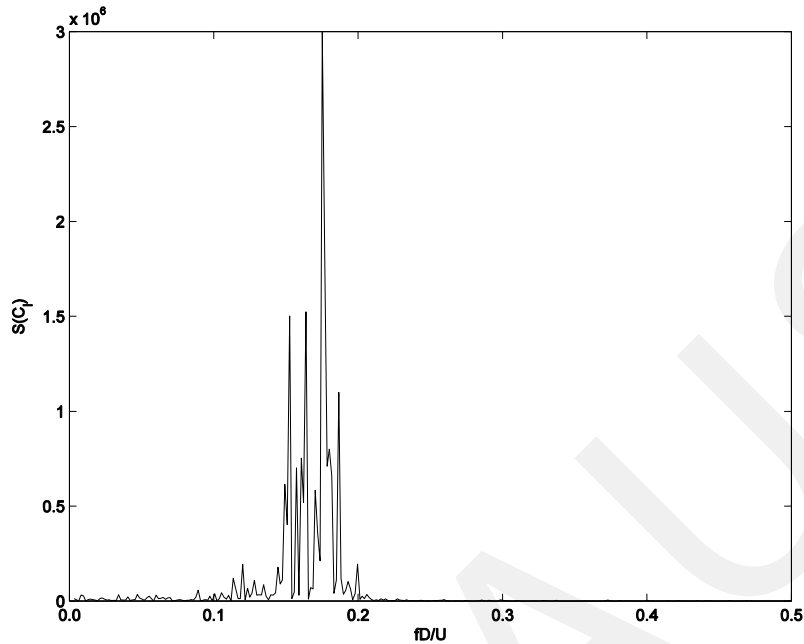
Figure 15. Spectral density of C_L for dynamic simulation, section D, wind speed at U=10m/s.

Fatigue life assessment

Fatigue performance of slab bridges is one of the main issues in design of new structures and in the assessment of existing ones. This problem is particularly complex due to the many uncertainties concerning the real effects of both passenger and freight traffic, and the real fatigue performances of structure. RC bridge slab subjected to fatigue has been a key issue in both maintenance and design rather than other members in the structural system. This investigation because of slab decks is thin for their span lengths and members which directly exposed to fatigue caused by cycling loading.

During the life cycle of bridges, varied amplitude of stress ranges on structural details are induced by the random traffic and wind loads. The progressive deteriorated road surface conditions might accelerate the fatigue damage accumulations. An effective structural modeling scheme and a reasonable fatigue damage accumulation rule are essential for stress range and fatigue life estimation. The present research targets at the development of a fatigue life and reliability prediction methodology for existing steel bridges under real wind and traffic environment with the capability of including multiple random parameters and variables in bridges' life cycle.

The main task is to know the critical wind induced strains measured in 100 m high depends on dynamics parameters in order to have the internal stresses and displacement amplitudes. The time history of the internal stresses will denote the number of cycles and the solutions provide remarkably good predictions of the S-N curve of the material.

Endo & Matsuishi 1968 developed the Rain flow counting method by relating stress reversal cycles to streams of rainwater flowing down a Pagoda.This is shown in Figure 15 and Table 2. The rain flow method is a method for counting fatigue cycles from a time history. The fatigue cycles are stress-reversals. The rain flow method is to assess the fatigue life of a structure subject to complex loading such as wind load. The algorithm is shown in following steps:

1. Reduce the time history to a sequence of stress peakes here to peak displacements.
2. Imagine that the time history.
3. Turn the sheet clockwise 90°, so the starting time is at the top.
4. Each peak is imagined as a source of water that "drips" down the pagoda.
5. Count the number of half-cycles by looking for terminations in the flow occurring when either:
   a. It reaches the end of the time history
   b. It merges with a flow that started at an earlier tensile peak;
   c. It encounters a trough of greater magnitude.
6. Repeat step 5 for compressive troughs.
7. Assign a magnitude to each half-cycle equal to the stress difference between its start and termination.
8. Pair up half-cycles of identical magnitude (but opposite sense) to count the number of complete cycles. Typically, there are some residual half-cycles.

From this stage the number of cycle loads will be repeated and the prediction of the S-N curve of the material will be denoted. These data have been used to verify a simple theoretical model of fatigue damage rate and fatigue life. Theoretical fatigue-life estimates appear to be reasonable, if a little conservative, in relation to experience of the shape of the cross section, span and the material of bridge model. Also, some uses of rain-flow method is to evaluate a structure's or component's failure potential using Miner's rule & S-N curve, compare the relative damage potential of two different vibration environments for a given component and derive maximum predicted environment (MPE) levels for nonstationary vibration inputs.
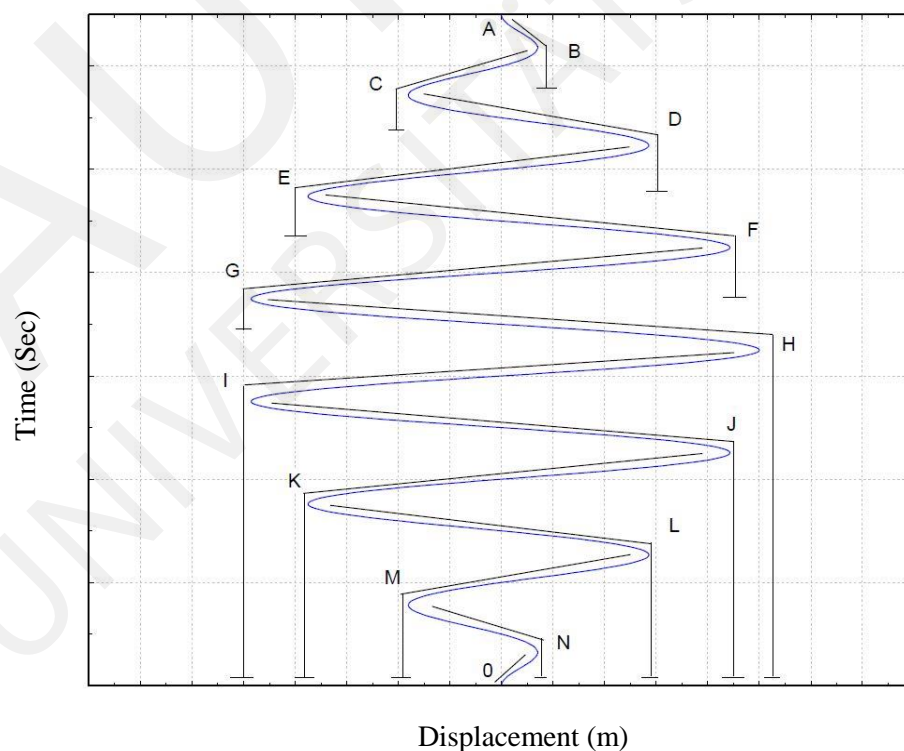
Figure 16. Time displacement curve of rain-flow counting method

Table 2. Rain flow cycle by path of displacement

Path	Cycles	Displacement
A-B	0.5	0.02
B-C	0.5	0.03
C-D	0.5	0.04
D-E	0.5	0.06
E-F	0.5	0.08
F-G	0.5	0.09
G-H	0.5	0.10
H-I	0.5	0.11
I-J	0.5	0.11
J-K	0.5	0.10
K-L	0.5	0.10
L-M	0.5	0.09
M-N	0.5	0.09
N-O	0.5	0.10

References

Gladwell, G. (2004). *A modern course in Areoelasticity*. London: Kluwer.

Ricardo Perera, E. A. (1986). Modlization of low cycle fatigue gamage in frames. *12WCEE 200*, 12.

Scanlan, R. (1996). *Wind Effects on Structures*. Canda: John Wiely.

Corriols A., Morgenthal G (2012). Computational analysis of VIV observed on existing bridge. BBAA7, Shaanhai 2012

Papers contributed by the participants

Modelling of circular concrete columns with CFRP sheets under monotonic loads by ATENA-3D

ALRAYES Omar

Institute of Structural Mechanics, Bauhaus-Universität Weimar, Germany

KÄSEBERG Stefen

Department of Civil Engineering and Architecture Leipzig, Germany

Abstract. Over the last years, performance based design has become acceptable in abnormal events assessment of structures. Therefore, using this design method, performance of existing and retrofitted reinforcement concrete (RC) buildings can be evaluated using nonlinear analysis. In this case, the performance of a fiber reinforced polymer (FRP)-retrofitted column is assessed under monitoring loading and the result is compared with unstrengthened ones. The results are examined and compared with models reported in literature such as Teng and Lam model (Teng et al., 2007). The reliability of the model is assessed through comparison with experiment results that were done in Institut für Betonbau (IFB), Leipzig in 2009. The comparison shows that within the practical range of the confinement model variables, the ATENA analytical model is in very good agreement with the empirically model (Vladimír, et al., 2012). This model is based on smeared crack method in order to develop a nonlinear finite element method that describes the behavior of the plasticity and mechanical damage of the material.

The number of structures in the world continues to increase, as does their average age. The need for increased maintenance is inevitable. Complete replacement is likely to become an increasing financial burden and is certainly a waste of natural resources if upgrading is a viable alternative. Therefore, maintenance, strengthening and monitoring of existing buildings have become more important. The way in which FRP composite material as carbon fiber reinforced polymer (CFRP) can apply in strengthening structures like buildings and bridges is illustrated in EUROCOMP Design Code (December 2004) and ACI committee 440 (Technical committee document 440. 2R-02, 2002). The predictions are confirmed as confinement efficiency depends on the strength of both concrete and confinement, the shape of cross section, lateral ties hoop and fiber orientation.

98

Historical evolution of shape and aerodynamics

ANAGNOSTOPULOS Danai Iris
Università degli Studi di Genova, Italy

Abstract. While airplanes, boats, cars, trains and windmills were born through a process of optimization of the shape, buildings will remain for a long time anchored in a different reality: first, an architect conceives a shape based on his stylistic taste and just later an engineer makes structurally secure an already defined and untouchable shape.

This conception will change at the end of the 20th century, when were born various researches aimed to optimize the form of skyscrapers on the basis of aerodynamics. This is the prelude of a new vision, where the architect and the engineer find a meeting point and work in team to achieve stylistic requirements and structural optimization.

High-speed railway traffic: challenges on the simulation of the dynamic response of the track

COLAÇO Aires, ALVES COSTA Pedro, CALÇADA Rui, SILVA CARDOSO António
Faculdade de Engenharia da Universidade do Porto, Portugal

Abstract. The dynamic amplification effects of the response due to a moving load on the surface of an elastic solid has been a topic of research for more than a century [1-3]. However, if in the beginning of the last century the problem has only theoretical interest, this is not true anymore. Indeed, the recent advances on the rolling stock, which can now reach speeds of more than 500 km/h, brought this kind of problems for the engineering practice, mainly for the railway engineering of high speed [4, 5]. Actually, the increase of the traffic speed that is expected to reach during the next years could give rise to the appearing of this kind of problems in several regions where the railway lines cross alluvionar regions with soft soils.

In the present communication, departing from the theoretical formulation of the critical speed problem of a moving load on the surface of an elastic solid, the problem is approached for the railway engineering. Since the mechanical soil behaviour is quite far away from the elastic approach, it is shown that non-linear methodologies are needed for the simulation of the dynamic response of railway tracks when subjected to very high speed traffic, i.e., when the circulation speed is high in comparison with propagation speed of the waves in the ground [4]. However, due to the complexity of the problem, involving a vast three-dimensional domain with non-linear response subjected to moving loads, several challenges are found, for which the engineering practice should give an efficient answer. To reach that target it is indispensable the development of efficient and accurate numerical models, without undesirable numerical complexity that could put them in a non-applicable level for practical situations.

The communication presents not only simplified approaches for the estimation of the critical speed of railway tracks but also comprehensive approaches where the effects of the soil non-linearity can be taken into account, without forgetting the demands of the time of computation. Moreover the theoretical background is discussed with the presentation of case studies where the proposed methodologies are applied and numerical and measured results are compared.

Overcladding of existing large precast concrete panel buildings using steel

FLORICEL Andra, UNGUREANU Viorel

Department of Steel Structures and Structural Mechanics, Politehnica University Timisoara, Romania

Abstract. A large part of the Romanian urban population, as that of Eastern Europe, lives in collective residential buildings made out of large prefabricated concrete panels, mostly built between 1960 and 1989, most of them with major structural and energetical deficiencies. However, the refurbishment of these buildings had to comply with these neccesities, without compromising the structural integrity and stability of the building. The solution of overcladding these buildings has become not only an inevitable approach, but rather a mandatory process in achieving the enlargement of the living space, as well as the refurbishment of the existing building stock in terms of energy consumption and environmental aspects, without bringing much extra weight to the structure. Present paper presents and compares three types of overcladding structural solutions based on intensive use of steel elements: a) hot rolled steel; b) rectangular hollow sections; c) cold-formed steel profiles. The solutions are analysed and compared from structural point of view, but also from environmental impact perspective, in order to determine the optimum solution for these large precast concrete panel buildings.

Evaluation of the effect of masonry infill walls presence in existing RC structures: Numerical and experimental study

FURTADO André, ARÊDE António
Faculdade de Engenharia da Universidade do Porto, Portugal

RODRIGUES Hugo
Departamento de Engenharia Civil – ESTG – Instituto Politécnico de Leiria, Portugal

Abstract. The quality of the built heritage play a central role on the quality of the daily human lives as they interact continuously with the built spaces, either in the work, social events and at home. In particular, the safety of the built spaces is indeed a demand of modern societies and remains a huge concern in prone seismic regions. The masonry infill walls represent the most traditional enclosure system and have demonstrated reasonable performance with respect to healthy indoor environment, temperature, noise, moisture, fire and durability. This study consists initially on a geometric characterization of the Portuguese masonry infill walls that allowed to define an experimental campaign of full scale masonry infill wall that are in preparation to be performed during the next days. Finally the last part of this research is about modelling of RC buildings with masonry infill walls, particularly the seismic assessment of existing buildings.

Modal pushover analysis for seismic vulnerability analysis

GARCIA Hernan Alfredo
KU Leuven, Belgium

Abstract. A simple introduction of inelastic structural analysis for seismic vulnerability by considering the definition of pushover analysis and using a simple elasto-plastic material model to compare analytical and numerical results. The modal pushover method is explained to approximate the response due to "El Centro 1940" ground motion for MDOF systems. The properties of Modal Pushover analysis is used to plot capacity curves vs. ground motion spectra in order to perform a one limit state fragility curve using the maximum likelihood method. All explanation are done by following a step by step procedure, then it is applied to a benchmark structure, the 9 storey SAC building.

Seismic behaviour study of Argostoli Museum's exhibits during Cephalonia earthquakes on 26 January & 3 February 2014

GIOTIS Georgios, SEXTOS Anastasios
Department of Civil Engineering, Structural Division, Aristotle University of Thessaloniki, Greece

Abstract. This paper aims at developing the tools that will be used for the assessment of the seismic performance of specific exhibits in the Archaeological Museum in Argostoli, Greece during the recent Cephalonia earthquakes (26/1/2014 & 3/2/2014).

These exhibits are considered as non-deformable and their responses are similar to these of rigid bodies. Unlike conventional constructions, the damping of seismic energy is not consumed internally with deformation of the body, but externally with movement of solid body. This non-linear, dynamic phenomenon is of most complexity and is dealt by using Abaqus, which is a powerful computational tool using Finite Element Method (FEM). Initially, the exhibits were investigated under sinusoidal ground acceleration in order to allow the qualitative differentiation and quantification of their potential response shape. Then, their responses were simulated under study earthquakes and the results were compared with the recorded ones.

Our scope is the understanding of the potential response shape of examined exhibits, the verification that accelerometer records reflect the actual seismic events and the calibration of a three-dimensional finite element numerical model.

Static wind loads on adjacent cooling towers considering flow interference

DONG Haotian, GE Yaojun

State Key Lab for Disaster Reduction in Civil Engineering, Tongji University, Shanghai, China

Abstract. Building Codes usually use 2-D symmetrical mean wind pressure curves to map spatial wind load distribution on cooling towers, multiplied by single amplification coefficient *"IF"*, namely interference factor, to consider wind-induced interference effects. These simplified methods neglect the redistribution of mean wind pressures due to flow interference. Significant rises of negative pressures on the leeside surface and variations of circumferential-average-pressure with height have been observed through wind tunnel tests about a diamond-shaped array of 6 cooling towers with central distance 1.5 times of inlet diameter. To simplify complex pressure distribution under interference conditions, improved equivalent static load expression is proposed, using displacements or internal forces to determine interference factors. In this study, reinforcement-based effect is introduced. Vertical and circumferential reinforcement percentage of tower shell can be a better alternative to present changes in the distribution of wind pressures and structural effects. Furthermore, reinforcement results are also good indicators of construction cost and structural redundancy. Different static wind pressures measured in wind tunnel tests are applied in structural analysis and reinforcement computations, and necessary comparison with building Codes items and several other methodologies are carried out. In general, traditional concept using single amplification coefficient prove to be conservative to some extent, while proposed methods has better precision and efficiency.

Simple method for the tensile catenary slab contribution in the 2D progressive collapse simulation

HATAHET Tareq, KÖNKE Carsten
Institute of Structural Mechanics, Bauhaus-Universität Weimar, Germany

Abstract. Progressive collapse simulation in reinforced concrete building is a challenge due to the complex inelastic behaviour of the composite material, large deformation, body motion, transit phenomenon and the size of the full building model; this becomes even more challenging when the collapse due to an extreme seismic excitation is simulated. 2D models of multi-story building are very common in academic literature, but the contribution of the RC slab to progressive collapse is not yet considered in 2D to the best of the author knowledge. One reason is the absence of alternative model to represent slab contribution in 2D, we propose and discuss the validity of the simple method which includes slab tensile catenary contribution in the 2D progressive collapse simulation of the RC building. Using the proposed method, the tensile catenary forces can be evaluated as compared to two tests from the literature. The far aim is to support stochastic analysis of progressive collapse safety in RC buildings.

Development of naturally buckling braces combining high strength and low yield steel

INAMASU Hiroyuki
Department of Architecture and Architectural Engineering, Kyoto University, Japan

NAKASHIMA Masayoshi
Disaster Prevention Research Institute, Kyoto University, Japan

Abstract. Steel concentrically braced frames inherently provide great strength and stiffness, and therefore are widely used for seismic resisting systems in buildings. The steel braced frames include conventional buckling braced frames and buckling restrained braced frames. Although the latter can prevent brace buckling and provide ductile behaviour, both types of braces provide no hysteretic damping at small drift levels, and offer very limited post-yield stiffness. In this study, we propose a new type of steel brace with a novel mechanism – the naturally buckling brace (NBB). The design combines high-strength and low-yield steels with a specified initial eccentricity along the brace length, providing ductile seismic behaviour. Tests with various design variables were conducted and subjected to cyclic loadings to examine the seismic performance of the proposed NBB. The results confirm that the proposed braces can achieve early yielding, or hysteretic damping, from around 0.11% story drift and prevent local buckling as well as deformation concentration until a very large story drift (greater than 3%) is reached. The proposed NBBs also enable to provide a large post-yield stiffness and a ductile performance with stable energy dissipation.

Experimental research on thermo-creep behaviour of soft sedimentary rock

JINBU Tomoya, ZHANG F, XIONG Yonglin, KAGEYAMA Sei, KURIMOTO Yuhei
Nagoya Institute of Technology, Nagoya, Japan

Abstract. In Japan, nuclear electricity generation has occupied about 30% of total power generation. On the other hand, we are faced with a serious problem of how to manage the nuclear waste disposal, especially the disposal of high-level radioactive waste (HRW). Until now, the deep geological disposal is regarded as one of the most viable and the safest ways of permanent disposal of HRW, and soft sedimentary rock is one of the host rocks suitable for the geological disposal of the nuclear waste. At the disposed site, however, HRW generates huge amount of thermal energy, and the half-decay period of many nuclear elements are very long. For this reason, it is worried about the influence of strength deterioration of surrounding rock due to the heat on the stability of the disposed site of HRW. To study the interacting factors related to the mechanical properties of host rock, author conducted triaxial compression and creep tests under different constant temperatures. The tests are still under way, but from these tests, it is known that: (1) peak strength of soft rock decreases as the temperature increases; (2) creep failure occurs more quickly as temperature increases. Taking these results, we conducted analysis and succeeded in simulating the element tests.

Dynamic behaviour of a railway viaduct with a precast deck under traffic loads

JORGE Pedro, NEVES Sérgio, CALÇADA Rui, DELGADO Raimundo
Department of Civil Engineering, Faculty of Engineering, University of Porto, Portugal

Abstract. In this article the dynamic effects of the passage of a high speed train on the Alverca's viaduct are evaluated. Two analysis methodologies are compared considering the vehicle-structure interaction. The first methodology follows the direct integration method and the modal superposition method to solve the train and bridge's systems of equilibrium equations respectively and the second methodology follows direct integration methods exclusively to solve both. In the first methodology the train and bridge's matrixes are considered separately and an iterative method is used to solve the interaction. In the second methodology a direct method that solves only one system involving the train, bridge and compatibility equations that relate the bridge and train's displacements is adopted. Both train and viaduct are modelled using finite elements in the ANSYS program.

Dynamic loads induced by human motion

KRUMKA Kasapova
University of Architecture, Civil Engineering and Geodesy (UACEG), Sofia, Bulgaria

Abstract. Considering the propensity in the last decades of using lightweight materials and in some sense extraordinary structures, one can realize the importance of dynamic loads resulting from human motion. Although not vulnerable regarding structural capacity and integrity in most cases, such structures may experience extreme levels of vibrations. When we talk about public buildings or structures which may be loaded by significant number of people, for instance concert halls, grandstands, long-span floors, staircases in malls etc. the issue concerning vibrations induced by humans becomes strongly pronounced – there is not only possibility of disturbing vibrations but the danger of destruction because of resonance, as well.

The dynamic features of a structure are significantly influenced by its stiffness. Lowering the structural stiffness, aiming to impart an attractive outlook to a building, leads to lowering the fundamental frequency and hence deteriorating the dynamic performance of the structure. Reducing the fundamental frequency makes it close to the frequency of any types of rhythmic motion. As an example of the above statement pointed out can be the measurements of Dr. J. Dickie (Manchester University, 1988) at the London Docklands Arena. He measured a fundamental sway frequency 2,5 Hz, when the grandstand was empty, compared with a frequency 1,7 Hz, when the grandstand was full of spectators.

When dynamic loads caused by human motion are present in a structure, we must take into account several matters. The designers must be familiar with the full loading and the effect of the dynamic part of it. If the structure is irregular and unconventional, a designer must resort special analysis – modal analysis based on finite element procedure, aiming to determine which masses and what part of the overall mass will be excited as a result of particular impact. As a consequence of the huge variability of human-induced loadings large number of load patterns should be made and taken into consideration. After assessing the influence of human motion countermeasures should be applied in order to avoid disturbing vibrations for the occupants or even damage to non-structural elements.

Evaluating the performance of tsunami propagation models

KIAN Rozita, YALCINER Ahmet Cevdet
METU Department of Civil Engineering, Ocean Engineering Research, Ankara, Turkey

ZAYTSEV, Andrey
Special Research Bureau for Automation of Marine Researches, Far Eastern Branch of Russian Academy of Sciences

Abstract. There are several numerical models computing the behaviour of long waves and tsunamis under different input wave and bathymetric conditions. Two of the applied models in this study are NAMI DANCE (developed in collaboration with METU, Turkey and Special Bureau of Automation of Research Russian Academy of Sciences, Russia) and FUNWAVE (developed by James T. Kirby et al. (1998), University of Delaware) with the capability of modelling the waves considering the hydrodynamic characteristic such as velocity and direction of the waves. The models consider the dispersion effect in the simulating the tsunami propagation. The numerical simulations are performed for various cases of uniform water depths, wave amplitudes and grid sizes and time steps using momentum equations with and without dispersion. Comparisons show that in the both cases of using nonlinear shallow water equations (without dispersion) and Boussinesq equations, the results are in agreement for both models. The suggestions for the effect of grid size and time step selection to have optimal simulation results in the long waves are presented and discussed.

Dynamic properties of multi-storey reinforced concrete tunnel-form building – a case study in Osijek, Croatia

KLASANOVIĆ Ivana, KRAUS Ivan, HADZIMA-NYARKO Marijana
Faculty of Civil Engineering, Osijek, Croatia

Abstract. Reinforced concrete shear wall (RCSW) dominant buildings, constructed using a special tunnel-form technique, are commonly built in the Republic of Croatia. The fundamental period of vibration plays a major role in predicting the expected behaviour of structures under dynamic excitations. Empirical formulas for the estimation of the fundamental period have been included in seismic codes, which mainly depend on building height, material (steel, reinforced concrete (RC)) and structural systems type (frame, shear wall, etc.). These formulas have been usually derived from empirical data through regression analysis of the measured fundamental period of existing buildings subjected to seismic actions. The main purpose of this paper is to compare the fundamental period obtained from numerical analysis of a real RC building constructed using a special tunnel-form technique with the periods obtained using formulas in different building codes.

Experimental study on vibration behaviour and reinforcement effect of an existing bridge retrofitted by ground anchor

LIANG Yufan

Department of Civil and Environmental Engineering, Waseda University, Tokyo, Japan.

Abstract. Bridges are strategic structures playing important roles in road and railway networks. Large-scale earthquakes have occurred in recent years, such as the Southern Hyogo Prefecture Earthquake in 1995 (M7.3), the 2008 Wenchuan Earthquake (M8.0), the 2011 off the Pacific Coast of Tohoku Earthquake (M9.0), and so on. They brought destructive damage to numerous construction structures including seismic designed bridge structures. Many bridges, designed and constructed based on the old "Specifications for Highway Bridges", cannot meet the demand of increasing high-level earthquake resistance at present.

Therefore, the ground anchor retrofit method, one of indirectly retrofitting methods, has been adopted to improve the seismic performance of the existing structures such as port facility, dam, slope, and so on. According to the previous researches, the retrofit method by connecting ground anchor to the superstructure of bridge was proved to be the most effective one to improve the seismic performance of the whole bridge system by using numerical analysis. The aim of this work is to further verify the reinforcement effect of this method by conducting shaking table tests.

In this study, the prototype bridge was a typical highway bridge as shown in Figure 1. The bridge was a 5-span continuous steel plate girder bridge with a total length of 200 m. The pier pillars were constructed of reinforced concrete and the foundation was constructed of concrete piles built on Type II ground. One of the bridge piers and the portion of superstructure weigh supported by the pier were considered in this study. The scale of the model was 1:16. To investigate the vibration behaviour and seismic performance of the structure, response accelerations, displacements and strains were recorded in the experiment. The detail of the experimental model and the instruments arrangement are shown in Figure 2 and Figure 3. Three types of waves were used as the input ground motions in this study. Sine waves were used to investigate the vibration properties, and the Type 1 and Type 2 seismic design waves were used to verify the seismic performance of the structure.

The ground anchor retrofit method has effective action to improve the seismic performance of bridge associating with the reinforcement amount in this test. The main findings are as follows: The response acceleration, the displacement of the superstructure and the deformation of the bearing were reduced by the introduction of ground anchor. These high performances by test result are almost the same as that by previous simulation result. To obtain more reinforcement effect, the number of ground anchors, stiffness and strength of tendons, direction and angle of the ground anchor axis, and dampers should be considered in future work.

Figure 1. Prototype bridge & concerned pier (P1)

Figure 2. Experimental model (front view & side view) and instruments arrangement

Figure 3. Photo of the experimental model

Crack growth investigation in Storström Bridge

MALEZANOV Lazar Lazarov
University of Architecture, Civil Engineering and Geodesy, Sofía, Bulgaria

Abstract. This report presents a newly developed crack growth model based on an energy criterion. The model is able to predict crack propagation, loading and deformation in mode I fracture. The crack propagation formula is a first order differential equation. The energy changes required may be determined using simple linear elastic finite element methods. The non-linearity is taken into account using Irwins crack length correction. A parametric study of crack propagation formula has been carried out, in order to evaluate the consistency of the theory. It is shown that the theory is able to predict size effects and crack propagation in ductile as well as brittle materials. In order to investigate the capability of the model a comparison carried out between theory and experimental results is obtained with three point bending tests on plain concrete. Full load-deflection curves for three point bending tests where material properties of concrete such as compressive strength and maximum aggregate size together with beam dimensions are varied, are compared with theoretical results. The crack propagation formula is able to predict the peak value and part of the descending branch of the load-deflection curve for different strength levels, notch height ratios and maximum aggregate sizes. A comparison between a proven theory and the presented one is being carried out for steel elements.

Slippage of thermal insulation subjected to seismic load

MIKEC Janez
University of Ljubljana, Faculty of Civil and Geodetic Engineering, Slovenia

Abstract. The present work is a part of a research performed within the BSC thesis of the author. Only some of the results that can be directly used in practice are summarized. The main goal of the study was to determine and predict the possibility of the slippage of thermal insulation when subjected to the seismic load. The design formula was defined for one-storey buildings. The base-shear stresses were compared with the available friction stresses. The friction coefficient was defined by an experimental study. The formula was evaluated on the example of an RC wall structure. It was found that the slippage of thermal insulation could occur especially when a structure has a fundamental period of vibration, which is in the resonant area of the acceleration spectrum, and the building responds essentially elastic to an earthquake load.

PREFLEX girders: Prefabricated composite bridges

PAP Zsuzsa Borbála
Budapest University of Technology and Economics, Hungary

Abstract. The focus of this paper is the presentation of PREFLEX beam through the designing of the B398 underpass bridge at the Makó-Csanádpalota/Nagylak section of the M43 motorway in Hungary. As well as the comparison of this bridge type with the most commonly used pre-cast pre-stressed RC beam superstructure by this bridge type. The paper also presents the newest developments and an analytical calculation method of the PREFLEX pre-stress girders. The pre-stressing girders are used usually at motorway projects. We show a hand-calculating method via analysis a conventional motorway bridge, which is a traditional method based on stress-super positioning and stiffness-changing. Accordingly, two preliminary calculations are made: one with pre-cast, pre-stressed reinforced concrete beam superstructure, and one with PREFLEX beam superstructure (Figure 1).
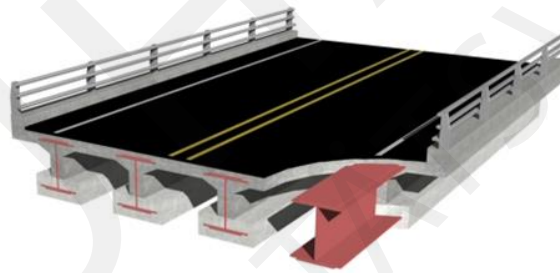
Figure 1. PREFLEX superstructure

Influence of the number of seismic records in the evaluation of structures behaviour

SANTOS Ricardo
Faculdade de Engenharia da Universidade do Porto, Portugal

Abstract. This study analyses the performance of various criteria to define the number of accelerograms that should be used in nonlinear dynamic analysis. The study was based on the analysis of the nonlinear behaviour of one degree of freedom systems having different characteristics in terms of cyclic behaviour. The work was essentially focused on the selection and scaling of earthquake records according to different restrictions for their selection. Subsequently, 24 groups of real earthquakes and one group of artificial earthquakes with different sizes were formed. The results were analysed from a statistical point of view, particularly in terms of the acceleration, displacement and force demands.

The analysis of the demand results was focused on two main aspects: the comparison between the maximum demand obtained for cases where the group of earthquakes had a smaller size and the average demand obtained for cases where the group of earthquakes had a larger size; and the evaluation of the dispersion of the structural demand has the level of restrictions imposed to the record selection process increased.

Regarding the first point, it was concluded that the maximum demand obtained with groups having a lower size is only comparable to the average demand obtained with groups having a higher size when using artificial records or real records selected using a stricter selection criterion. With respect to the second point, it was observed that there is a significant reduction in the dispersion of the demand from the initial selection criterion – the one defined by EC8 – to the more restrictive selection criterion defined in this study.

Model for the seismic performance assessment of masonry houses in Slovenia

TRILLER Petra

University of Ljubljana, Faculty of Civil and Geodetic Engineering, Slovenia

Abstract. Two global models for the seismic performance assessment of masonry houses in the Škofja Loka region are introduced. The models were developed on the basis of survey of ten masonry houses, built in the period from 1970 to 1990. Firstly a statistical analysis of important geometrical features of investigated buildings was performed. All surveyed buildings were then analysed by the pushover-based method (N2 method) and the results were the pushover curves. In order to define the global model of pushover curves, the forces were normalized by the weight of the building or with respect to the average effective floor area of the walls in the given direction whereas the top displacements were normalized by the building's height. The advantage of the proposed global model, represented at the end of the paper, is that only a few data of a house are required for its seismic performance assessment.

Wind characteristics near bridge during strong typhoon procedures

WANG Shouqiang
State Key Laboratory for Disaster Reduction in Civil Engineering, Tongji University, Shanghai, China

Abstract. In recent years, the southeast coastal areas are frequently influenced by strong typhoon. Based on the data of typhoon Muifa (Muifa 1109) measured by the bridge health monitoring system, the wind fluctuating characteristics of two places were analysed. The characteristics, such as turbulence intensity (TI), turbulence scale (TS), gust factor (GF), distribution of fluctuating wind, were mainly discussed. The results show that before and after typhoon landing TI is scattered than it during typhoon. Lateral TI is greater than longitudinal TI ($I_v = 1.011I_u$) at 205.5m, so value according the Standard is bad for the wind resistance of bridge. TSs are larger than the Standard, especially lateral value (larger by 16.4%). Fitting curve of GF changing with TI is under Ishizaki curve and above Choi curve & Cao fitting curve.

Antiseismic study of 15-storey building without beams, of large layout and large spans: Inspection of seismic movements and raft foundation

ZIAKAS Rafail, TEGOS Ioannis, PSARRAS Konstantinos
Department of Civil Engineering, Aristotle University of Thessaloniki, Greece

Abstract. The purpose of this research is to prove the feasibility of constructing buildings without beams at locations with high seismicity. The finite elements model used, involves big internal spans between the supports, central shear walls core system and no internal columns, all of which lead to the application of pre-stressing tendons. After the application of the gravity loads and the transaction of dynamic spectral analysis, the study focuses on restricting the harmful horizontal displacements caused by seismic stresses. To achieve that, different ways of simulation of coupling beams are explored, in order to connect the shear walls to each other. Another concern of the study is to preserve the vertical displacements of the slabs inside acceptable limits, by adjusting the position and geometry of the tendons. Subsequently, the research deals with the treatment of the bending stress requirements of the components, as well as the slab punching shear problems. The last part of the study examines the possibility of activation of the entire body of the raft foundation in order to receive the vertical building loads. The results that emerge will, hopefully, dispel the doubts that accompany this sort of constructions at high seismicity areas.

Activities

Bauhaus Summer School

The Bauhaus Summer School is the summer programme of the Bauhaus-Universität Weimar and offers courses in Architecture & Urbanism, Art & Design, Engineering & Environment and Languages. It is open to prospective students, undergraduate and graduate students. Each year approximately 400 participants from 70 countries around the world create a unique atmosphere. Be a part of the experience!

The Bauhaus Summer School is a great opportunity to meet people all over the world, to connect to an international network and broaden your cultural and academic horizons. Furthermore, the team of Bauhaus Summer School creates a diverse programme that participants can tailor to their interests. Even if you would like to use the weekends to venture outside of Weimar or enjoy a reading, concert or film in the evenings. The guided tours, the international gaming night, the international dinner, all Summer School parties and the film programme are free of charge for those who have a Bauhaus Summer School ID card. Moreover Bauhaus Summer School offers excursions at a reduced cost. Experience the beauty of Weimar, the city of Johann Wolfgang von Goethe and Bauhaus, and make friendships that will last a lifetime!

Guided tours

Every Wednesday between 2 p.m. and 5 p.m., participants can enjoy a cultural programme about the history of Thuringia, Weimar and the Bauhaus-Universität Weimar. The topics vary from week to week:

Johann Wolfgang von Goethe: The Last Universal Genius. Travel cloak, volcanic rock, puppet theatre, Weimar?! On this tour, attendees learn what these things say about one of the most important dramatic artists of the German classical period and how they are connected. Goethe's complexity is as striking today as ever. He not only produced literary masterpieces such as Faust, but also was active in politics and art.

In Franz Liszts Footprints. From 1848-1861, Franz Liszt had a significant influence on Weimar's "Silver Era" as the Court Music Director. In January of 1869, he returned to Weimar on the Grand Duke's invitation and lived on the upper floor of the former court nursery during his summer stays. Together, we will explore the elegant rooms that the Grand Duchess appointed for him.

Experience the World of Music from 200 Years Ago. Participants experience the music culture of the 18th and 19th centuries in an authentic environment as pianists bring historical grand pianos to life in rooms in the castle. Musicologists explain in which direction the sound aesthetics of the piano moved and the role music played in cultural life around 1800.

Discover the Green Heart of Weimar. Two hundred years ago, the Duchy of Weimar was little more than a tiny village with a burned-out castle and was almost bankrupt. A tour through the Park an der Ilm and Johann Wolfgang von Goethe's garden house will show why this city succeeded within a span of 20 years in becoming a cultural centre with a European flair.

Bauhaus Walk. Participants take a walk through Weimar, follow the traces of the early Bauhaus and experience the exciting past and present of the Bauhaus-Universität Weimar. The beginnings of the Bauhaus-Universität Weimar can be traced back to the 19th century. Originally an art academy, it was enlarged after 1945 to include a number of engineering disciplines which gave the university a modern technical character. With the inclusion of the Faculty of Art and Design, founded in 1993, and the Faculty of Media, founded in 1996, the Bauhaus-Universität Weimar has once again coupled the fields of art and engineering into one institution and has been carrying the name of the famous school of design since 1996.

Campus Tour. The programme introduces prospective students to the Bauhaus-Universität Weimar, its laboratories and workshops. The programme aims to establish contact with these potential students and reduce their anxiety to study. You can visit all faculties: Art & Design, Media, Architecture and Engineering. Afterwards you get an introduction in »How to study at Bauhaus-Universität Weimar«.

Summer school parties

Three big parties traditionally take place during the Bauhaus Summer School. The first party, titled „Bonvena", welcomes all the participants to Weimar. Students discover that music and good food are the best ice-breakers. Everyone comes wearing the colours of their home country or those of the country whose language they're going to learn at the Summer School.

Another great tradition is the „Bauhaus Gots Talent Show" held midway through the Bauhaus Summer School course. It's the last party for some participants, but for others, it marks the half-way point. A lot of fun for everyone involved.

Each year Bauhaus Summer School pick a different motto for the last big party. Here students can exchange telephone numbers and e-mail addresses, and celebrate the final hours of the Bauhaus Summer School together. And as always, dancing is strongly encouraged!

International gaming night and food evening

Students make their learning process a game! What is the best way to get to know other people? Correct, the best way is to play games. So, that is why attendees have the opportunity to participate in an international gaming night on every Monday during Bauhaus Summer School at 8 p.m., where they can meet other people from different courses. The purpose of this event is to overcome language barriers in a playful way.
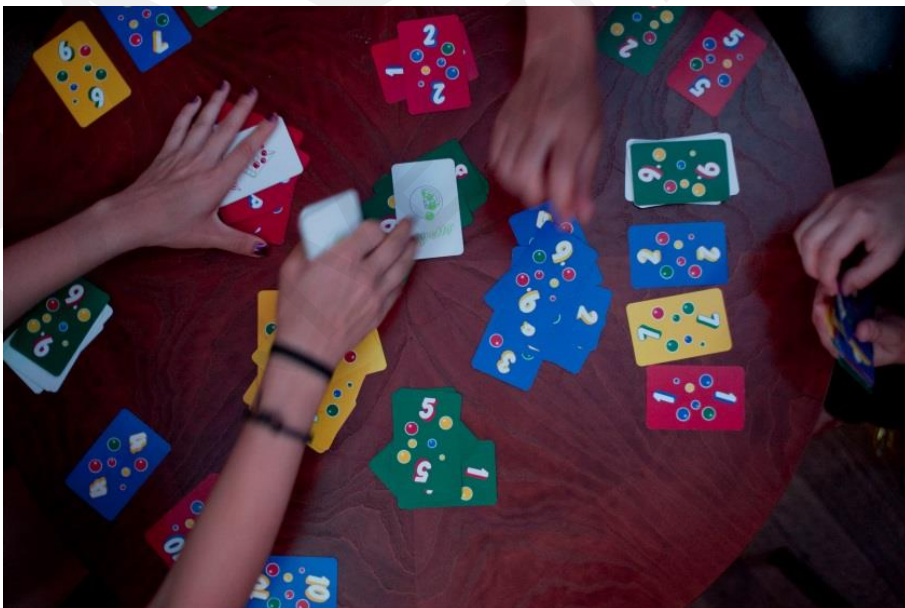
We all know it: nothing brings people together and guarantees good times like a delicious meal. Take a break from the food at the Mensa and the Bratwurst you can get on every corner, and decide for yourself what's on the table. What better way to get to know people from other cultures than by sharing food? We invited all participants to the International Food Evening to meet other students at Bauhaus Summer School who are in different courses. All were requested to prepare the food at home so that all could sample the delight of various cuisines.

Excursions

Berlin. Bauhaus Summer School offers a trip to one of the most fascinating cities in Europe. After a relaxing dinner on Friday evening, participants can go discover the nightlife of Berlin. On Saturday morning, they meet for a boat tour and cruise the Spree River while take in the sights and learn about the "New Berlin". In the afternoon attendees can use their free time to visit museums, go shopping or just even enjoy the rhythm of Berlin. The weekend in the capitol city ends with a visit to the "Reichstagsgebäude".

The Bauhaus in Dessau. Are you interested in learning more about the Bauhaus? Then join us on an excursion to the Bauhaus city of Dessau. The Bauhaus was founded in 1919 inWeimar and experienced political pressure and financial difficulties. So the school moved to Dessau in 1925. The Bauhaus Building in Dessau was designed by Walter Gropius. It was constructed in 1926 to house the schools of art, design and architecture in Dessau. We will tour this iconic building of classical modernism first. Not only its architecture followed the Bauhaus idea consequently, but also furniture and furnishings. Following lunch at the Bauhaus Club, we will tour the settlement of the Bauhaus masters where famous instructors like Gropius, Moholy-Nagy, Feininger, Muche, Schlemmer, Kandinsky and Klee lived and worked. Even today, nearly nighty years later, the settlement still looks surprisingly modern.

Rubber Rafting Tour. Participants enjoy an unforgettable experience with their fellow Bauhaus Summer school friends paddling down the Saale river from Camburg to Bad Kösen. The rubber rafting tour takes attendees gently down the stream past castles, manors, vineyards, massive limestone cliffs and breathtaking landscapes. And the occasional rapids will certainly get their adrenaline pumping!

Sports. As Participants don`t have to miss out on anything during Bauhaus Summer School, not even their weekly sport activities. Every Tuesday, between 5 p.m. and 7 p.m., they can meet with other participants at the Falkenburg University Sports Centre and work up a sweat. There`s something for everyone, from volleyball to badminton to football.

Cinema. As every year the communal cinema mon ami in cooperation with the language centre and the Bauhaus Summer School will show several movies in their original language with German subtitles.

All photos taken by Barbara Proschak || http://www.barbaraproschak.com/